Materials and Interfaces

Scilight

Review

Check for updates

Polymer Microfibers: Fabrication, Structural Design, Functionalization, and Biomedical Applications

Bidya Mondal [1], S. M. Shatil Shahriar [1], Syed Muntazir Andrabi [1], and Jingwei Xie [1,2,*]

[1] Department of Surgery-Transplant and Mary & Dick Holland Regenerative Medicine Program, College of Medicine, University of Nebraska Medical Center, Omaha, NE 68198, USA
[2] Department of Mechanical and Materials Engineering, University of Nebraska-Lincoln, Lincoln, NE 68588, USA
* Correspondence: jingwei.xie@unmc.edu

Received: 31 March 2026; Revised: 10 May 2026; Accepted: 12 May 2026; Published: 22 May 2026

Abstract: Microfibers are rapidly emerging as versatile building blocks for next-generation biomedical devices due to their precisely tunable morphology, chemistry, and functionality. However, most existing reviews primarily focus on electrospun nanofibers or broadly discuss nanofiber systems, where the focus on microfiber areas is limited. Herein, this review presents a comprehensive and systematic roadmap for the design and fabrication of microfibers tailored for healthcare applications. We first survey state-of-the-art fabrication technologies emphasizing their respective capabilities in controlling fiber diameter, alignment, internal architecture, and production throughput. We then discuss material selection strategies encompassing natural, synthetic, and hybrid composite systems. Subsequently, we examine key structural motifs, and elucidate how architectural design governs mass transport, cell-fiber interactions, and spatiotemporally controlled therapeutic release. We further outline functionalization strategies that transform passive microfibers into smart platforms. Finally, we highlight representative biomedical applications with high translational potential and commercial microfiber-based products. We conclude by discussing current translational challenges and future perspectives. Thus, this review provides practical design principles and strategic insights to accelerate the development and clinical translation of microfiber-based biomedical technologies.

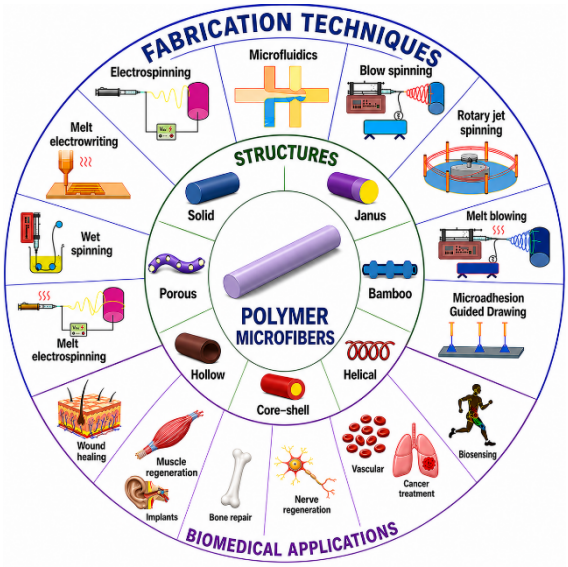

Keywords: microfiber; fabrication; material selection; structural design; functionalization; biomedical applications

1. Introduction

The convergence of materials science and biomedical engineering has opened new frontiers in developing advanced materials for healthcare, among which microfibers have emerged as one of the critical component [1–4]. Microfibers, fibers with diameters typically ranging from 1 to few hundred micrometers, possess tunable structural, mechanical, and functional properties that make them ideal candidates for a wide range of biomedical applications [5–7]. Their unique ability to mimic the architecture of native extracellular matrices (ECM), combined with high surface-area-to-volume ratios, provides a favourable environment for cell adhesion, proliferation, and differentiation, making them particularly attractive in regenerative medicine and tissue engineering [8–11]. Over the past two decades, significant progress has been made in fabricating microfibers using a variety of top-down and bottom-up approaches [12]. Techniques such as electrospinning, melt blowing, rotary jet spinning, wet spinning, microfluidic spinning [13], and melt electrowriting [14] have enabled the production of microfibers with diverse morphologies, including solid, porous, core-shell, and hollow [15] structures [16–21]. Each fabrication technique offers distinct advantages and limitations, influencing the fiber properties and subsequent application

performance [22]. The evolution of these fabrication strategies has also allowed for precise control over fiber alignment, diameter, mechanical strength, and hierarchical organization, which are essential for designing application-specific microfiber scaffolds [23].

In addition to structural control, the integration of functional materials into microfibers has transformed them from passive matrices into dynamic and responsive platforms [24–26]. The incorporation of bioactive molecules, drugs, nanoparticles, and conductive or stimuli-responsive polymers has led to the development of smart microfibers capable of performing therapeutic or diagnostic tasks in response to biological cues [27–29]. These functionalized fibers are being actively explored in wound healing, controlled drug delivery, biosensing, and the tissue regenerations such as bone, nerve, and blood vessels [30,31]. Furthermore, the choice of base materials, ranging from biocompatible natural polymers like collagen, chitosan, and silk fibroin to synthetic biodegradable polymers such as polylactic acid (PLA), polycaprolactone (PCL), polyglycolide (PGA) and polyurethane (PU) plays a vital role in determining the degradation rate, mechanical behaviour, and biological response of microfibers [32,33]. Material selection, combined with smart design and surface engineering, enables the development of multifunctional systems tailored to specific biomedical needs [34].

This review aims to provide a comprehensive overview of the strategies employed to develop microfibers for biomedical applications. We first explore various fabrication techniques and their principles, followed by a discussion on the selection of materials and control over microfiber structure. Next, we focus on functionalization strategies that impart stimuli-responsiveness, therapeutic activity, or sensing capabilities to microfibers. Finally, we highlight major biomedical applications where these fibers are making a transformative impact, such as in wound healing, bone and muscle regeneration, nerve and vascular repair, biosensing, and cancer treatment.

2. Fabrication Techniques

Microfibers are prepared in a number of processes, starting with the selection of appropriate precursor materials and fabrication techniques. The choice of preparation techniques is determined by the desired characteristics of microfibers, including structure design, porosity, surface area, and mechanical strength. Figure 1 shows an overview of different techniques.

2.1. Solution Electrospinning

Electrospinning is a versatile and extensively used technique for fabricating microfibers, particularly in biomedical applications [35–37]. The method employs electrostatic forces to stretch a charged polymer solution into ultrafine fibers that are collected on a conductive substrate [38]. This approach allows precise control over fiber diameter, morphology, and alignment, enabling the design of scaffolds that closely mimic the fibrous architecture of native ECM [11,39].

The electrospinning process involves applying a high voltage (typically 5–30 kV) to a polymer solution dispensed through a needle connected to a syringe pump [40]. Once the electrostatic forces exceed the surface tension of the solution, a charged jet is ejected from the tip of the needle, forming what is known as a Taylor cone [41–43]. This jet undergoes elongation and thinning due to electrostatic repulsion and bending instabilities, and as the solvent evaporates in flight, solid fibers are deposited on the collector. The final fiber morphology can be finely tuned by adjusting key parameters such as solution viscosity, conductivity, and concentration, applied voltage, tip-to-collector distance, and environmental conditions like temperature and humidity [44,45]. Advanced forms of electrospinning have been developed to extend its functionality and address specific biomedical needs. Coaxial electrospinning enables the formation of core-shell fibers, useful for drug encapsulation and sustained release [46]. Needleless electrospinning enhances production throughput by generating multiple jets from a free liquid surface [47].

In electrospinning, different types of natural and synthetic polymers are explored [48]. Moreover, by integrating conductive or electroactive materials, the morphology and properties of fibers are tuned for different applications [49]. For example, Schönlein et al. fabricated nanocomposite microfiber scaffolds with PLA and polydopamine-coated barium titanate (BTO) for enhanced piezoelectric properties of 120% in comparison to pristine PLA microfiber scaffolds [50]. One key trend in utilizing electrospinning is the creation of highly specialized fiber architectures and composites. Mares-Bou et al., for instance, employed both uniaxial and coaxial electrospinning to fabricate polyvinyl alcohol (PVA)-based microfibers for controlled drug release [51]. Similarly, Li et al. explored the complexity of fiber morphology by generating ultraporous interweaving microfibers from immiscible PCL- polyethylene oxide (PEO) binary blends [52]. Beyond morphology, the electrospinning technique is instrumental in integrating bioactivity directly into the fiber structure. Roman et al. electrospun and incorporated the therapeutic agent paclitaxel into aligned PLA microfibers to treat spinal cord injuries [24]. Furthermore, for bone tissue engineering, Steffi et al. developed electrospun PCL/silk fibroin (SF) microfibers

loaded with 17-B estradiol (E2) [53]. The capacity of electrospinning technique for cell encapsulation is also critical for creating complex tissue constructs. Guo et al. modified an aqueous solution-electrospinning method (cell-electrospinning) to directly encapsulate C2C12 myogenic precursors within aligned fibrin/PEO microfiber bundles, overcoming the common limitation of cells only adhering to the exterior of conventional scaffolds [54]. Expanding on structural control, Fattahi et al. introduced 3D near-field electrospinning (3D-NFES), a low-cost, high-resolution method utilizing hobbyist 3D printers to fabricate repeatable 3D polymeric fiber patterns [55]. Neuhäusler et al. specifically highlighted the integration of electrospun microfibers into bioinks and 3D-bioprinted constructs to address the diffusion limit inherent in hydrogels, demonstrating the crucial role of electrospinning in the future of scalable biofabrication [56].

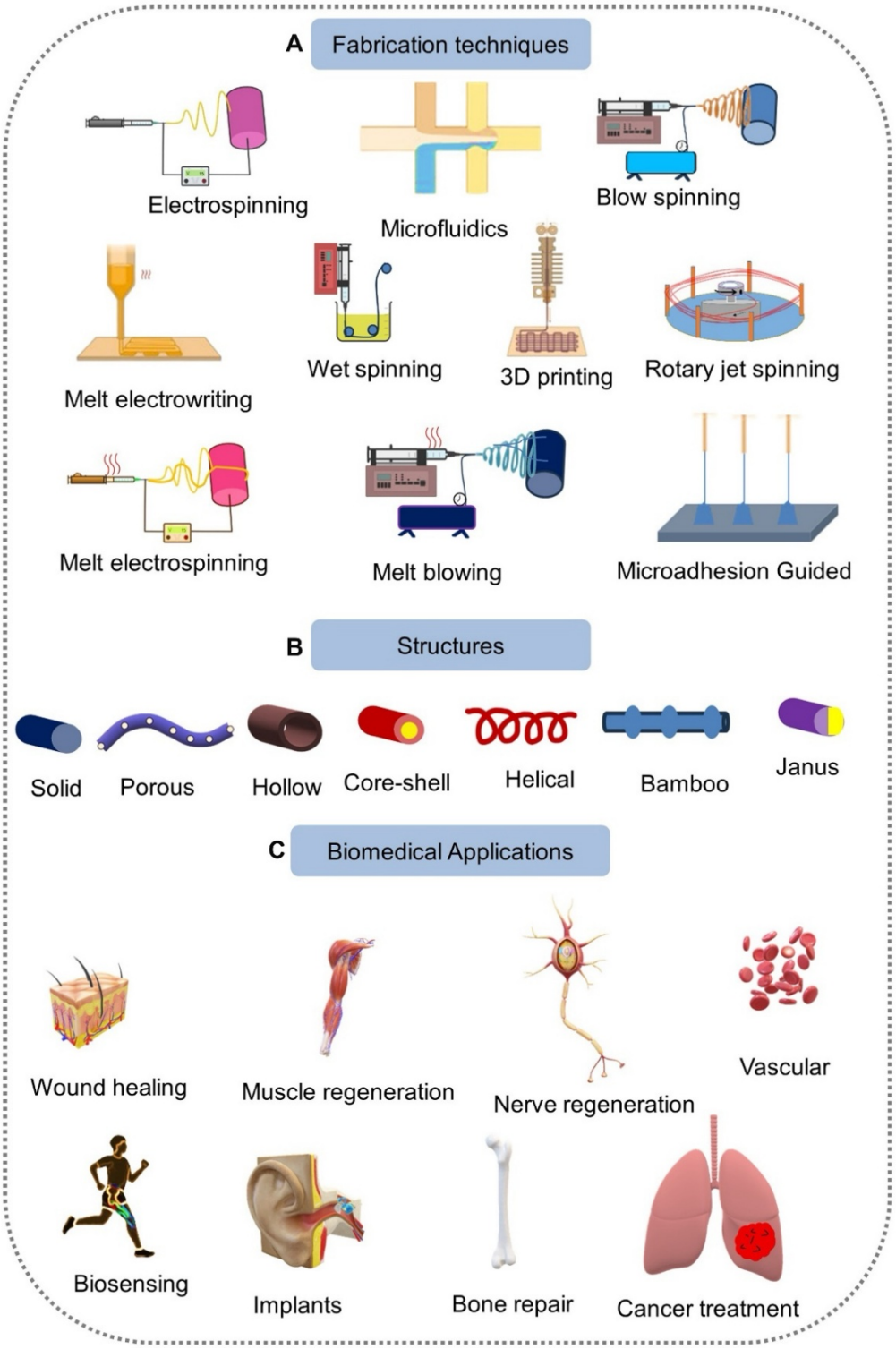

Figure 1. A brief outline of the contents discussed in this review illustrating (**A**) microfiber fabrication techniques, (**B**) secondary structures, and (**C**) their biomedical applications.

2.2. Melt Electrospinning

Melt electrospinning is a fiber fabrication technique that combines the principles of electrospinning and melt processing, using a polymer melt instead of a solvent-based solution to produce continuous microfibers [57–59]. In melt electrospinning, a thermoplastic polymer such as PCL, PLA, or PEO is heated above its melting point and extruded through a nozzle under the influence of a high-voltage electric field [60,61]. The molten polymer is drawn into thin fibers as it travels from the nozzle to the collector, where it solidifies upon cooling. The applied voltage, melt temperature, flow rate, and collector distance play critical roles in determining the fiber diameter and morphology [62–64]. Unlike solution electrospinning, where solvent evaporation contributes to jet thinning, melt electrospinning relies purely on electrostatic stretching and thermal behaviour, often leading to fibers in the range of 1–50 μm [65–67]. Melt electrospun fibers exhibit good mechanical strength, slow degradation rates, and excellent biocompatibility, making them ideal for long-term implantation and load-bearing tissue scaffolds [68,69]. Additionally, unlike solution-based methods, melt electrospinning eliminates toxic solvents, making it highly desirable for direct clinical applications and pharmaceutical manufacturing [70].

In melt electrospinning, the fine control over fiber architecture is invaluable for mimicking the native ECM. Castilho et al. employed melt electrospinning to fabricate highly organized scaffolds from a hydroxyl-functionalized polyester, poly(hydroxymethylglycolide-co-ϵ-caprolactone) (PHMGCL), for cardiac tissue engineering [71]. They showed that the prepared scaffolds significantly improved the alignment and differentiation of cardiac progenitor cells compared to traditional electrospun counterparts. Beyond single polymers, melt electrospinning is a powerful platform for engineering composite and blend microfibers with complex internal morphologies. Talebpour et al. conducted the comprehensive study on morphology development in melt-electrospun fibers from immiscible binary polymer systems, specifically polystyrene (PS) and PCL [72]. They demonstrated that by tuning parameters such as composition ratio, viscosity, and the use of a PS-b-PCL block copolymer as a compatibilizer, they could control the internal morphology, producing highly aligned microfibrils within the fibers. This level of internal structure control is crucial for designing smart microfibers with advanced functions, such as anisotropic mechanical response or directional drug release. Moreover, addressing the challenge of industrial scalability, Koenig et al. investigated the effect of additives and process parameters on the pilot-scale manufacturing of PLA sub-microfibers using melt electrospinning [73]. By combining a 600-nozzle pilot-scale device with conductive and viscosity-reducing additives like sodium stearate (NaSt) and sodium chloride (NaCl), they optimized the process to achieve sub-micron fiber diameters. This research is vital for translating melt electrospinning from a laboratory technique into a high-throughput, environmentally friendly manufacturing platform for polymer microfibers, making the technology viable for mass production in the biomedical and textile industries.

Despite its advantages, melt electrospinning faces challenges such as high processing temperatures, limited material options (thermoplastics only), and relatively low resolution and throughput [74–76]. Nevertheless, its solvent-free nature and compatibility with biodegradable polymers used in FDA-approved medical devices have positioned it as a promising technique for fabricating microfibers for tissue regeneration and other biomedical applications.

2.3. Rotary Jet Spinning (RJS)

RJS, also known as forcespinning, is a centrifugal fiber fabrication technique that produces microfibers by harnessing high-speed rotational forces instead of relying on electrostatic fields, as in electrospinning [77–79]. RJS has gained increasing attention in the biomedical field due to its ability to process a wide variety of polymer solutions or melts without the need for high voltage or electrical conductivity, and it offers significantly higher fiber production rates [80]. The technique is simple, cost-effective, and particularly well-suited for large-scale manufacturing of fibrous scaffolds for wound healing, tissue engineering, and drug delivery [81–83].

In a typical RJS setup, a polymer solution or melt is loaded into a rotating reservoir or cylindrical spinneret equipped with one or more orifices. When the spinneret is rotated at high speeds (typically thousands of revolutions per min), centrifugal forces eject the polymer through the orifices as fine jets [84]. As these jets travel outward, solvent evaporation or melt cooling causes the polymer to solidify into continuous microfibers, which are collected on a surrounding surface or drum collector. The morphology and diameter of RJS fibers can be tuned by adjusting key parameters such as polymer concentration and viscosity, spinneret rotation speed, nozzle diameter, ambient temperature and humidity, and solvent volatility [85]. With optimized conditions, RJS can produce fibers ranging from tens of nanometers to several micrometers in diameter [17]. The remarkable versatility and scalability of RJS have established it as a pivotal technology for fabricating advanced polymer microfibers in regenerative medicine, by offering high throughput and control over fiber morphology and alignment, enabling the precise recapitulation of native ECM architecture [86]. For example, Machado-Paula et al. explicitly leveraged RJS to create PCL

scaffolds embedded with hydroxyapatite (nHap) and carbon nanotube (CNT) for bone repair [87]. Further, Zamproni et al. fabricated porous PLA microfibers for mesenchymal stem cell (MSC) delivery to treat central nervous system injuries [85]. Beyond simple nonwoven meshes, the RJS platform has been ingeniously modified to fabricate complex three-dimensional devices and hierarchically structured materials. Motta et al. introduced focused rotary jet spinning (FRJS), a system combining RJS with a focused air stream, to achieve the on-demand manufacturing of heart valves (FibraValves) in a matter of minutes [88]. Similarly, Yang et al. employed wet rotary jet spinning (WRJS) combined with a salting-out process to produce PVA hydrogels with biomimetic hierarchical structures [77].

The adaptation of RJS into the immersion approach further expands its utility in producing hydrogel-based and tissue-specific constructs. MacQueen et al. employed the immersion rotary jet spinning (IRJS) process to produce gelatin microfibers at high production rates (~100 g/h) [89]. By tuning process conditions, they achieved fiber diameters comparable to natural collagen fibers, fabricating aligned scaffolds that successfully guided the formation of aligned muscle tissue from smooth muscle and myoblast cells. This versatile IRJS technique was also critical for developing smart therapeutic wound dressings. Ahn et al. engineered biomimetic and estrogenic fiber dressings composed of soy protein isolate (SPI) and hyaluronic acid (HA) [90]. For rapid hemostasis using RJS microfibers, Fu et al. developed a highly porous cellulose acetate/thermoplastic polyurethane aerogel and demonstrated a substantial reduction in blood loss and clotting time in trauma models [91].

Additionally, the ability to use polymer melts instead of solutions makes RJS an environmentally friendly option by eliminating organic solvents and their associated toxicity [80]. This melt-based variant is particularly useful for producing implantable devices and scaffolds where solvent residues are undesirable. Despite its many benefits, RJS does face some limitations [92]. The resulting fiber mats are typically non-aligned unless specific collection strategies or modifications are used. The resolution and spatial patterning of fibers are also less precise compared to melt electrowriting or microfluidic spinning [93–95]. Nevertheless, ongoing developments in collector design, multi-nozzle configurations, and hybrid processes are improving the versatility of RJS.

2.4. Melt Blowing

Melt blowing is a solvent-free, high-throughput fiber fabrication technique that utilizes the combination of polymer extrusion and high-velocity hot air to produce micro- and submicron-scale fibers [96,97]. Unlike electrospinning, which relies on electrostatic forces, melt blowing uses mechanical and aerodynamic forces to attenuate polymer melts into fine filaments [98]. The process is industrially scalable and widely used for applications requiring nonwoven fibrous mats with high porosity and surface area, such as filtration, wound care, and barrier materials.

In a typical melt blowing setup, a thermoplastic polymer, commonly polypropylene, PCL, PLA etc. is melted in an extruder and pushed through a die consisting of narrow capillaries [99]. Simultaneously, streams of hot, high-pressure air are directed through orifices adjacent to the polymer nozzles [100]. These air jets exert drag forces on the extruded polymer, causing rapid fiber stretching and thinning. The solidified fibers are collected on a rotating or stationary collector as a random, nonwoven web. Fiber diameters typically range from 0.5 to 20 μm, though submicron fibers can also be achieved with process optimization. The key parameters influencing the melt blowing process include polymer melt viscosity, air pressure and temperature, die-to-collector distance, throughput rate, and ambient conditions [101,102]. These variables control fiber diameter, web thickness, pore size, and fiber orientation. Compared to electrospinning, melt blowing generally results in thicker, randomly oriented fibers but offers significantly higher production rates and eliminates the use of potentially toxic solvents.

Melt-blown microfibers are particularly attractive due to their breathability, softness, and adaptability to large-area manufacturing. Nonwoven mats fabricated by melt blowing can be engineered to have antibacterial, absorbent, or barrier properties, making them suitable for wound dressings, surgical masks, and protective medical garments. Additionally, biodegradable polymers like PLA and PCL have expanded the use of melt-blown fibers in temporary implants and resorbable scaffolds. Although melt blowing offers less control over fiber alignment and architecture compared to techniques like melt electrowriting or electrospinning, its speed, scalability, and simplicity make it a valuable method for producing microfiber-based biomaterials, especially where large-area coverage and economic feasibility are essential.

To this end, Wang et al. successfully enhanced the performance of PLA-based fabrics by preparing PLA/polyethylene glycol@sodium dodecyl sulfate (PLA/PEG@SDS) microfibers using a modified melt-blown process [103]. Their work highlighted the ability to tune the average fiber diameter between 1 and 13.9 μm by regulating key process parameters. These modified nonwovens demonstrated remarkably efficient wetting performance, paving the way for their industrial application as wound dressings. In the domain of high-efficiency

air filtration for filtering respiratory protective devices (FRPDs), Brochocka et al. developed a multifunctional composite from polypropylene (PP) and poly(ethylene terephthalate) (PET) using a melt-blowing technique [104]. This method involved the simultaneous application of powdered functional modifiers, a biocidal agent (biohaloysite) and a superabsorbent polymer via independent injection systems directly into the elementary fiber stream. This innovation yielded a nonwoven with very good antimicrobial activity, high filtration efficiency, and excellent water absorption capacity, which is critical for improving wearer comfort by mitigating the adverse effects of moisture accumulation in the breathing zone. Similarly, González-Sánchez et al. employed melt-blowing to incorporate copper nanoparticles (CuNP) into polyester to create antimicrobial non-woven fabrics, demonstrating activity against pathogens like *E. coli* for use in hospital environments [105]. For composite structures, Kang et al. utilized melt-blown thermoplastic polyurethane (TPU) nonwovens as a mechanically robust substrate layer onto which an electrospun nanofiber layer containing AgCl nanoparticles was deposited [106]. This double-layered approach provided a composite with superior mechanical properties, improved filtration efficiency, and potent antimicrobial activity of 99.9%.

2.5. Wet Spinning

Wet spinning is one of the oldest and most established fiber fabrication techniques, traditionally used in the textile and biomedical industries to produce continuous fibers from polymer solutions [107–110]. Unlike electrospinning methods, wet spinning is a solvent–non-solvent exchange process in which a polymer solution is extruded through a spinneret into a coagulation bath containing a non-solvent that induces phase separation and fiber solidification. This technique is particularly valuable for processing natural or bio-derived polymers that are difficult to electrospin due to poor solubility, low viscosity, or sensitivity to electric fields [111,112].

The process begins by preparing a homogenous polymer solution, which is then pumped through a fine nozzle into a coagulation bath, typically water, ethanol, or a salt solution, depending on the solvent system used [113–115]. Upon contact with the non-solvent, the polymer undergoes rapid precipitation or gelation, forming solid or semi-solid fibers. These fibers are then collected, washed to remove residual solvent or coagulant, and often subjected to post-processing steps such as stretching, crosslinking, or drying to enhance mechanical properties and dimensional stability. Key process parameters include polymer concentration, flow rate, nozzle diameter, bath composition, temperature, and the draw ratio applied to the fibers during collection [116]. One significant application of wet spinning lies in engineering gradient scaffolds for the complex interfaces found in the body. Calejo et al. pioneered the use of wet spinning to create a 3D fibrous scaffold with a continuous transition from mineralized to non-mineralized tissue [25]. They produced continuous, aligned composite microfibers from polycaprolactone (PCL)/gelatin and PCL/gelatin/hydroxyapatite (HAp).

Wet spinning is also crucial for synthesizing scaffolds with tailored mechanical and morphological features. Han et al. introduced a method to create microribbon-like elastomers by wet-spinning gelatin microfibers and subsequently drying them in acetone [117]. This drying process caused an asymmetrical collapse of the microfibers, yielding microribbons that could then be photocrosslinked into macroporous and highly flexible 3D scaffolds. This architecture supported robust proliferation of hASCs, illustrating how solvent choice and post-processing steps can be exploited in wet spinning to transition from simple fibers to complex, macro-porous elastic structures. In the realm of tissue engineering, Zhang et al. developed a new wet-spinning system using a blended solution of edible oil and hexane as the coagulation bath to fabricate PCL microfiber scaffolds [118]. They achieved control over fiber diameter (7–27 μm) and porosity (68–82%), demonstrating that the resultant oriented microfibers guided the oriented growth and infiltration of smooth muscle cells (SMCs).

Furthermore, the technique is adept at incorporating functional materials for advanced electronic and smart applications. Zheng et al. successfully fabricated biocompatible CNT-based hybrid microfibers via wet spinning for use as implantable electrochemical actuators and flexible electronics [119]. Similarly, Wang et al. achieved continuous meter-scale wet-spinning of cornlike composite fibers by anchoring polyaniline (PANI) onto regenerated cellulose (RC) from recycled waste cotton fabrics [109]. This green approach allowed for the mass production of multifunctional electronic fibers, with the corn-like morphology of the PANI layer, controlled by the coagulation bath's ammonium persulfate (APS) content, enhancing the fiber's performance as an eco-friendly flexible strain sensor.

The inherent structure of wet-spun fibers, characterized by a dense outer skin and a porous inner core, offers unique advantages. Puppi et al. applied an additive manufacturing protocol involving the patterned deposition of a polysulfone (PSU)/N-methyl-2-pyrrolidone (NMP) solution into a coagulation bath [120]. The resulting PSU medical implants possessed a transversal cross-section with a dense external skin and a macroporous/microporous inner structure due to the non-solvent induced phase separation (NIPS), highlighting the intrinsic architectural

control offered by the technique for medical implants. In a similar vein, Yang et al. fabricated shear-patterned alginate hydrogel microfibers using wet spinning [121]. They demonstrated that the shear force during spinning introduced microgroove patterns on the fiber surface.

However, wet spinning also presents certain limitations. The fiber diameters are generally larger than those obtained via electrospinning (typically in the range of tens to hundreds of micrometers), and the process is less amenable to producing ultra-fine structures [122–124]. In addition, precise control over fiber alignment and deposition requires specialized collection systems. Despite these challenges, wet spinning remains a valuable technique in the fabrication of biomedical microfibers due to its versatility in material compatibility, ability to form continuous and robust fibers, and potential for biofunctionalization.

2.6. Microfluidic Spinning

Microfluidic spinning is an innovative and highly controlled fiber fabrication technique that utilizes microfluidic devices to generate continuous microfibers through the manipulation of fluid flows within microscale channels [125–127]. This method offers exceptional control over fiber diameter, composition, morphology, and structure, making it especially valuable for biomedical applications that demand uniformity, reproducibility, and multifunctionality [128,129]. Unlike traditional spinning techniques that rely on bulk processes or high mechanical forces, microfluidic spinning enables gentle processing conditions, making it suitable for incorporating sensitive biological components [130].

The basic setup for microfluidic spinning involves a microfluidic chip with one or more inlet channels where polymer solutions and crosslinking agents flow in a co-axial or side-by-side configuration [131]. The spinning fluid (typically a hydrogel precursor or polymer solution) is sheathed or surrounded by a coagulating or crosslinking stream. As the fluids interact within the microchannels, solidification occurs through ionic crosslinking, solvent exchange, or photopolymerization, depending on the system. The resulting fibers are continuously extruded from the outlet and collected in a bath or on a moving stage. Parameters such as flow rate ratio, channel geometry, fluid viscosity, and external stimuli (e.g., UV light or temperature) govern the final fiber properties [132,133]. Microfluidic spinning excels in fabricating microfibers with advanced architectures such as core-shell, hollow, multilayered, and anisotropic structures. Chen et al., for instance, utilized a co-axial microfluidic spinning strategy to continuously produce all-polymeric, core-shell stretchable conductive fibers [134]. These fibers featured a polyurethane (PU) elastic shell and a conductive core of poly(3,4-ethylene dioxythiophene) polystyrene sulfonate (PEDOT:PSS). This design imparted a high conductivity (over 220 $S \cdot m^{-1}$) alongside an impressive stretchability (up to 400% strain). Similarly, Geiger et al. highlighted the use of microfluidic spinning to create microfibers entirely from the conductive polymer PEDOT:PSS for neural applications [135]. By precisely adjusting the flow rates of the spinning dope and shear fluid within a PDMS microfluidic chip, they were able to precisely control the fiber diameter between 1.2 to 3 μm. These conductive microfibers possessed mechanical properties comparable to natural fibrin fibers.

Beyond basic structural and conductive properties, microfluidic spinning allows for the intricate design of microfibers with complex, bio-inspired topographies and therapeutic capabilities. Shang et al. developed bioinspired multifunctional microfibers featuring spindle-knots and joints using a microfluidic spinning [136]. This integrated technique, which involves fluid coating and knot emulsification precisely tuned by adjusting flow rates, grants high controllability over the size and spacing of the knots. For post-operative care, Peng et al. demonstrated the fabrication of multifunctional analgesic sutures [137]. By using microfluidic spinning coupled with a solvent extraction process, PCL microfibers were continuously produced with encapsulated ropivacaine (ROP), a potent analgesic. Furthermore, microfluidic spinning is instrumental in constructing sophisticated *in vitro* tissue models and engineered scaffolds. Masuda et al. focused on the maturation of human induced pluripotent stem cell (iPSC)-derived cardiac microfibers (CMFs), fabricated by using a double-coaxial laminar flow microfluidic device to achieve the desired shape [138]. The architectural control is further emphasized by Liu et al., who proposed a phase inversion-based microfluidic spinning (PIMS) method to produce strong, stretchable, and biocompatible helical microfibers [139]. Thus, the meticulous control offered by microfluidic spinning thus makes it a pivotal technique for creating the smart, functional, and geometrically complex polymer microfibers.

Despite its advantages, microfluidic spinning is currently limited by low throughput and complexity in device fabrication [140]. Producing large quantities of fibers requires parallelization or scale-up of microfluidic channels, which adds to fabrication challenges. Moreover, the process often requires careful optimization of fluid compatibility and surface treatments to prevent clogging and ensure reproducible fiber formation [141]. Nonetheless, the precision and adaptability of microfluidic spinning make it a powerful tool for producing next-generation microfibers for biomedical applications [142,143]. Ongoing developments in soft lithography, 3D

printing of microfluidic chips, and integration with bioprinting platforms are expected to enhance the scalability and functionality of this technique.

2.7. 3D Printing

3D printing, also known as additive manufacturing, is a transformative fabrication technique that enables the layer-by-layer construction of three-dimensional structures from digital models [144–146]. In the context of microfiber fabrications, 3D printing offers precise control over scaffold geometry, pore size, and internal architecture, factors that are critical for mimicking the structural and functional characteristics of native tissues [147–149].

In 3D printing of microfibers, polymers are usually extruded through a nozzle and deposited layer by layer in a predefined pattern to form a solid structure [150]. Depending on the technique, the printing material may be a thermoplastic polymer, hydrogel, or composite bioink. Thermoplastic-based printing methods like fused deposition modeling (FDM) use heat to melt and deposit the polymer, which solidifies upon cooling [151]. Some systems also incorporate ultraviolet (UV) or visible light sources to induce rapid crosslinking of photocurable bioinks during or after deposition [152]. Moreover, by adjusting printing parameters such as nozzle speed, pressure, and deposition path, it is possible to control fiber orientation, gradient properties, and multiscale architecture, thereby influencing cell behavior and tissue integration [153–155].

The integration of smart functionalities into 3D-printed microfibers is rapidly advancing, with a focus on remote stimulation and targeted regeneration. Cedillo-Servin et al. reported the rational design and fabrication of magneto-active microfiber meshes using 3D printing of a magnetized PCL-based composite [156]. By incorporating uniformly dispersed iron oxide nanoparticles, they created hexagonal scaffolds with tunable fiber diameter and a zonal distribution of magnetic material. Beyond structural and magnetic control, 3D printing enables the precise immobilization of growth factors to drive functional tissue outcomes. Ainsworth et al. combined 3D printing with atmospheric-pressure plasma jet (APPJ) treatment to create PCL microfiber meshes with covalently immobilized transforming growth Factor beta-1 (TGFB1) for guided cartilage regeneration [157]. 3D printing is also addressing the challenge of fabricating vascular grafts that are both mechanically stable and anti-thrombogenic. Shen et al. developed a 3D-printed electrospun graft loaded with tetramethylpyrazine [158].

Despite its immense potential, 3D printing faces challenges in microfiber fabrication, primarily related to resolution, throughput, and material limitations [151,159]. Achieving fiber diameters in the micron or submicron range requires precise control over printing parameters and specialized equipment, which can increase cost and complexity [160]. Additionally, ensuring long-term mechanical stability, biodegradation kinetics, and regulatory approval for printed constructs remains an active area of research. Nevertheless, 3D printing continues to evolve rapidly, driven by advances in bioprinting, multi-material integration, and in situ fabrication techniques [161].

2.8. Melt Electrowriting (MEW)

MEW is an emerging fiber fabrication technique that merges principles from electrospinning and additive manufacturing to produce highly controlled, micron-scale fiber architectures [162–164]. Unlike conventional electrospinning, which typically results in randomly deposited fibers due to jet instability, MEW enables direct, layer-by-layer (LbL) desposition of molten polymer filaments with minimal jet whipping, allowing precise control over fiber placement and scaffold geometry [165–167]. This deterministic fiber deposition makes MEW particularly attractive for biomedical applications where structural fidelity and pore architecture are critical [168].

In MEW, a thermoplastic polymer such as PCL is heated above its melting point and extruded through a fine nozzle under low pressure [169,170]. A moderate voltage (typically 2–10 kV) is applied between the nozzle and a conductive collector, which guides the fiber's trajectory and enhances stretching [171]. The collector, often mounted on a programmable stage, moves in predefined patterns to direct fiber deposition and build up 3D scaffolds with high spatial resolution [172]. Unlike traditional solution-based electrospinning, MEW operates at much lower flow rates and avoids solvent-related issues, making it more suitable for biomedical applications where solvent toxicity and residuals are a concern. Several parameters govern the MEW process, including melt temperature, applied voltage, nozzle-to-collector distance, polymer viscosity, and collector speed [68,173,174]. These variables influence fiber diameter, deposition accuracy, inter-fiber spacing, and scaffold porosity. The resulting microfibers can be arranged in well-defined grid-like or biomimetic architectures. A major advantage of MEW is its ability to produce mechanically robust scaffolds with highly organized, reproducible structures [175]. These scaffolds exhibit superior load-bearing capacity and support cell alignment and tissue organization, making them ideal for regenerating mechanically active tissues such as cartilage, intervertebral discs, and tendons. Furthermore, MEW scaffolds can be functionalized with bioactive agents, coated with ECM proteins, or combined with hydrogels to create hybrid systems with improved biological performance [176–178].

A key strength of MEW lies in its ability to rationally design and fabricate scaffolds with specific mechanical properties tailored to target tissues. For instance, Mueller et al. established a design strategy to create small-diameter vascular grafts with programmable compliance [179]. By meticulously controlling the helical microfiber winding angle in PCL scaffolds, they exploited the structure-function relationship of the MEW architecture, achieving tailored compliance that spanned the physiological range of both arteries and veins. This precise mechanical matching is critical for minimizing the compliance mismatch that often leads to high failure rates in synthetic grafts. Similarly, Castilho et al. leveraged MEW to engineer ultrastretchable scaffolds for cardiac tissue engineering [173]. Their work demonstrated that controlled hexagonal microstructures could exhibit large biaxial deformations, delivering up to 40 times more elastic energy than rudimentary MEW fiber scaffolds.

Beyond mechanical stability, MEW is increasingly utilized in advanced composite scaffold design and microphysiological systems. Lai et al. combined MEW with solution electrospinning to produce antibacterial and osteogenic dual-functional micro-nano composite PCL scaffolds for calvarial defect repair [180]. The precision of MEW also extends to constructing sophisticated *in vitro* models, as shown by Janssen et al., who engineered an immunocompetent Intestine-on-a-Chip (IoC) [181]. This model integrated half-pipe-shaped MEW scaffolds with extrusion-based bioprinted hydrogels, allowing for spatial epithelial-immune cell interactions. Moreover, MEW demonstrated its potential to control over polymer processing and architecture to produce smart microfibers, where high porosity is crucial for rapid dissolution kinetics. Keßler et al. utilized MEW to create highly porous, rapid-dissolving scaffolds loaded with an amorphous solid dispersion of Indomethacin [177].

While MEW offers customized design control, and reproducibility, it also has some limitations [182–184]. The range of usable polymers is restricted to thermoplastics with appropriate melt rheology, and the process throughput is relatively low due to its single-nozzle, LbL nature [185,186]. Nonetheless, ongoing developments such as multi-nozzle arrays, temperature-gradient control, and integration with biological printing are expanding its capabilities.

2.9. Micro-Adhesion Based Drawing

Micro-adhesion based drawing technique mimics spider silk drawing by utilizing adhesion between a polymer droplet and a collector surface to generate fibers during mechanical withdrawal [187,188]. Fiber diameter and alignment can be finely controlled by adjusting pulling speed, contact time, and surface tension [189]. This technique allows direct deposition of microfibers onto complex geometries or moving surfaces, making it ideal for site-specific fabrication on biomedical devices, implants, or skin-interfacing electronics. The simplicity and precision of micro-adhesion based drawing hold promise for personalized therapeutic textiles and soft robotics [190].

In summary, microfiber fabrication techniques have evolved significantly, enabling precise control over fiber diameter, architecture, alignment, porosity, and multifunctionality for diverse biomedical applications. As summarized in Table 1, each technique possesses distinct advantages and limitations in terms of resolution, material compatibility, throughput, cost, and clinical applicability, making the selection of fabrication strategy highly dependent on the intended biomedical application. Continued advances in fabrication technologies, process integration, and scalable manufacturing are expected to further accelerate the clinical translation of microfiber-based biomedical systems.

Table 1. Comparative overview of key microfiber fabrication techniques for biomedical applications.

Technique	Scalability	Resolution	Material Compatibility	Cost	Ref.
Electro-spinning	Moderate to high; scalable using multi-nozzle, or roll-to-roll systems	High control; typically fiber diameter in nano–micro range)	Broad	low to moderate cost; but scale-up requires advanced collectors	[56,191]
Melt electro-writing	Low to moderate; slower fabrication rate than electrospinning	high spatial precision; fibers in microscale range	Limited	High equipment complexity; requires controlled heating, pressure, voltage, and motion stage	[172]
Rotary jet spinning	High; can produce large-area fibrous mats rapidly	Moderate diameter control; fibers often in nano- to microscale range	Broad	Moderate cost; simpler than electrospinning for large-scale production	[77,81]
Melt electro-spinning	Moderate; but process control is challenging	Moderate control; usually produces microfibers larger than solution electrospun fibers	Limited	Moderate to high; requires heating and high-voltage control	[75,76]
Wet spinning	High; industrially scalable and continuous fiber production is possible	Moderate; fiber diameter controlled by system parameters	Broad	Moderate; relatively simple setup but requires coagulation chemistry optimization	[77,109]

Table 1. *Cont.*

Technique	Scalability	Resolution	Material Compatibility	Cost	Ref.
Microfluidic spinning	Low to moderate; excellent control but limited throughput	Very high control over cross-section, diameter, core-shell, hollow, Janus, and multicompartment structures	Broad	High device-design complexity; requires microfluidic chips and precise pumps	[140,192]
Melt blowing	Very high; industrially scalable and used for nonwoven production	Low to moderate; produces mostly random fibers with broad diameter distribution	limited	High industrial equipment cost but low cost per unit at scale	[101,106]
3D printing	Moderate; scalable for customized constructs	Moderate to high; depends on nozzle size, ink rheology, and printing system	Broad	Moderate to high; requires printer, optimized bioink, and post-crosslinking	[193,194]
Micro-adhesion-guided drawing	Low; currently mainly laboratory scale	High control over fiber placement and alignment at small scale	Limited	Moderate; requires patterned substrates and controlled drawing/spinning	[187,188]

3. Choice of Materials

The selection of appropriate materials is a critical step in the design and fabrication of microfibers for biomedical applications [171,195]. The material not only determines the mechanical and degradation properties of the fiber but also influences its biocompatibility, drug-loading capacity, and interaction with cells and tissues [196]. Depending on the intended function, whether for tissue regeneration, wound healing, drug delivery, or biosensing, materials must be carefully chosen to ensure structural integrity, biological performance, and compatibility with the selected fabrication technique [197,198]. Table 2 provides a comprehensive summary of the polymers, including fabrication process, microfiber diameter, final structure, and their biomedical applications or significant outcomes.

Table 2. List of different polymers and fabrication techniques of microfibers and their biomedical applications.

Materials	Fabrication Technique	Fiber Diameter (μm)	Secondary Structure	Applications	Ref.
PCL	Wet spinning	15	Solid	Tissue regeneration	[199]
PLLA/cBTO	Electrospinning	1.8	Solid	Piezoelectric scaffold	[50]
Alg-GelMA	Microfluidic spinning	380–510	Hollow	Peripheral nerve regeneration	[200]
PEDOT: PSS	Microfluidic wet-spinning	3	Solid	Nerve guidance conduits	[135]
PLA	FDM 3D printing	45	Solid	Piezoelectric biosensor	[201]
GelMA	Bioprinting	20–120	Solid Janus	Tumor angiogenesis	[202]
PHB/ε-PLL	Solution blowing	1	Solid	Antimicrobial activity	[203]
Gelatin	Microfluidic spinning	685–715	Hollow	Application in blood capillary	[193]
poly(styrene-b-isobutylene-b-styrene)	solution blow spinning	1–20	Solid	Antibacterial and antithrombosis coating	[204]
Na-alginate	Microfluidic spinning	140–200	Janus-hollow	Tissue construction	[142]
PDO	Centrifugal spinning	15–19	Solid	Skin tissue engineering	[205]
PEDOT/PDA/Silk	extraction-protection	10	Core-sheath	Wound healing	[206]
Polyacrylamide/Mxene	Microfluidic spinning	233	Porous	Joint monitoring	[207]
hyaluronic acid/SWCNT	Wet Spinning	50	Porous	Implantable electrochemical actuator	[119]
PCL	Electrospinning	2–10	Solid	Biomedical application	[19]
PLGA	Microfluidic spinning	20–230	Porous	Tissue engineering	[127]
PCL	3D printing	11	Solid	Bone regeneration	[208]
PEG/PVA/Alginic acid	Microfluidic spinning	300–500	Cavity knot	Tissue engineering	[209]
PCL	Melt electrowriting	10–15	Solid	Tympanic membrane replacement	[162]

Natural polymers are widely used due to their inherent biocompatibility and resemblance to the native ECM in both composition and function [210]. Materials such as collagen and gelatin are frequently employed in skin and cartilage regeneration owing to their cell-adhesive properties [211]. Silk fibroin, another natural protein polymer, offers superior mechanical strength and is often used in bone, nerve and ligament scaffolds [212]. Polysaccharides like chitosan provide antimicrobial activity and are suitable for wound healing, while alginate and hyaluronic acid are commonly used in hydrogel-based spinning systems that encapsulate cells or bioactive agents [213]. Despite these advantages, natural polymers often require blending or crosslinking to improve mechanical stability and consistency.

Synthetic polymers offer greater control over fiber properties, including degradation rate, mechanical strength, and processability [214]. PCL, PLA, PGA, and poly(lactic-co-glycolic acid) (PLGA) are among the most commonly used biodegradable polyesters, well-suited for a wide range of tissue engineering and drug delivery applications [169,213,215]. Polyurethane (PU) is valued for its elasticity and durability in skin and cardiovascular devices, while polyvinylidene fluoride (PVDF) is often selected for its piezoelectric properties in sensing applications [84,216]. Water-soluble polymers like PEO and PVA are used in systems requiring rapid dissolution or transient performance [217]. Synthetic polymers are generally easier to process and offer more predictable performance, but often lack intrinsic bioactivity and require surface modification to enhance cell interactions.

To overcome the limitations of individual polymers, composite and hybrid materials are increasingly employed [218,219]. These combine the bioactivity of natural polymers with the structural integrity of synthetics. For example, blending gelatin or collagen with PCL can enhance both cell adhesion and mechanical strength [46]. Hybrid systems can also be enhanced with nanoparticles such as silver to provide antibacterial effects, hydroxyapatite to support bone regeneration, and carbon-based nanomaterials to improve electrical conductivity [119]. This material modularity enables the design of multifunctional microfiber systems tailored to specific biomedical challenges.

The choice of material also varies according to application-specific demands. For wound healing, materials that maintain moisture balance, prevent infection, and promote tissue closure are essential. Bone tissue scaffolds require materials with higher stiffness and bioactivity, such as calcium phosphate composites. Nerve and muscle regeneration benefit from elastic materials that support aligned fiber orientation and directional cell growth. In biosensing applications, materials must combine flexibility, conductivity, and chemical stability to ensure signal fidelity and user comfort.

Recent advances in smart and stimuli-responsive polymers have further expanded the material landscape for microfibers [220]. Polymers that respond to temperature, pH, light, or magnetic fields allow for dynamic, on-demand functionalities such as controlled drug release or actuation [221]. Examples include poly(N-isopropylacrylamide) (PNIPAM) for temperature responsiveness, poly(acrylic acid) for pH sensitivity, and iron oxide nanoparticle-laden composites for magnetic actuation [222]. These smart materials enable microfibers to transition from passive scaffolds to active, responsive platforms capable of interacting intelligently with their biological environment.

4. Secondary Structures

The structural properties of microfibers play a pivotal role in determining their mechanical behaviour, surface interactions, biological responses, and overall performance in biomedical applications [223]. By tailoring the internal and external morphology of fibers, such as producing solid, porous, hollow, core-shell, helical, bamboo knot, and Janus architectures, researchers can achieve specific functionalities, ranging from controlled drug release to enhanced cell adhesion, electrical responsiveness, and tissue integration (Figure 2) [72,224–226]. The following subsections describe each structural configuration in detail, emphasizing fabrication strategies, physicochemical properties, and biomedical relevance.

Solid microfibers represent the simplest and most common architecture, typically formed through electrospinning, melt electrowriting, wet spinning, or rotary jet spinning (Figure 2A) [5,135]. They consist of a homogeneous cross-section with a uniform polymer matrix, providing high mechanical strength, structural stability, and tunable flexibility depending on polymer type and molecular weight. Their dense morphology ensures durability under mechanical loading, making them ideal for structural scaffolds, sutures, and load-bearing applications such as bone or ligament regeneration. The simplicity of solid fibers allows for easy control of diameter, alignment, and orientation, which can direct cellular responses such as fibroblast elongation or osteoblast differentiation [163]. However, their limited internal surface area has motivated the development of modified variants such as porous or core-shell fibers. Surface functionalization through plasma treatment, coating, or chemical grafting can further improve hydrophilicity and bioactivity, allowing these dense fibers to serve as fundamental building blocks for multifunctional tissue-engineering constructs.

Porous microfibers are characterized by the presence of interconnected pores or cavities within their matrix, resulting in significantly enhanced surface area and permeability (Figure 2B) [217,227]. Porosity can be introduced via phase separation, salt leaching, electrospinning, or gas foaming methods [228,229]. The porous structure promotes nutrient and oxygen diffusion, supports cellular infiltration, and provides additional sites for drug loading. The pore size and distribution can be tuned by varying solvent volatility, polymer concentration, and humidity during spinning [230,231]. For example, electrospinning under high humidity generates breath figure-induced pores, while emulsion electrospinning allows oil-in-water systems to form controlled microcavities [232,233]. Porous

microfibers are especially valuable in wound dressings and regenerative scaffolds where moisture retention, gas exchange, and controlled degradation are critical for healing.

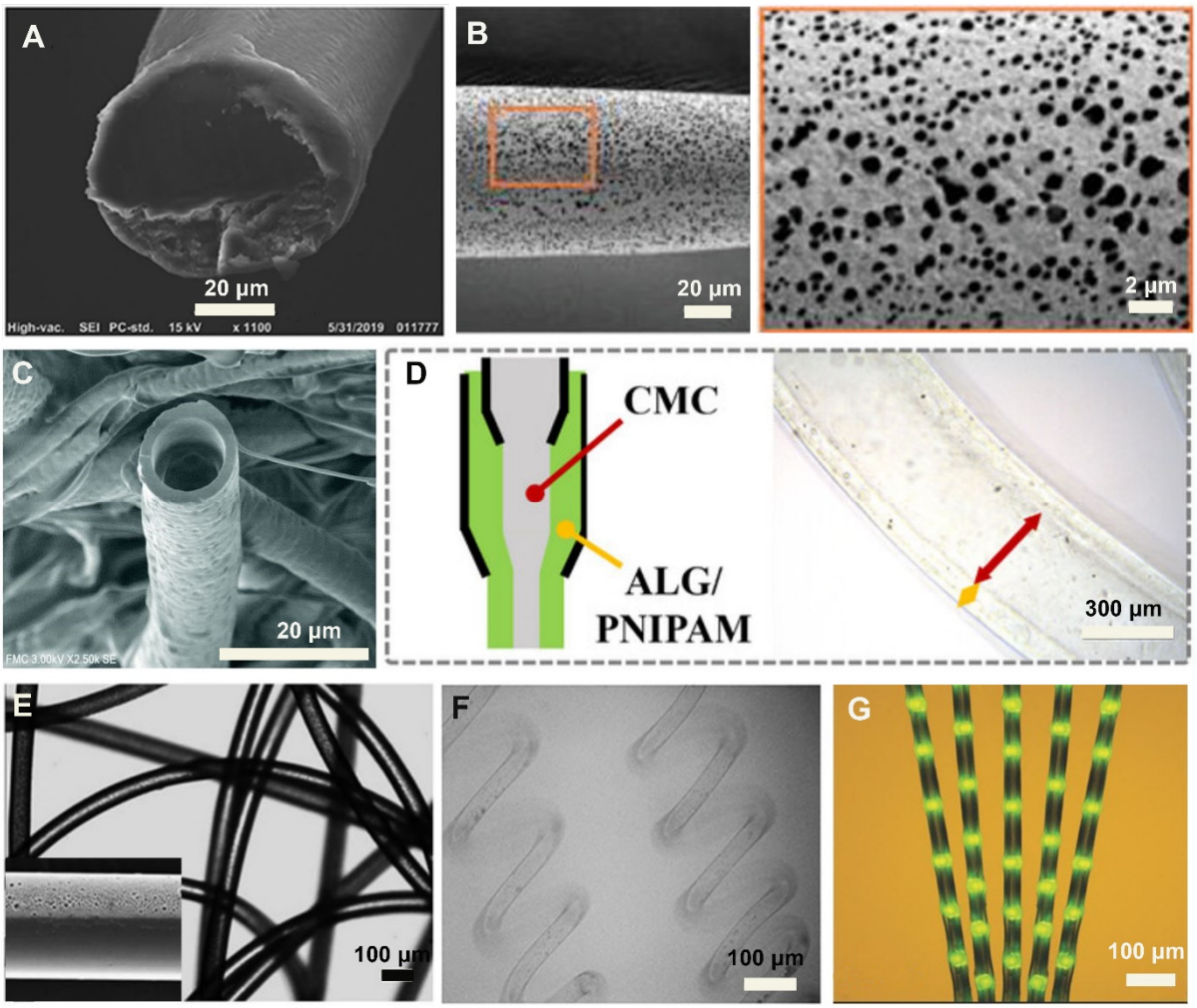

Figure 2. Different structural designs of microfibers. (**A**) Solid microfibers of alginate. Reproduced with permission [234]. Copyright 2020, Frontiers. (**B**) Porous prolamin microfibers and its high-magnification view. Reproduced with permission [235]. Copyright 2024, Wiley-VCH. (**C**) Hollow microfibers of PCL. Reproduced with permission [16]. Copyright 2020, RSC Publishing. (**D**) Core-shell microfibers, featured as an alginate/poly (N-isopropyl acrylamide) (ALG/PNIPAM) shell encapsulating a carboxymethyl cellulose (CMC) core. Reproduced with permission [236]. Copyright 2023, Wiley-VCH. (**E**) Janus polyurethane microfibers. Reproduced with permission [216]. Copyright 2009, RSC Publishing. (**F**) Helical microfibers of Na-alginate. Reproduced with permission [192]. Copyright 2017, Wiley-VCH. (**G**) Bamboo shaped calcium alginate microfibers. Reproduced with permission [237]. Copyright 2014, Wiley-VCH.

Hollow microfibers contain an empty central lumen surrounded by a solid shell, mimicking natural tubular structures such as blood vessels and nerve conduits (Figure 2C) [238,239]. These fibers are typically fabricated using coaxial electrospinning or microfluidic spinning, where two immiscible fluids are extruded simultaneously to form a core-shell structure, and the core phase is later removed [217,240]. Hollow fibers combine lightweight mechanical behaviour with large internal volume, enabling encapsulation and sustained release of therapeutic agents, growth factors, or even living cells [241]. The internal channel allows fluid transport, making them ideal for vascular grafts, nerve guides, and controlled drug delivery systems [242]. By adjusting core and shell flow rates, shell thickness and lumen diameter can be finely tuned, affecting permeability and mechanical strength [6,243]. Materials such as PCL, PLA, and silk fibroin are often used as shells, while hydrogels or bioactive materials can serve as the core template. Their biomimetic tubular morphology has made hollow microfibers a preferred structure for fabricating artificial blood vessels and nerve guidance conduits.

Core-shell microfibers possess a composite structure with distinct inner (core) and outer (shell) layers, offering superior multifunctionality and controlled release properties (Figure 2D) [224]. Fabrication typically

involves coaxial electrospinning or 3D printing with dual nozzles, where the core and shell are independently formulated to achieve complementary functionalities. The core can encapsulate sensitive bioactive molecules, such as proteins, growth factors, or drugs, shielded by the protective shell that regulates diffusion and degradation. This configuration prevents premature drug loss and preserves bioactivity. The shell often provides mechanical strength, environmental protection, or targeted surface chemistry for cell adhesion. For instance, hydrophilic shells can promote biocompatibility, while hydrophobic shells control drug release kinetics. Core-shell designs have been successfully applied to wound healing (sustained antibiotic release), nerve regeneration (encapsulated neurotrophic factors), and bone repair (dual-phase mineralization). Moreover, the use of stimuli-responsive materials in the core or shell, such as pH-, temperature-, or enzyme-sensitive polymers, enables smart therapeutic systems capable of on-demand release in response to physiological changes.

Janus microfibers feature two distinct sides or compartments with contrasting physical or chemical properties, typically achieved through side-by-side electrospinning, microfluidic co-extrusion, or bicomponent melt spinning (Figure 2E) [197,216]. This asymmetric structure allows simultaneous incorporation of multiple functionalities within a single fiber. One side can be hydrophilic to promote cell adhesion and drug release, while the other remains hydrophobic for barrier or mechanical stability [244]. Alternatively, one hemisphere may contain magnetic nanoparticles or conductive fillers, while the other contains growth factors or biomolecules. Such anisotropy enables directional interactions and programmable responses [245,246]. Janus fibers are ideal for stimuli-responsive or gradient delivery systems, where each phase reacts differently to environmental cues such as temperature, pH, or electric fields.

Helical microfibers exhibit a coiled or spring-like morphology that provides exceptional elasticity, stretchability, and energy dissipation (Figure 2F) [247]. They can be fabricated through mechanical twisting of aligned fibers, controlled jet instabilities during electrospinning, or direct 3D printing using rotating collectors or predesigned helical paths. The helical configuration allows these fibers to withstand cyclic strain and recover their shape, making them suitable for soft tissue engineering (e.g., muscle, tendon, and vascular applications). The coiled structure also enhances surface area, improving interactions with cells and biomolecules. In biomedical devices, helical fibers can function as artificial tendons, stretchable biosensors, or electroactive actuators. When made from conductive or piezoelectric polymers, they can convert mechanical deformation into electrical signals, useful for self-powered sensors and dynamic scaffolds. Additionally, the geometric flexibility of helices provides unique mechanical cues that influence stem cell mechanotransduction and alignment, enhancing muscle and nerve tissue regeneration [248,249].

Bamboo knot microfibers are characterized by a periodic alternation of thick and thin segments along the fiber axis, resembling the joints of bamboo (Figure 2G) [226]. These structures can be created by modulating flow rate, voltage, or collector movement during electrospinning, leading to uneven mass deposition. The “knot” regions serve as mechanical reinforcements and local reservoirs for drug encapsulation. This architecture enables a unique combination of flexibility and localized functionalization. For biomedical applications, bamboo-like fibers are particularly advantageous for sequential or site-specific drug delivery, as the nodal segments can contain different therapeutic agents. Additionally, the varying diameter creates differential mechanical stiffness along the fiber, which can influence cellular behaviour and tissue integration. Bamboo knot structures are also being investigated for hierarchical scaffolds where graded mechanical properties are desirable, such as tendon-to-bone or muscle-to-tendon interfaces [250–252].

In summary, the structural versatility of microfibers, spanning from simple solid configurations to complex Janus or helical architectures, offers powerful means to tailor mechanical performance, surface chemistry, and biological activity. By leveraging advanced fabrication technologies such as coaxial, side-by-side, and microfluidic spinning, researchers can precisely design fiber architectures suited for diverse biomedical applications, including regenerative scaffolds, drug delivery systems, wearable biosensors, and implantable therapeutic devices [253]. The continued evolution of controlled structural engineering at the microscale will enable the next generation of multifunctional, adaptive microfiber systems capable of interacting intelligently with biological environments.

5. Functionalization

Functionalization plays a vital role in modifying the physicochemical and biological properties of microfibers to meet specific biomedical demands. A wide range of physical and chemical methods are available to impart functionality to microfibers post-fabrication, as shown in Figure 3, including dry etching, wet etching, electrospray, sputtering, dip coating, and LbL assembly to tailor surface morphology, reactivity, and bioactivity.

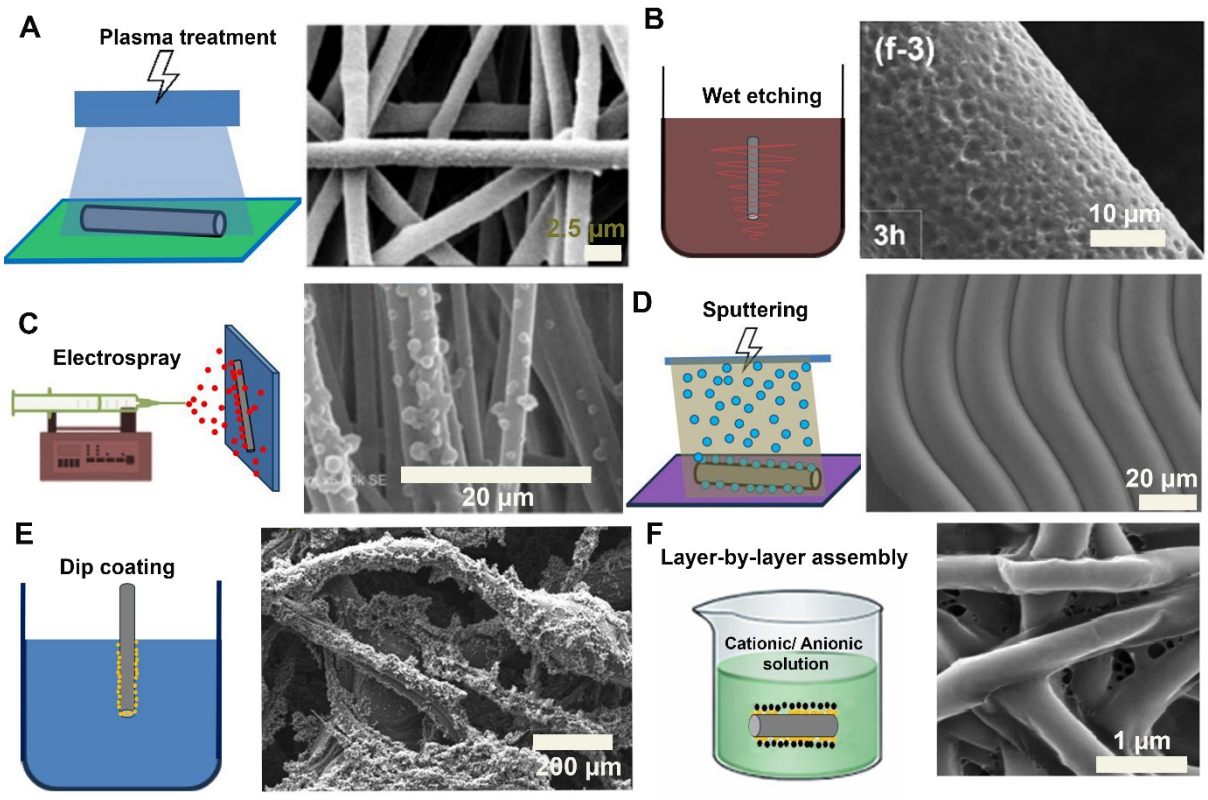

Figure 3. Different methods for functionalization of microfibers. In each case, representative SEM images of postprocessed microfiber scaffolds show the modifications on the fiber surface by the methods described respectively. (**A**) Dry etching or plasma treatment. Reproduced with permission [254]. Copyright 2013, Wiley-VCH. (**B**) Wet etching. Reproduced with permission [255]. Copyright 2022, Elsevier. (**C**) Electrospray coating. Reproduced with permission [256]. Copyright 2022, Sage Journals. (**D**) Sputtering. Reproduced with permission [257]. Copyright 2023, Springer Nature. (**E**) Dip coating. Reproduced with permission [84]. Copyright 2025, Wiley-VCH. (**F**) Layer-by-layer assembly. Reproduced with permission [258]. Copyright 2012, Elsevier.

Plasma treatment or dry-etching is a highly effective surface modification technique used to functionalize microfibers by altering their surface chemistry and topography without affecting their bulk properties (Figure 3A) [259,260]. This method employs ionized gas (plasma) composed of reactive species such as ions, electrons, radicals, and photons to activate or etch the fiber surface. Plasma treatment is particularly valuable for microfibers because it enables the introduction of reactive functional groups, increases surface roughness and energy, and enhances wettability, factors that significantly improve cell adhesion, protein adsorption, coating adherence, and overall biological performance [261,262]. In a typical plasma treatment process, microfiber mats are placed in a vacuum or low-pressure chamber where a gas, commonly oxygen (O_2), argon (Ar), nitrogen (N_2), or air is ionized using radiofrequency (RF) or microwave energy. The resulting plasma interacts with the fiber surface, breaking molecular bonds and forming new polar functional groups such as hydroxyl (-OH), carboxyl (-COOH), amine (-NH_2), or carbonyl (C=O) [254,263]. These groups serve as anchoring sites for subsequent chemical conjugation, such as the attachment of bioactive molecules. Plasma treatment also enhances coating adhesion in post-processing steps. For instance, plasma-treated microfibers exhibit better bonding with drug-loaded polymers, or hydrogel coatings due to the increased density of surface functional groups and roughness [264]. This makes it an essential pre-treatment step in multilayer microfiber systems and sensor-integrated scaffolds. Importantly, plasma treatment is a solvent-free, low-temperature, and rapid process, making it compatible with thermally sensitive polymers and biologically active molecules. The depth of surface modification is typically limited to a few nanometers, which ensures that the mechanical properties of the fibers remain unchanged [259]. In biomedical applications, plasma functionalization has been effectively utilized to enhance the performance of microfiber-based systems. It improves cell adhesion and proliferation in scaffold structures, increases drug loading efficiency by enhancing surface wettability and interactions, and enables site-specific immobilization of biomolecules such as peptides, antibodies, and enzymes for biosensing applications. Additionally, it facilitates the integration of hydrogels, supporting the development of smart wound dressings and moisture-responsive systems.

Wet etching involves immersing fibers in a reactive chemical solution that selectively dissolves specific components of the fiber or modifies the surface (Figure 3B) [265,266]. Acidic or basic solutions such as hydrochloric acid, nitric acid, or sodium hydroxide are commonly used. Wet etching creates increased surface roughness, opens up surface pores, and modifies surface chemistry. This process is valuable for improving hydrophilicity, increasing protein or drug adsorption, and enhancing cell attachment. For instance, alkaline etching of PLA or PCL microfibers exposes carboxyl and hydroxyl groups, which promote collagen adsorption or subsequent chemical grafting. Wet etching is also used to remove sacrificial layers or surface coatings to reveal internal fiber layers or cores.

Electrospray coating is a precise and versatile surface modification technique that enables the deposition of micro- or nanoscale droplets onto a target substrate using an electrically driven spraying process (Figure 3C) [39,267]. In contrast to conventional spray coating, which relies on pneumatic or thermal atomization, electrospray utilizes electrostatic forces to produce a fine mist of charged droplets from a polymer or functional material solution. This technique allows for the uniform and controlled coating of microfiber surfaces with excellent resolution, making it especially suitable for biomedical applications where spatial precision, minimal material waste, and gentle processing conditions are essential. The electrospray process involves applying a high voltage (typically 5–20 kV) to a capillary needle containing the solution to be deposited [268]. Under the influence of this electric field, a Taylor cone forms at the needle tip, and charged droplets are emitted from its apex. These droplets travel toward a grounded collector, which may be a microfiber mat, individual fiber, or rotating substrate. As the solvent evaporates mid-flight, the solute is deposited onto the target surface as a thin film or particulate layer. Key parameters such as solution concentration, flow rate, applied voltage, tip-to-substrate distance, and solvent volatility influence droplet size, deposition rate, and coating morphology. Electrospray coating is particularly advantageous for functionalizing delicate or highly porous microfiber structures, as it provides conformal coverage without fiber bundling or morphological collapse. The technique has been used to deposit a wide range of functional materials including therapeutic drugs, nanoparticles (e.g., silver, hydroxyapatite, magnetic), bioactive polymers, enzymes, and conductive materials. Its ability to deposit material LbL also supports the fabrication of multilayered or gradient coatings with tunable properties. In biomedical applications, electrospray coating has been employed to endow microfibers with antibacterial activity (e.g., electrosprayed silver or zinc oxide nanoparticles), controlled drug release (e.g., coating with hydrophobic or stimuli-responsive drug reservoirs), and bioactivity (e.g., growth factor-loaded coatings for regenerative scaffolds). The low temperature and solvent-based processing also make it suitable for encapsulating and immobilizing sensitive biomolecules such as proteins or peptides without denaturation. Furthermore, electrospray allows selective functionalization by directing the spray to specific areas or patterns on the microfiber surface, which is advantageous in biosensing, wound healing patches, and organ-on-fiber constructs where spatial functionality is required. Despite its advantages, electrospray coating requires careful optimization to ensure consistent deposition, especially on 3D fibrous architectures where charge accumulation and droplet trajectory may affect uniformity. However, with advances in nozzle design, multi-nozzle arrays, and real-time feedback control, electrospray is becoming increasingly scalable and reliable for industrial and clinical translation.

Sputtering, a form of physical vapor deposition (PVD), enables the deposition of ultra-thin metallic or metal oxide layers onto fiber surfaces (Figure 3D) [269]. The process occurs in a vacuum chamber, where a target material (e.g., gold, silver, titanium, zinc oxide) is bombarded by inert gas ions (usually argon), causing ejection of atoms that condense on the fiber surface [270]. The key advantages of sputtering include conformal coverage, high purity, and excellent adhesion. Sputtered coatings are often used to add electrical conductivity, antimicrobial properties, or photothermal activity to microfibers [271]. For example, sputtered silver or copper layers provide antimicrobial effects for wound healing, while gold coatings support biosensor functionality. Titanium and zinc oxide coatings offer biocompatibility and UV protection. The deposition parameters, such as power, time, pressure, and substrate orientation, affect the coating's thickness, crystallinity, and surface energy.

Dip coating is one of the most accessible and widely used methods for surface functionalization (Figure 3E) [272]. In this process, microfiber mats or single fibers are immersed in a solution containing the functional agent (e.g., drug, polymer, nanoparticle) and then withdrawn at a controlled rate [273,274]. Upon drying or curing, a uniform coating forms on the fiber surface. Multiple cycles can be performed to increase coating thickness or to build multilayers. Dip coating is highly adaptable and compatible with a wide range of functional agents and solvents [275]. It is widely used to impart antibacterial, anti-inflammatory, or hemostatic functionality to wound dressings and implantable fibers [276]. For example, chitosan or alginate coatings can provide antimicrobial action, while dip coating with silver nanoparticles or drug-loaded polymers enables therapeutic release [277]. Parameters such as immersion time, withdrawal speed, and solution viscosity determine the coating thickness and uniformity.

LbL assembly is a versatile surface modification technique that relies on the sequential adsorption of oppositely charged polyelectrolytes or biomolecules onto a substrate [278]. In microfiber scaffolds, this method enables the formation of ultrathin multilayer coatings with precise control over composition and thickness [279]. The process typically involves alternating immersion of the fibers in positively and negatively charged solutions, resulting in the gradual buildup of functional layers through electrostatic interactions, hydrogen bonding, or covalent bonding [280]. LbL coatings can incorporate bioactive molecules such as growth factors, enzymes, antimicrobial agents, or nanoparticles, thereby imparting multifunctional properties to microfiber scaffolds [258]. Because the process occurs under mild conditions, it is particularly suitable for loading sensitive biomolecules without compromising their biological activity. Consequently, LbL functionalization has been widely explored to enhance cell adhesion, control drug release, and introduce antibacterial or immunomodulatory properties in microfiber-based biomedical devices [281].

Thus, these functionalization techniques offer a powerful toolkit for tuning the surface and interface properties of microfibers. By selecting and combining these methods, it is possible to endow microfibers with antibacterial, anti-inflammatory, osteoinductive, conductive, or sensing capabilities. The compatibility of these techniques with different fiber materials and structures, whether porous, hollow, aligned, or core-shell, makes them adaptable across a wide range of biomedical applications, from wound care and implants to wearable sensors and organ scaffolds.

6. 3D Assemblies

Three-dimensional (3D) assemblies of microfibers represent a critical structural advancement beyond individual fibers or simple 2D mats, enabling hierarchical architectures that better recapitulate native tissue organization. By organizing microfibers into nonwoven meshes, woven constructs, or precisely patterned 3D frameworks, it is possible to tailor porosity, mechanical anisotropy, interconnectivity, and cell-matrix interactions at multiple length scales. Such assemblies bridge the gap between microscale fiber engineering and macroscale tissue constructs, offering improved structural stability and functional performance.

Nonwoven microfiber meshes are the most widely used 3D assemblies and are typically produced through electrospinning, rotary jet spinning, or air-blowing techniques [11,282,283]. In these systems, fibers are deposited randomly or semi-randomly to form an interconnected network without a defined weaving pattern. The resulting architecture is highly porous, lightweight, and ECM-mimetic, closely resembling the fibrillar structure of natural connective tissues. The key advantages of nonwoven meshes include high surface area, tunable pore size distribution, and ease of fabrication at large scale. Porosity and thickness can be controlled by adjusting spinning time, collector distance, humidity, and fiber diameter [45]. However, conventional electrospun nonwoven mats often suffer from limited cell infiltration due to small pore sizes. To overcome this, strategies such as multilayer stacking, incorporation of sacrificial porogens, gas foaming, or combining micro- and nanofibers have been employed to create thicker, highly porous 3D constructs [284]. Additionally, non-woven meshes can be thermally bonded or chemically crosslinked to improve mechanical stability and structural durability under physiological loading [22,285].

Woven microfiber meshes introduce a higher level of structural organization by interlacing fibers in defined patterns (e.g., plain weave, twill, satin) [286,287]. Unlike nonwoven constructs, woven assemblies provide predictable mechanical behaviour, enhanced tensile strength, and improved load-bearing capacity due to ordered fiber interconnections. Woven architectures allow precise control over pore geometry, anisotropy, and directional stiffness. Fabrication of woven microfiber scaffolds may involve many different techniques such as micro-weaving, textile braiding, knitting, and 3D weaving [288,289]. The interlaced structure enhances resistance to tearing and delamination while maintaining interconnected porosity for cell migration and nutrient diffusion. Moreover, woven scaffolds can be engineered with gradient stiffness by varying fiber density or material composition, enabling the recreation of complex tissue interfaces. However, fabrication complexity and limited flexibility compared to nonwoven meshes can be challenges.

3D patterned meshes represent the most advanced category of microfiber assemblies, where fibers are deposited or organized in predefined spatial geometries to create architecturally precise scaffolds. These structures are typically fabricated using MEW, 3D printing, direct ink writing (DIW), or programmable textile engineering [156,157]. Unlike conventional nonwoven or woven meshes, 3D patterned constructs allow micron-level control over fiber spacing, orientation, stacking sequence, and hierarchical layering [68]. This approach enables the creation of lattice, hexagonal, honeycomb, gradient, or biomimetic patterns tailored to specific tissue requirements [163,290]. Mechanical properties such as stiffness, elasticity, and anisotropy can be finely tuned by adjusting fiber diameter, inter-fiber spacing, and stacking angle. Moreover, pore size can be precisely controlled to enhance cell infiltration,

vascularization, and tissue integration. Multi-material deposition further allows incorporation of bioactive or conductive fibers within specific regions, creating functionally graded scaffolds. Compared to nonwoven and woven systems, 3D patterned assemblies offer superior reproducibility, customization, and integration with digital design platforms [171]. However, scalability and manufacturing speed remain ongoing challenges for widespread clinical translation.

In summary, 3D microfiber assemblies whether nonwoven, woven, or precisely patterned, provide a versatile framework for translating microscale fiber engineering into functional tissue-scale constructs. The strategic selection and combination of these assembly approaches allow microfiber-based systems to address diverse biomedical requirements, ranging from soft tissue repair to mechanically demanding regenerative therapies and advanced bioengineered implants.

7. Biomedical Applications

Microfiber-based systems have demonstrated remarkable versatility across a broad spectrum of biomedical applications, owing to their tunable architecture, surface functionality, mechanical adaptability, and capacity for bioactive integration. In this section, the applications are organized to reflect a progression based on the increasing structural and functional complexity of target tissues, as well as the expanding technological demand. The discussion begins with wound healing, representing surface-level tissue repair, where microfibers primarily act as protective and ECM-mimicking scaffolds. It then advances to bone and muscle regeneration, which require enhanced mechanical strength, and structural anisotropy, followed by nerve and vascular regeneration, where guidance cues and bioelectrical or tubular architectures become essential. Finally, the scope extends beyond regenerative scaffolding to multifunctional biomedical interfaces, including biosensing and diagnostics, and therapeutic systems for cancer treatment. This structured progression highlights how microfiber technologies evolve from passive structural supports to dynamic, smart, and clinically translatable platforms capable of addressing increasingly complex biomedical challenges.

7.1. Wound Healing

Wound healing is a complex, dynamic biological process involving hemostasis, inflammation, proliferation, and remodeling phases [11,291,292]. Effective wound care materials must therefore protect the wound site, manage exudate, prevent infection, and promote tissue regeneration [293]. Microfiber-based scaffolds, due to their high surface area, porosity, mechanical flexibility, and tunable architecture, are increasingly being explored as advanced wound dressings. These materials can mimic the structure of the ECM, support cell migration and proliferation, and deliver therapeutic agents in a controlled manner to accelerate healing [294].

Electrospun microfibers are among the most widely used for wound healing applications, primarily because they can form nonwoven mats with closely resembling native skin ECM [295]. Their high porosity ensures gas exchange while maintaining a moist environment that is critical for re-epithelialization. Additionally, the interconnected pores facilitate nutrient transport and cell infiltration, while the tunable mechanical properties allow for conformity to irregular wound geometries. Microfibers for wound healing are often functionalized with antibacterial, anti-inflammatory, or regenerative agents to enhance therapeutic outcomes [143]. Antibacterial functionalization is particularly important to prevent infection, a common complication in chronic wounds. This can be achieved by directly incorporating silver compounds, silver nanoparticles, zinc oxide nanoparticles, magnesium oxide nanoparticles, antibiotics, or antimicrobial peptides into the fiber matrix via above-mentioned functionalization strategies [32,296]. Anti-inflammatory drugs such as curcumin or corticosteroids can also be loaded into microfibers for sustained release, reducing prolonged inflammation and promoting timely progression to the proliferative phase [206,294]. Another promising approach involves bioactive molecule or growth factor incorporation, such as vascular endothelial growth factor (VEGF), epidermal growth factor (EGF), platelet-derived growth factor (PDGF), and basic fibroblast growth factor (bFGF), to stimulate angiogenesis and cellular proliferation [296,297]. Recent studies have also investigated stimuli-responsive microfibers as intelligent wound-healing systems. These systems, which respond to changes in temperature, pH, or moisture, can release therapeutic agents in a controlled, on-demand manner or dynamically alter their structure to adapt to the wound microenvironment [32,295,298]. Microfibers also support skin tissue regeneration by guiding cell alignment, supporting ECM deposition, and modulating the wound microenvironment [299]. Aligned fibers, for example, promote directional migration of keratinocytes and fibroblasts, which can accelerate re-epithelialization [300,301]. In deeper wounds, microfiber scaffolds serve as dermal substitutes, supporting angiogenesis and integration with surrounding tissue. These scaffolds can be fabricated with multilayered structures to mimic the epidermis and dermis, with different porosity, degradation rates, and bioactive contents in each layer. *In vivo* studies have shown

that microfiber-based wound dressings can significantly enhance the rate and quality of wound closure, reduce inflammation, and promote collagen deposition and neovascularization [302,303]. Some commercial products based on electrospun microfibers have already entered clinical use, highlighting their translational impact to the patients [304].

In addition, hydrogel-forming microfiber mats are gaining traction due to their superior hydration capacity and soft tissue conformity [235]. These systems combine the benefits of fibrous structure with hydrogel swelling and drug release properties, making them especially suitable for treating burn wounds and diabetic ulcers. These hydrogel systems can accelerate wound closure, reduce scarring, and enhance epithelialization. Recent research efforts increasingly emphasize precision fabrication techniques and the utilization of the materials' intrinsic biological activity to enhance therapeutic performance. Shen et al. demonstrated the utility of microfluidic spinning to create an injectable "Fibro-Gel", an all-aqueous network of entangled polyethylene glycol diacrylate (PEGDA) microfibers (Figure 4A) [305]. This injectable system allows for minimally invasive application to irregularly shaped wounds and provides a key mechanism for accelerating wound closure and vascularization *in vivo* through the tunable and sequential release of distinct therapeutic agents, such as antibiotics and growth factors. Similarly, using a one-step microfluidic spinning technique, Wang et al. developed porous hydrogel microfibers assembled from prolamins (Figure 4B) [235]. They showcased that the porosity and morphology of these microfibers could be precisely tailored, enabling them to serve as flexible delivery vehicles for actives like bacitracin and VEGF, ultimately displaying superior *in vivo* capability in treating diabetic wounds. Expanding on microfiber complexity, Yu et al. reported the use of coaxial capillary microfluidic spinning to create sophisticated core-shell microfibers with an alginate shell and a core containing copper- or zinc-vitamin framework (Figure 4C) [306]. The controlled release of vitamins and metal ions from this system provided combined antibiosis and antioxidation for accelerated tissue healing.

Beyond drug delivery, microfibers are being engineered for active therapy and diagnosis. Jia et al. demonstrated a significant leap by fabricating ultralong conductive silk microfibers (mSFs) via a bioinspired coating of polydopamine (PDA) and Poly(3,4-ethylenedioxythiophene) (PEDOT) (Figure 4D) [206]. This resulted in a flexible patch that acts as a conformable bioelectronic for monitoring physiological signals. Importantly, they showed the patch's active therapeutic role in chronic diabetic wound healing, where the conductive mSFs' intrinsic anti-oxidative activity actively reduced inflammation and regulated oxidative stress. For straightforward, real-time monitoring, Ha et al. created a multifunctional electrospun bilayer-dressing patch (Figure 4E) [307]. The protective layer of this patch incorporated curcumin as a sensing agent, enabling a visible colour change (pH 6–9) for non-invasive, real-time monitoring of wound status, while also providing enhanced antimicrobial protection.

Furthermore, researchers have addressed infection and structural integrity using probiotic therapy [308]. However, probiotic therapy has large obstacle and potential biosafety risks for proper application. Lu et al. reported an effective, probiotic-free strategy for promoting infected wound healing by regulating the wound flora balance (Figure 4F) [271]. They engineered a poly(4-methyl-1-pentene) (PMP) microfiber membrane that exhibited strong bacterial adhesion, allowing for the efficient removal of pathogenic bacteria through sdressing changes to maintain a low-concentration, pro-healing environment. Moreover, to address the low structural integrity issues, Xu et al. reported a blended membrane composed of chitosan (CS) and chemically hydrolyzed silk microfibers (mSFs) (Figure 4G) [309]. Their findings demonstrated that incorporating mSFs substantially enhanced the membrane's mechanical strength and decreased its swelling ratio, which in turn improved wound healing performance, as evidenced by increased epithelialization and greater collagen deposition.

In summary, microfiber scaffolds offer a multifunctional platform for wound healing by integrating mechanical protection, moisture regulation, antimicrobial activity, and therapeutic delivery into a single system. With continued advancements in fabrication, functionalization, and clinical validation, microfiber-based wound dressings are poised to become a next-generation solution for managing acute and chronic wounds.

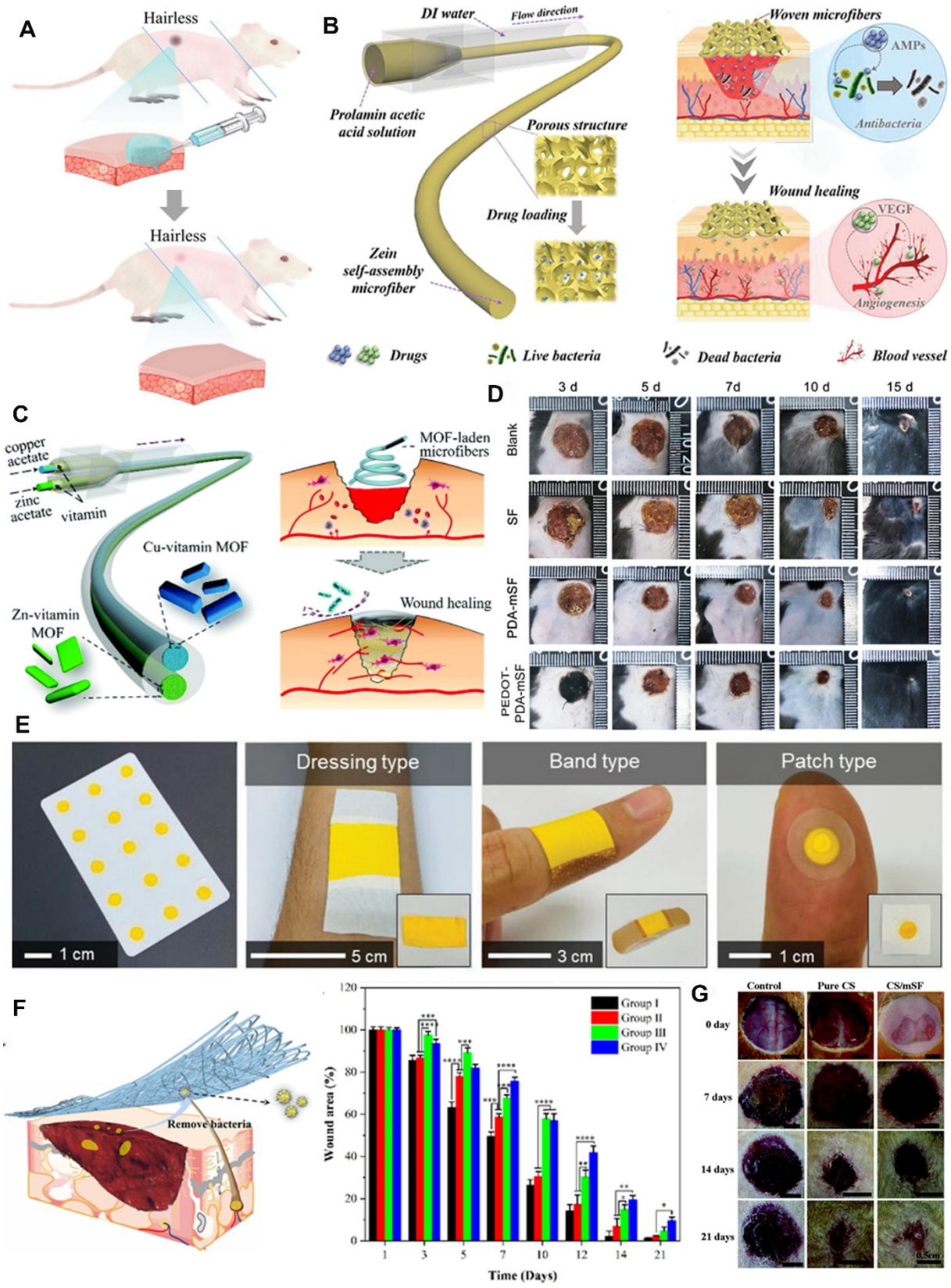

Figure 4. Applications in wound healing. (**A**) Schematic of the mice excision skin model where the mice were dressed with the PEGDA fibro-gel. Reproduced with permission [305]. Copyright 2023, Wiley-VCH. (**B**) Schematic diagram of the prolamins-assembled porous hydrogel microfibers from microfluidic spinning technology for wound healing. Reproduced with permission [235]. Copyright 2024, Wiley-VCH. (**C**) Schematic illustration of the formation of vitamin MOF-laden microfibers using a microfluidic spinning approach and their application in the wound healing. Reproduced with permission [306]. Copyright 2018, RSC Publishing. (**D**) PEDOT-PDA-silk microfiber patch accelerated dermal wound healing in diabetic mice. Reproduced with permission [206]. Copyright, Wiley-VCH. (**E**) The multifunctional wound dressing patch containing dexpanthenol,

hyaluronic acid, and gelatin (DHG), curcumin and polycaprolactone (C-PCL). Various types of wound treatments (dressings, bands, and patches) suitable for the size of the lesion can be applied. Reproduced with permission [307]. Copyright 2023, Wiley-VCH. (**F**) Schematic illustrating the regulation of wound flora balance using the poly(4-methyl-1-pentene) microfiber membrane. Right side bar graph shows wound area after therapy *in vivo*. (* $p < 0.05$, ** $p < 0.01$, *** $p < 0.001$, **** $p < 0.0001$). Reproduced with permission [291]. Copyright 2022, ACS Publications. (**G**) Digital images of macroscopic wound condition depicting wound size at different durations. Wound size is compared at different days with control (covered with vaseline cream), pure chitosan (CS) membrane and CS/mSF (80% CS/mSF blended membrane). Reproduced with permission [309]. Copyright 2015, Wiley-VCH.

7.2. Bone Repair

Bone tissue engineering aims to restore, repair, or replace damaged bone by creating biomimetic scaffolds that provide structural support and promote cellular activity essential for osteogenesis [310]. Microfiber-based scaffolds have emerged as highly promising platforms for bone regeneration due to their ability to mimic the hierarchical structure of native bone ECM, guide cell behavior, and deliver bioactive cues in a spatially and temporally controlled manner [181,311]. Their tunable mechanical properties, degradability, and functionalization potential make them excellent candidates for load-bearing and non-load-bearing bone defects. The mechanical integrity of microfiber scaffolds is essential in bone applications, especially for supporting load-bearing sites. Aligned or grid-patterned fiber scaffolds produced via melt electrowriting or 3D printing offer high compressive strength and structural anisotropy, which mimic the architecture of trabecular bone [312]. These features not only support mechanical loads but also direct cell alignment and matrix deposition in the direction of applied stress. To enhance osteoinductive and osteoconductive properties, microfiber scaffolds are often functionalized with bioactive molecules or inorganic fillers [87,313]. These fillers can be blended into the polymer prior to spinning or deposited via electrospray coating, sputtering, or dip coating [48,314].

Moreover, microfiber scaffolds can be biofunctionalized with growth factors such as bone morphogenetic protein-2 (BMP-2), VEGF, or transforming growth factor-β (TGF-β) to stimulate osteogenic differentiation, angiogenesis, and matrix remodeling [46,311]. Controlled release of these factors from core-shell or porous microfibers provides a sustained stimulatory environment that mimics natural bone healing processes. Scaffold surfaces can also be modified with RGD peptides or collagen to enhance osteoblast attachment and proliferation [46,227]. Another emerging strategy involves the use of electroactive microfiber scaffolds, incorporating piezoelectric materials such as PVDF or BTO nanoparticles [315,316]. These materials generate electrical signals under mechanical stress, mimicking the endogenous bioelectric cues that naturally stimulate bone regeneration during physical activity. Such scaffolds have shown promise in promoting osteogenic gene expression and enhancing mineral deposition, particularly under dynamic loading conditions. Depending on the design, these scaffolds can degrade over time in synchrony with new tissue formation, eliminating the need for surgical removal.

Despite the progress, challenges remain in translating microfiber scaffolds for clinical bone regeneration. These include achieving optimal load-bearing capacity, matching degradation kinetics to tissue regeneration rates, scaling up fabrication processes, and ensuring regulatory compliance. However, continued advancements in material science, additive manufacturing, and functionalization technologies are rapidly addressing these issues. The current research focuses intensely on developing composite scaffolds that not only provide mechanical support but also actively induce osteogenesis and angiogenesis through smart material design and tailored drug/ion delivery. Zhou et al. reported the formulation of an injectable, composite hydrogel system for the minimally invasive treatment of osteonecrosis (Figure 5A) [313]. This scaffold comprised an alginate (SA)/tricalcium phosphate (β-TCP) hydrogel matrix reinforced with P34HB/MgO+PEG coaxial electrospun microfibers. They demonstrated that by varying the microfiber concentration, the composite's injectability and mechanical strength could be optimized, while the controlled release of magnesium ions (Mg^{2+}) from the MgO-laden core promoted osteogenic differentiation and bone repair. Wu et al. employed dual-nozzle hybrid electrospinning to address the insufficient mechanical properties and biocompatibility of single-polymer systems (Figure 5B) [48]. They fabricated composite scaffolds using a blend of PVA, polyhydroxybutyrate (PHB), and multiwalled CNTs (MWCNTs). This strategy resulted in microfibers with enhanced mechanical properties and improved surface characteristics that significantly promoted the osteogenic differentiation of stem cells *in vitro* and accelerated bone regeneration *in vivo*.

Several studies have aimed to design bone scaffolds that better replicate the natural mineralized structure of bone in order to improve osteogenic activity. In this context, researchers have developed biomineralized and dynamic scaffold systems that combine organic matrices with calcium-based mineral components. Shi et al. developed a self-healing silk fibroin (SF)-based hydrogel for bone regeneration, utilizing a dynamic metal-ligand

coordination chemistry approach (Figure 5C) [311]. Their system involved reversible crosslinking between silk fibroin microfibers (mSF), which were biomineralized with calcium phosphate, and a polysaccharide binder. This dually crosslinked (DC) hydrogel exhibited shear-thinning and autonomous self-healing properties, allowing it to conform perfectly to irregularly shaped defects. They successfully showed that this scaffold could accelerate bone regeneration in cranial critical size defects without the need for additional exogenous morphogens. Similarly, Wei et al. created a mechanically enhanced biodegradable scaffold based on pure silk fibroin microfibers and mineralized collagen (Figure 5D) [212]. This composite scaffold significantly improved mechanical properties and demonstrated superior efficacy in repairing bone defects in the distal femur of rats.

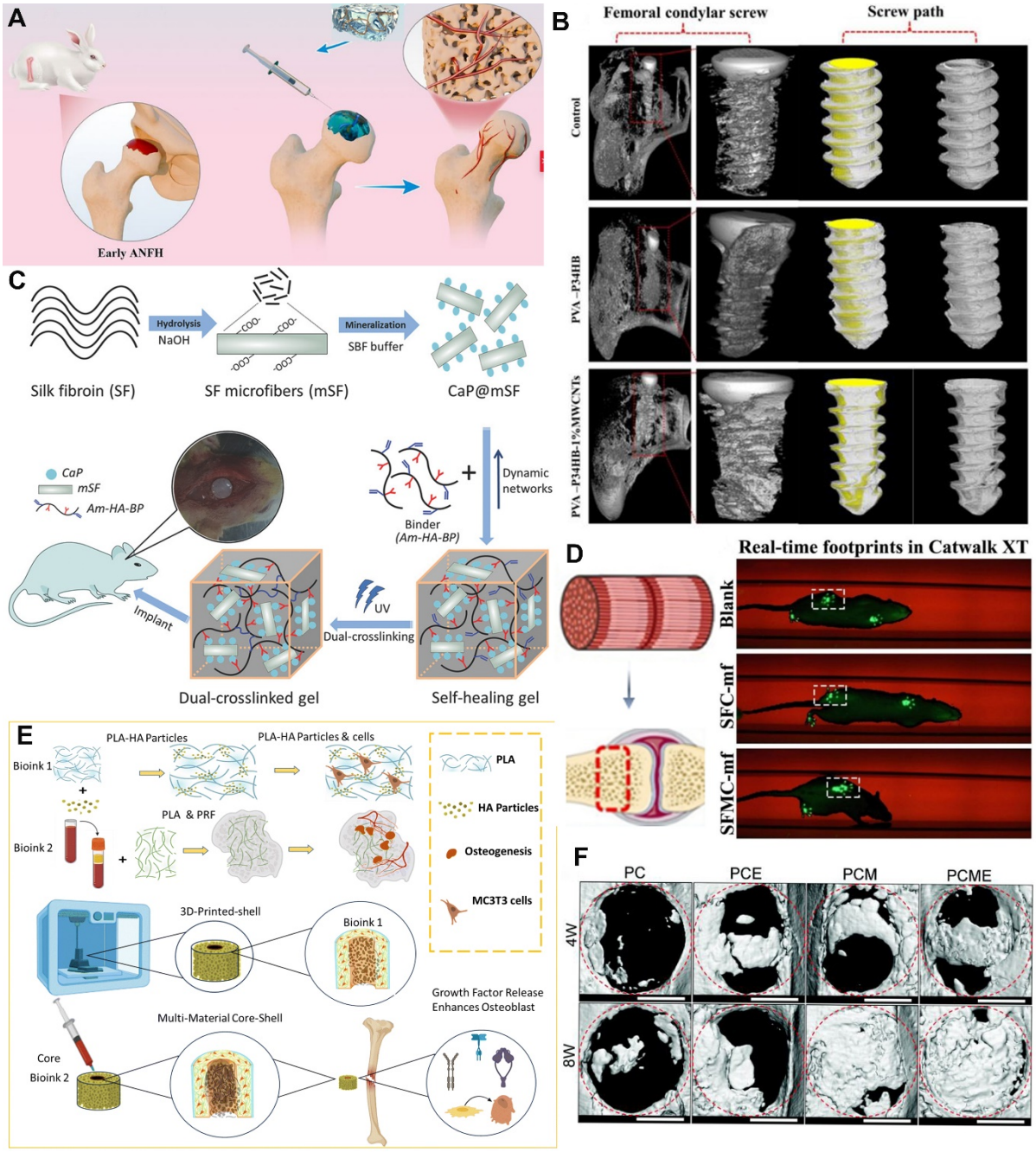

Figure 5. Applications in bone regeneration. (**A**) Schematic of injectable alginate/β-TCP hydrogel reinforced with coaxial electrospun P34HB/MgO+PEG microfibers for treating early-stage avascular necrosis of the femoral head (ANFH) in a rabbit model. Reproduced with permission [313]. Copyright 2025, Wiley-VCH. (**B**) Micro-CT imaging of rabbit femoral condyles at 8 weeks post-implantation of PVA-P34HB based microfiber scaffolds, indicating new bone formation along the screw-bone interface. Reproduced with permission [48]. Copyright 2025, Elsevier. (**C**) Schematic illustrating the fabrication of mineralized silk fibroin microfiber based hydrogels for repairing rat cranial bone defects. Reproduced with permission [311]. Copyright 2017, Wiley-VCH. (**D**) Implantation of mechanically enhanced biodegradable silk fibroin microfiber scaffold in rat femoral bone defects

and thereafter gait analysis demonstrating mechanical and functional recovery. Reproduced with permission [212]. Copyright 2024, Elsevier. (**E**) Schematic illustration of bioink preparation and the fabrication method of multi-material bioactive bone substitutes. Reproduced with permission [213]. Copyright 2024, RSC Publishing. (**F**) Illustration depicting radiographic reconstruction of cranial bone defects at 4- and 8-weeks after microfiber scaffolds implantation, highlighting new bone growth at surgery sites. Reproduced with permission [46]. Copyright 2019, RSC Publishing.

Furthermore, recent studies have explored the integration of microfibers with advanced biofabrication strategies to improve the structural and biological performance of bone scaffolds. Moghimi et al. reported the development of short microfiber-reinforced printable hydrogels for personalized bone repair (Figure 5E) [213]. By employing 3D bioprinting, they fabricated a core-shell bone graft from a hybrid composite of hydroxyapatite-coated poly(lactic acid) (PLA) fibers embedded within a methacryloyl gelatin (GelMA)/alginate hydrogel matrix. This construct was designed to incorporate platelet-rich fibrin (PRF) to enhance the biological cues for regeneration. Focusing on cell recruitment and differentiation, Chi et al. constructed a dually optimized polycaprolactone (PCL)/collagen I microfiber scaffold using coaxial electrospinning (Figure 5F) [46]. This scaffold was specifically engineered to capture bone marrow stem cells (BMSCs) and deliver BMP2-derived peptides from the core. Their work demonstrated that this design promoted the osteogenic differentiation of the enriched stem cells, ultimately leading to synergistic bone regeneration.

In conclusion, microfiber-based scaffolds offer a customizable, multifunctional, and biomimetic approach to bone regeneration. By tuning fiber structure, surface chemistry, mechanical properties, and biological cues, these systems can effectively guide bone repair and integration, offering a promising alternative to traditional grafts and metallic implants.

7.3. Muscle Regeneration

Skeletal muscle has a remarkable regenerative capacity following minor injuries, however, in cases of severe trauma, volumetric muscle loss (VML), or degenerative diseases such as muscular dystrophy, the endogenous repair mechanisms are insufficient to restore full structure and function [282,317–319]. To address this clinical challenge, microfiber-based scaffolds have emerged as one of promising platforms for muscle tissue engineering due to their ability to replicate the fibrous architecture of native muscle ECM, support cellular organization, and deliver biological or electrical cues to guide regeneration [320].

The structural alignment of muscle fibers plays a fundamental role in skeletal muscle regeneration because the native muscle tissue exhibits a highly organized, anisotropic architecture that enables efficient force generation and transmission [297]. Therefore, biomaterial scaffolds designed for muscle repair must replicate this aligned microenvironment to support proper myoblast orientation and maturation. Microfibers fabricated using techniques such as electrospinning, microfluidics, and 3D printing can be engineered with precise orientation to promote myoblast alignment, fusion into multinucleated myotubes, and anisotropic tissue formation [107,321]. Aligned microfiber scaffolds provide topographical cues that guide cell elongation and cytoskeletal organization, closely mimicking the architecture of native skeletal muscle [317,319]. In addition to structural guidance, muscle tissue relies on electrical signaling to regulate contraction and cellular function, which has motivated the development of conductive microfiber-based scaffolds to better replicate this physiological environment. Incorporating conductive materials such as polypyrrole (PPy), PANI, CNTs, or graphene into fiber matrices enables scaffolds to transmit bioelectrical signals, enhance myogenic differentiation, and improve muscle fiber contractility [322]. These scaffolds can be used with external electrical stimulation setups or integrated with wireless bioelectronics for smart, on-demand stimulation [297]. Microfibrous scaffolds with dynamic mechanical properties or shape-memory behavior can be designed to deliver periodic stretching, which enhances cytoskeletal organization and mimics muscle loading during movement [323,324]. Microfiber scaffolds have been also seeded with myoblasts, MSCs, and induced pluripotent stem cell-derived myogenic progenitors (iPSC-MPs), often in combination with bioactive fibers, to support muscle formation [319,325].

Building on these design principles, several studies have developed biomimetic microfiber-based scaffolds that recreate the hierarchical microfibrillar structure of skeletal muscle. Kim et al. reported a 3D-printed biomimetic scaffold that simulates the microfibril structure of muscle (Figure 6A) [326]. They employed a microfibrillation/leaching process of poly(vinyl alcohol) (PVA) from a PVA/PCL mixture to create a micropatterned PCL microfiber strut. This structure, supplemented with Type-I collagen, successfully promoted C2C12 myoblast proliferation and myogenic differentiation in vitro, demonstrating its potential as a platform for realistic 3D muscle tissue modeling. Similarly, for complex tissue structures, Chen et al. developed a flexible, mechanically robust, and well-aligned bi-layered tubular microfiber scaffold based on silk protein (Figure 6B) [327].

This design specifically mimicked the native human intestinal smooth muscle structure, supporting the alignment and elongation of primary human intestinal smooth muscle cells in two orthogonal layers, which is essential for achieving functional innervation in engineered intestinal smooth muscle tissue.

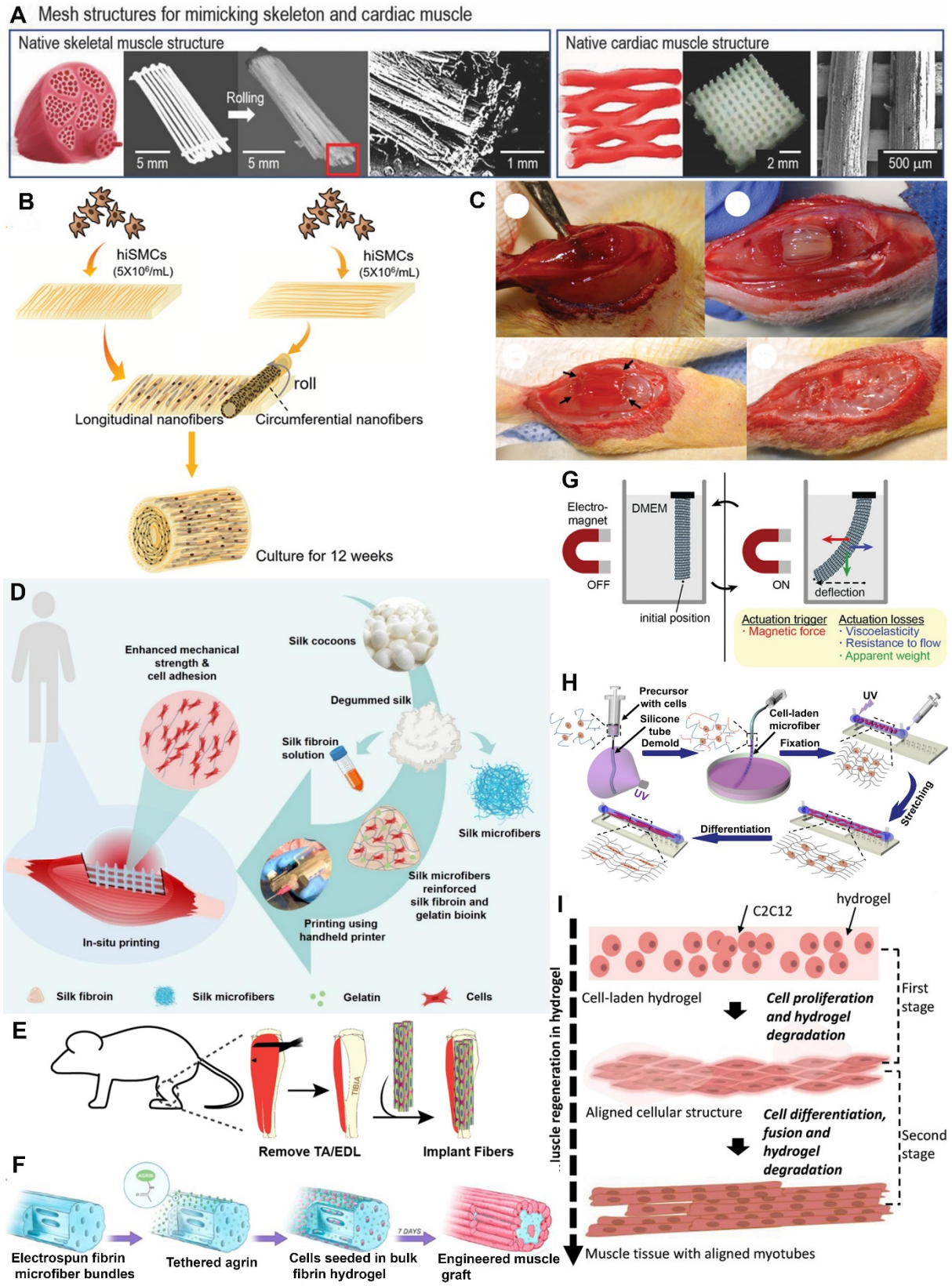

Figure 6. Applications in muscle regeneration and engineering muscle constructs. (**A**) Skeletal and cardiac muscles mimicked by rolling aligned microfiber membranes and 3D printing. Reproduced with permission [326]. Copyright 2018, Wiley-VCH. (**B**) Schematic illustrating a cell seeding strategy for making hiSMC-derived 3D intestinal smooth muscle constructs. Reproduced with permission [327]. Copyright 2020, Wiley-VCH. (**C**) Defect creation,

initial placement of a collagen fiber implant, suture placement for implant attachment, and fascia replacement during functional recovery in a rodent VML model. Reproduced with permission [325]. Copyright 2022, Wiley-VCH. (**D**) Schematic representation of silk fibroin solution and silk microfibers preparation from silk cocoons and their application as a bioink for in situ 3D bioprinting using custom-made handheld 3D printer for VML repair. Reproduced with permission [318]. Copyright 2025, Elsevier. (**E**) Schematic illustrating fibrin miccrofiber implantation into a murine VML defect model. Reproduced with permission [319]. Copyright 2018, Sage Publications. (**F**) Schematic illustrating engineered muscle graft generated by agrin tethering and cell seeding on electrospun fibrin microfiber bundles. Reproduced with permission [282]. Copyright 2020, Elsevier. (**G**) Schematic showing magneto-mechanical stimulation of magneto-active skeletal muscle constructs reinforced with magneto-active microfiber scaffolds. Reproduced with permission [156]. Copyright 2024, Wiley-VCH. (**H**) Schematic representation of the fabrication process, the fixation, and the uniaxial stretching of C2C12 myoblasts laden microfibers. Cells within microfibers are elongated with the application of uniaxial stretching during culture and the differentiation of myoblasts is further promoted. Reproduced with permission [320]. Copyright 2020, ACS Publications. (**I**) Schematic showing the skeletal muscle regeneration within the microfiber based 3D hydrogel. Reproduced with permission [328]. Copyright 2024, Wiley-VCH.

While such biomimetic mirofiber scaffolds are effective for reproducing structural features of muscle tissue in vitro, translation toward therapy requires fabrication platforms capable of generating larger, cellularized implants with robust mechanical integrity and reproducible organization. Addressing this need, Christensen et al. invented an advanced biomanufacturing platform called assembled cell-decorated collagen (AC-DC) bioprinting (Figure 6C) [325]. This platform rapidly creates living biomaterial implants using strong, microfluidic wet-extruded collagen microfibers and clinically relevant cells. They showed that AC-DC implants approximate the strength and stiffness of native musculoskeletal tissue and, critically, promoted functional recovery in a critically sized muscle injury model *in vivo*, demonstrating their therapeutic potential for VML. For customized, in situ fabrication, Kamaraj et al. proposed a bioink composed of silk microfiber-reinforced silk fibroin (SF) hydrogel (Figure 6D) [318]. They validated the use of a custom-made handheld 3D printer for in situ printing of these fiber-reinforced scaffolds, which were predesigned to provide the structural support and fiber alignment necessary to promote muscle regeneration for VML treatment.

Beyond fabricating structurally organized implants, another important strategy is to combine aligned microfiber scaffolds with stem cells that may enhance regeneration through direct differentiation or paracrine support. In this regard, Gilbert-Honick et al. assessed the regenerative potential of human adipose-derived stem cells (ASCs) seeded onto electrospun uniaxially aligned fibrin hydrogel microfiber bundles (Figure 6E) [319]. Although the ASCs exhibited alignment and elongation in vitro, they failed to fully recapitulate myotube characteristics. However, when implanted *in vivo* in a VML model, the ASC-seeded microfiber bundles enabled moderate muscle reconstruction. In a separate study, Gilbert-Honick et al. also investigated the delivery of the ECM protein agrin from an engineered scaffold (Figure 6F) [282]. They found that agrin, delivered from a scaffold, significantly increased the presence of regenerated neuromuscular junctions (NMJs) and promoted functional recovery following VML.

Furthermore, in addition to static structural design, recent strategies incorporate dynamic, stimuli-responsive features to better mimic the active mechanical environment of skeletal muscle. For example, Cedillo-Servin et al. reported the rational design and fabrication of magneto-active microfiber meshes using melt electrowriting (MEW) of a magnetic PCL-based composite (Figure 6G) [156]. This solvent-free MEW process allowed for the creation of skeletal muscle-inspired hexagonal scaffolds whose zonal distribution of magnetic material enabled out-of-plane reversible deformation triggered by external magnetic fields, providing a platform for remote stimulation and guided organization of 3D muscle models. Chen et al. demonstrated that the uniaxial stretching of cell-laden microfibers, generated via a silicone-tube-based method, effectively promoted the alignment of C2C12 myoblasts and subsequent myofiber formation *in vitro* (Figure 6H) [320]. To efficiently identify optimal culture conditions, Chen et al. introduced a high-throughput method using microfluidic spinning to produce skeletal muscle microphysiological models (microPMs) (Figure 6I) [328]. They developed a micromanipulation-actuated large-scale screening technique to assess the viscoelasticity and contractile force of these microPMs, establishing screening criteria that integrate these parameters to examine the effects of various culture conditions on skeletal muscle regeneration.

In summary, microfiber scaffolds, when rationally designed for anisotropy, mechanical compliance, electrical functionality, and biochemical delivery, offer a comprehensive toolkit for muscle regeneration. Future efforts should emphasize scalable manufacturing, integrated vascular and neural reconstruction, and closed-loop stimulation strategies to translate engineered muscle constructs into clinically practical therapies for VML and other severe muscle pathologies.

7.4. Nerve Regeneration

Peripheral nerve injuries (PNI) and neurodegenerative conditions often result in significant loss of sensory and motor function [329,330]. Although peripheral nerves have some innate regenerative capacity, the outcomes are often suboptimal in cases of large-gap injuries or complex trauma. Autografts, the current clinical gold standard, are limited by donor site morbidity and availability. Consequently, microfiber-based scaffolds have attracted increasing attention as promising alternatives for nerve regeneration, as their fibrous architecture closely resembles the native nerve ECM and can provide physical guidance for axonal extension while also enabling the incorporation of biochemical and biophysical cues that support neural repair [331].

The application of smart polymer microfibers is rapidly advancing the field of neural tissue engineering, particularly for bridging large-gap PNI and addressing spinal cord injury (SCI). The effective design of these scaffolds, which focuses on mimicking the native neural microenvironment by controlling physical, chemical, and electrical properties, is crucial for guiding successful axon regeneration and functional recovery. In this regard, Yu et al. developed the biomimicking microfibers with controllable core-shell structures generated through capillary microfluidic devices (Figure 7A) [200]. Their approach included integrating these microfibers into a multitrack nerve-on-a-chip system, allowing for the systematic *in vitro* assessment of nerve fiber formation before confirming rapid *in vivo* nerve regeneration and functional recovery in a rat sciatic nerve injury model. To further enhance structural and functional guidance for regenerating axons, Fang et al. designed a hierarchical conductive multiscale filled nerve guidance conduit (MF-NGC) using a combination of electrospinning and 3D printing (Figure 7B) [332]. This multiscale conduit consisted of electrospun PCL/collagen nanofibers forming the outer sheath, aligned PCL microfibers providing anisotropic guidance for axonal growth, and reduced graphene oxide (rGO)/PCL microfibers supplying mechanical stability and electrical conductivity. The hierarchical architecture promoted Schwann cell elongation, neurite extension, and vascular recruitment, while *in vivo* studies demonstrated enhanced axon myelination and improved functional recovery in a rat sciatic nerve defect model.

Further, electrical conductivity has also been incorporated into microfiber scaffolds to regulate neuronal behavior and enhance neural differentiation. Wang et al. fabricated three-dimensional conductive scaffolds from PLCL microfibers using near-field electrostatic printing and followed by coating with rGO (Figure 7C) [281]. They demonstrated the capability of these scaffolds to induce oriented neuronal-like network formation in PC-12 cells and primary mouse hippocampal neurons when coupled with external electrical stimulation, with both the electric field strength and microfiber diameter acting as critical regulatory parameters for neurite outgrowth. Building on this concept of electrically active microfiber scaffolds, Guo et al. further demonstrated a self-powered electrical stimulation platform to enhance neural differentiation using conductive hybrid microfibers composed of PEDOT and rGO (Figure 7D) [9]. In this system, the conductive microfiber scaffold served as both the cellular substrate and the electrical signal transmission medium, while pulsed electrical stimulation was supplied by a triboelectric nanogenerator. This integrated system significantly enhanced the neural differentiation of MScs without the need for additional biochemical factors, highlighting the potential of self-powered electroactive scaffolds for neural regeneration.

The regulatory role of microfibers extends beyond structural and electrical cues to include the modulation of the immune microenvironment. Dong et al. systematically interrogated the topological cues delivered by oriented microfibers, engineering nerve conduits with oriented microfiber cores and random nanofiber sheaths (Figure 8E) [333]. They elucidated a clear cascade where the aligned microfibers facilitated macrophage recruitment and polarization toward a pro-healing M2 phenotype, which consequently promoted Schwann cell migration, myelinization, and axonal extension, leading to pronounced functional improvement in a PNI model. Similarly, Kim et al. developed electrospun nerve guidance conduits (NGCs) integrating milk-derived casein protein (MDP) into aligned PCL and PLGA microfibers (Figure 7F) [334]. Their MDP-AF NGC provided both topographical guidance and chemoattraction from the bioactive protein, synergistically promoting Schwann cell migration, macrophage polarization, and enhanced regeneration of injured sciatic nerves *in vivo*.

Moreover, microfibers have proven essential as carriers for cell-based therapies, particularly for central nervous system injuries. In addressing the challenge of low stem cell survival and uncontrollable migration, Yao et al. fabricated three-dimensional MSCs-laden hydrogel microfibers using a hierarchically aligned fibrin hydrogel system for long-distance SCI repair [335]. The implantation of these cell-laden microfibers significantly enhanced the donor MSCs' neural differentiation, encouraged host neuron migration into the injury gap, and promoted nerve fiber regeneration across the injury site, ultimately improving limb motor function. Furthermore, Kim et al. reported a 3D neurosupportive culture system where astrocytes were cytoprotectively encapsulated within hydrogel based microfibers (Figure 7G) [26]. These microfibers significantly enhanced neuronal circuit generation by accelerating

neurite outgrowth, guiding its directionality, and enhancing synaptic formation, even without direct physical contact between the glial cells and the neurons, providing a cell-based therapeutic platform for injuries such as SCI.

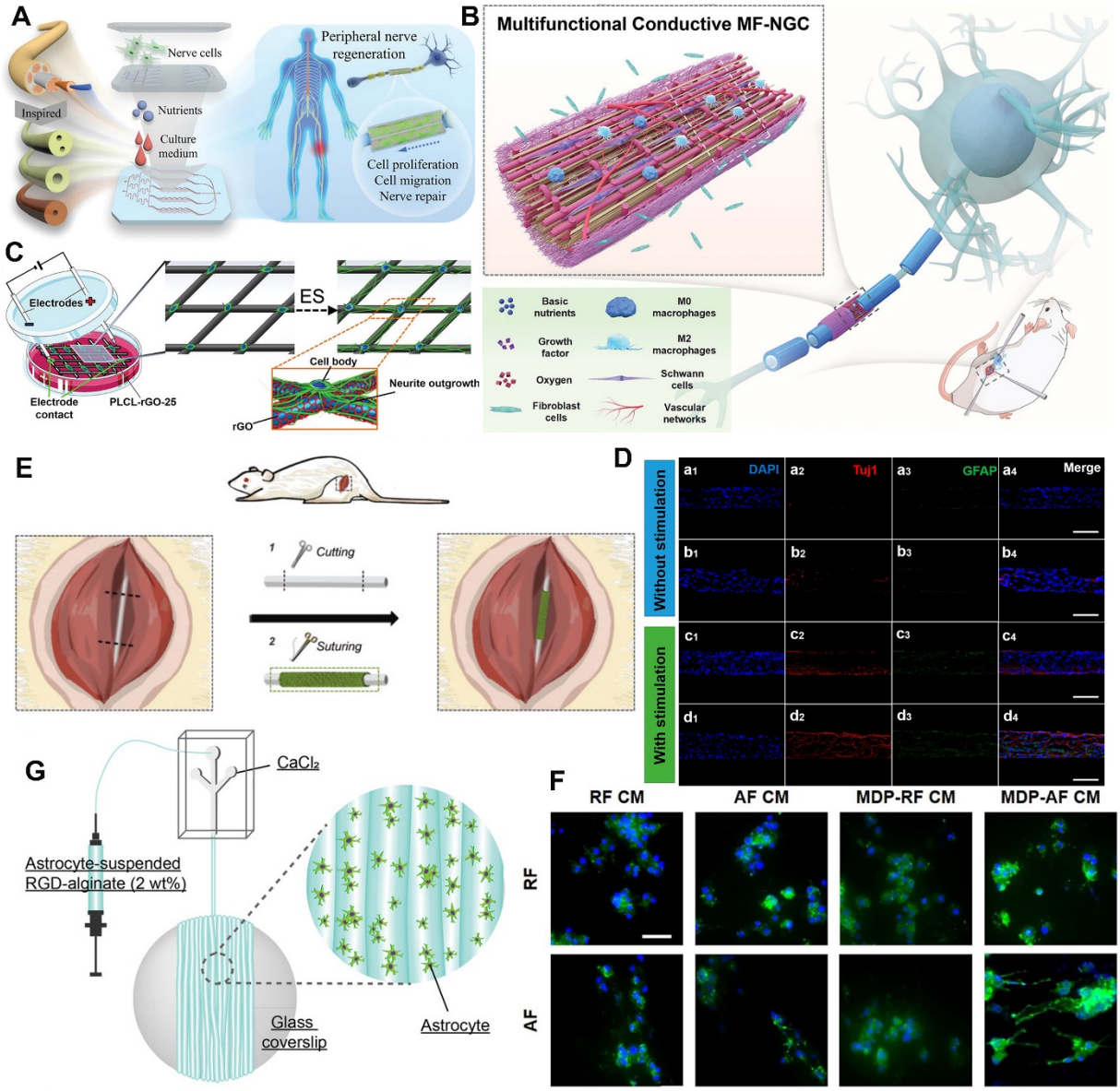

Figure 7. Applications in nerve regeneration. (**A**) Schematic showing nerve-on-a-chip derived biomimicking microfibers and their applications in peripheral nerve generation. Reproduced with permission [200]. Copyright 2023, Wiley-VCH. (**B**) Schematic overview of a multifunctional conductive nerve guidance conduit with hierarchical fibers for PNI treatment. Reproduced with permission [332]. Copyright 2023, Wiley-VCH. (**C**) The culture setup to regulate the neurite outgrowth of PC-12 cells on conductive microfiber patterns under electrical stimulation. Reproduced with permission [281]. Copyright 2020, Wiley-VCH. (**D**) Neural differentiation of mesenchymal stem cells on reduced graphene oxide (rGO) microfibers (**a**,**c**) and rGO-PEDOT hybrid microfibers (**b**,**d**) under triboelectric nanogenerator based electrical stimulation. Reproduced with permission [9]. Copyright 2016, ACS Publications. (**E**) Schematic showing transplanting nerve conduits to the rat sciatic nerve defects. Reproduced with permission [333]. Copyright 2021, Elsevier. (**F**) Fluorescence image of PC12 cells demonstrating higher neurite outgrowth of PC12 cells for aligned microfiber based nerve guidance conduits. Reproduced with permission [334]. Copyright 2025, ACS Publications. (**G**) Schematic illustration of astrocyte encapsulation in the RGD-modified alginate microfibers for enhancing neuronal circuit generation. Reproduced with permission [26]. Copyright 2020, Wiley-VCH.

Microfiber-based platforms offer a biomimetic and highly tunable solution for nerve regeneration. By combining aligned architecture, bioactive molecule delivery, electrical conductivity, and cellular support, these

systems can closely replicate the native neural microenvironment and promote long-distance, functional nerve repair. Continued research integrating multifunctional materials, microelectronics, and gene-delivery approaches will further enhance the efficacy of these systems, paving the way for clinically viable, next-generation neural interfaces and repair devices.

7.5. Vascular Regeneration

Vascular regeneration is critical for restoring blood flow in ischemic tissues, healing wounds, and engineering functional tissues and organs [336,337]. Microfibers have emerged as versatile and promising scaffolding platforms for vascular tissue engineering, owing to their ability to mimic the ECM, support endothelialization, and deliver biochemical cues that promote angiogenesis and vascular remodeling [338]. Their high surface-area-to-volume ratio, tunable porosity, and alignment make them ideal for constructing both microvascular and large-diameter vascular grafts. One of the key challenges in vascular regeneration is preventing thrombosis and intimal hyperplasia, particularly in small-diameter vascular grafts [339,340]. To address this, microfibers can be modified with antithrombotic agents (e.g., heparin, nitric oxide donors) or endothelial cell-attracting peptides to accelerate in situ endothelialization [341]. Additionally, surface coatings or in-fiber incorporation of antioxidants and anti-inflammatory agents (e.g., curcumin, aspirin, ROS-scavenging materials) help modulate the post-implantation inflammatory response and support long-term graft patency [5]. Bioactive microfiber mats have also been used as angiogenic dressings for ischemic wounds or myocardial infarction, supporting local neovascularization [342].

The advancement of polymer microfibers in vascular regeneration is focused on creating sophisticated scaffolds that mimic the native vessel's structure and function, addressing critical challenges like thrombosis, compliance mismatch, and poor endothelialization, especially in small-diameter applications. The challenge of engineering small-diameter vascular grafts necessitates scaffolds that not only match the mechanical compliance of native vessels but also orchestrate the complex biological processes of immunomodulation, cell recruitment, and anti-thrombogenicity. Federici et al. developed a multicomponent vascular graft using MEW technique to produce a tubular scaffold with vascular-mimetic fiber architecture (Figure 8A) [343]. This MEW framework was combined with a lyophilized fibrinogen matrix for tailored degradation, further functionalized with heparin for anti-thrombogenicity, and encased in an outer electrospun layer to mimic the tri-layered structure of the vessel wall and reduce permeability. Further, Wang et al. utilized a bio-inspired 4D printing strategy to design Janus-structured scaffolds capable of programmable multi-step transformations (Figure 8B) [344]. Inspired by the curling behavior of leaves, these scaffolds transition from a flattened 2D construct into a tubular 3D structure upon dehydration, followed by a crucial secondary transformation *in vivo* to adapt to the local intravascular geometry, thus enabling on-demand vascular reconstruction. In parallel, Liu et al. focused on enhancing vascular regeneration by creating immunomodulatory hybrid scaffolds composed of PCL microfibers and human placental ECM nanofibers via co-electrospinning, demonstrating a method to leverage natural ECM components within a mechanically robust synthetic framework while modulating the host immune response (Figure 8C) [339].

In addition to structural design approaches, biofunctionalization has been explored to enhance endogenous regenerative responses. Wang et al. demonstrated improved vascular regeneration by developing anti-Sca-1 antibody-functionalized vascular grafts (Figure 8D) [345]. This surface modification allows the selective capture of endogenous vascular stem/progenitor cells (SPCs), effectively utilizing the host's innate regenerative capacity to improve tissue outcomes. In addition to promoting regenerative cell recruitment, improving hemocompatibility and controlling inflammatory responses are critical for maintaining long-term graft patency. Shi et al. reported an inflammation-responsive PCL/gelatin microfiber scaffold that provided sustained release of both nitric oxide (NO) and heparin (Figure 8E) [341]. This scaffold not only improved blood compatibility but also suppressed the excessive proliferation of smooth muscle cells, thus preventing intimal hyperplasia and promoting desirable endothelialization. For fabricating microscale vascular structures, Wu et al. reported the microfluidic printing of tunable hollow microfibers using a composite bioink comprised of alginate, gelatin methacrylate, and silk fibroin (Figure 8F) [346]. This approach allowed for the rapid seeding and perfusion of human umbilical vein endothelial cells (HUVECs) into the hollow chambers, leading to the formation of vessel-like tissue structures with high cell viability within three days. Further, Sun et al. used magnetic alginate microfibers as scaffolding elements (Figure 8G) [347]. By loading these microfibers with cells and applying a controlled magnetic field, they were able to induce the self-assembly of cells into micro-scale toroidal cellular modules, which can serve as versatile building blocks for the bottom-up construction of complex microvascular-like structures.

In summary, microfiber-based scaffolds provide a versatile platform for vascular regeneration due to their ability to mimic the structural features of native ECM and support endothelialization and tissue integration. Their architecture, material composition, and surface functionalization can be tailored to regulate cellular responses and

vascular remodeling. These advances highlight the potential of microfiber-based systems for next-generation vascular grafts and regenerative vascular therapies.

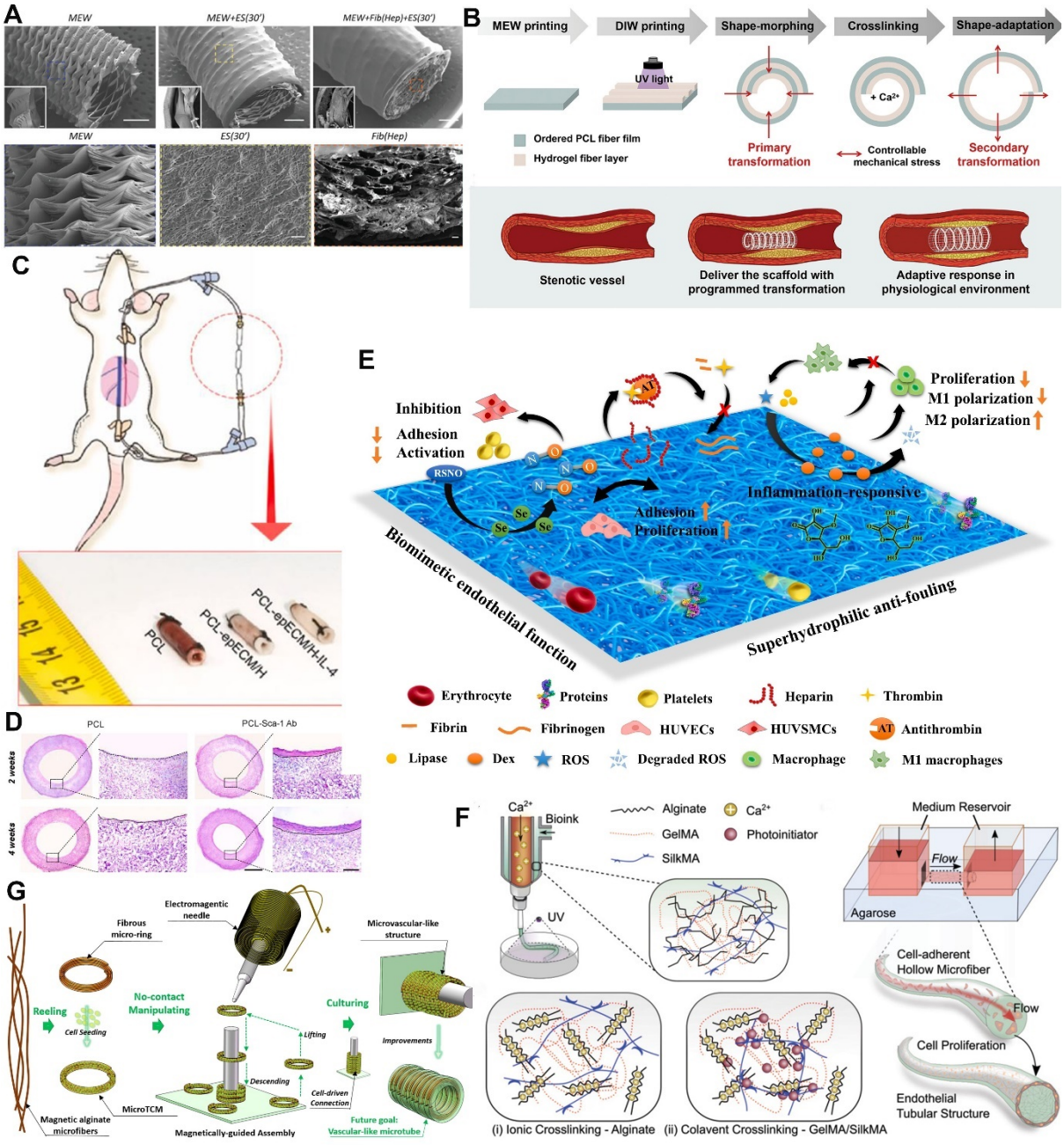

Figure 8. Applications in vascular tissue engineering. (**A**) SEM images of vascular graft. From left to right: MEW frame alone, enclosed in an electrospun PLCL nanofiber layer, and MEW infused with a lyophilized crosslinked fibrinogen ECM covered on the outside with an electrospun PLCL nanofiber layer. Reproduced with permission [343]. Copyright 2024, Wiley-VCH. (**B**) Schematic showing fabrication process, intravascular delivery and *in vivo* shape-adaptation of the scaffolds into blood vessels. Reproduced with permission [344]. Copyright 2024, Wiley-VCH. (**C**) Schematic representation of the arteriovenous shunt process and brightfield photographs of different vascular grafts after arteriovenous shunt. Reproduced with permission [339]. Copyright 2023, Elsevier. (**D**) Tissue regeneration within PCL microfiber based vascular grafts, analysed by H&E staining. The neo-tissue was bordered by dashed lines. Scale bars, 1 mm or 100 μm (magnified images). Reproduced with permission [345]. Copyright 2022, Elsevier. (**E**) Schematic illustrating a microfiber scaffold with long-term blood compatibility. Reproduced with permission [341]. Copyright 2024, Elsevier. (**F**) Schematic illustrating the formation of engineered vascular tissues through bio-printing and microfluidic perfusion. Reproduced with permission [346]. Copyright 2021, Wiley-VCH. (**G**) Schematic illustrating the formation of microvascular-like structures through magnetically-guided assembly of magnetic alginate microfiber rings. Reproduced with permission [347]. Copyright 2018, Elsevier.

7.6. Biosensing and Diagnosis

Biosensing and diagnostic technologies play a crucial role in modern healthcare by enabling early disease detection, continuous monitoring, and personalized medicine [348,349]. The confluence of polymer science, textile engineering, and microfabrication has ushered in a new era for biosensing and diagnostics, fundamentally redefining the interface between electronic devices and the human body [36]. This burgeoning field, largely anchored by the development of polymer microfibers, represents a paradigm shift from rigid, planar electronics to soft, textile-integrated systems capable of seamless, continuous physiological monitoring [15,350]. The sophisticated control over fiber geometry and material composition now permits the creation of functional architectures that are not only highly sensitive to biological signals but also mechanically compliant with human tissue, overcoming the pervasive issues of signal instability and wearer discomfort inherent in first-generation wearable sensors [351].

For a notable example, Yu et al. first demonstrated a significant advancement in functional material integration by introducing a dynamic liquid metal-microfiber interlocking strategy, enabling the realization of highly conductive and strain-insensitive metastructured fibers for wearable electronics (Figure 9A) [352]. Recognizing that embedding solid conductive materials severely compromises electrical pathways under strain, their approach utilized a mixture of Copper and Eutectic Gallium-Indium (Cu-EGaIn) partially embedded within a porous polymer microfiber mat. This composite structure was then rolled up into a spiral-layered, metastructured fiber. This dynamic solid-liquid interfacial interlocking mechanism enabled self-compensating conductive pathways, resulting in fibers that maintained an ultra-stable conductance, exhibiting only a 16% relative resistance change even at 100% strain, far exceeding theoretical predictions for similar composites. Crucially, the fiber boasted a high conductivity of 1.5×10^6 S m^{-1} and considerable stretchability up to 629%, making it an exceptionally stable platform for applications such as temperature-visualizing electrothermal fabrics and stretchable smart sensing displays. Similarly, to address the challenges of achieving both mechanical robustness and high sensitivity, Gao et al. engineered ultra-robust and extensible conducting microfibers for wearable smart healthcare (Figure 9B) [353]. Their fabrication process yielded fibers with a remarkable tensile strength of 17.6 MPa and extensibility up to 700%. This mechanical superiority translated directly into a high-performance mechanical sensor capable of detecting strains across an unprecedented range, from 0.0075% to 400%, while also demonstrating the capacity to monitor low-frequency biological vibrations in the 0 to 40 Hz range, effectively capturing tremors and micro-movements pertinent to neurological health monitoring. This work underscored that mechanical resilience is not merely a durability feature but a prerequisite for stable and wide-range biosensing performance.

Inspired by the need to match the mechanical behavior of biological tissues, researchers have increasingly explored biomimetic fiber designs to improve interface stability and functional performance. In this context, Hanif et al. developed a bio-inspired nanofiber-reinforced microfiber designed to replicate the mechanical behavior of natural biological tissue [354]. They constructed a core-shell system using a soft polyurethane (PU) microfiber, which mimics the elasticity of elastin, wrapped with PVDF nanofibers, which mimic the strain-limiting function of collagen. The resulting microfiber exhibited a J-shaped stress-strain curve, characterized by elasticity at low strains and a rapid increase in modulus at high strains, effectively providing a strain-limiting mechanism. This mechanical profile is critical for wearable electronics, offering both comfort at rest and structural protection during vigorous activity, thus ensuring continuous and accurate data acquisition without sensor damage or detachment. Similarly, Guo et al. introduced an innovative electronic skin based on an elastic MXene hydrogel microfiber for effective joint monitoring (Figure 9C) [207]. Using the microfluidic technology, they fabricated a double-network hydrogel microfiber composed of covalently cross-linked polyacrylamide and ionically cross-linked alginate, reinforced by highly conductive MXene nanosheets. The resulting microfiber possessed superior superelasticity and high electrical conductivity, allowing it to conform perfectly to dynamic, large-scale body movements, such as the bending of fingers and wrists. This MXene-hydrogel electronic skin demonstrated excellent stability and sensitivity for monitoring large-scale joint motions, providing a precise digital readout for human posture tracking and rehabilitation diagnostics.

Furthermore, achieving high sensitivity for detecting subtle physiological signals remains a major challenge in biosensing applications. In this direction, Jiang et al. developed a coaxial heterogeneous microfiber for ultrasensitive pressure monitoring of living organisms [355]. Their design featured a core of rGO- PPy aerogel encased in a flexible polymer sheath. The unique three-dimensional porous structure of the aerogel core maximized the piezoresistive effect by creating a vast network of inter-fiber contact points. This coaxial structure enabled the microfiber sensor to achieve exceptional sensitivity, making it capable of comprehensive surveillance and monitoring of living organisms through the detection of minute micropressure changes associated with organ activity, a capability previously unachievable by traditional e-skin systems. In addition to the sensitivity of the biosensor, wearability and comfort is also crucial factors for continuous monitoring. In this context, Mondal et al.

presented an all-organic rotary jet-spun textile piezoelectret dressing for biosignal-monitored wound healing (Figure 9D) [84]. This work elegantly combined sensing and therapeutic functions. The textile, fabricated through a scalable spinning method, exhibited outstanding piezoelectric properties, yielding a sensitivity of 400 mV kPa^{-1}. The enhanced piezo-potential was attributed to trapped polarized charges within the fiber matrix, confirmed by finite element modeling. Functionally, the textile seamlessly monitored vital physiological signals, including pulse and respiratory rate, while also acting as a pressure-mapping array with 98% accuracy. Crucially, the piezoelectric output, which generates micro-electrical stimulation, was demonstrated to accelerate the proliferation and migration of L929 cells, highlighting its potential for active, signal-guided wound healing and regeneration. Similarly, Kim et al. introduced a wireless breathable face mask sensor designed for spatiotemporal 2D respiration profiling and respiratory diagnosis (Figure 9E) [356]. Developed in response to the growing need for comfortable and quantitative pulmonary monitoring post-pandemic, their sensor array was integrated into a porous, breathable substrate. Unlike single-pixel sensors, this flexible pressure-sensing mask allowed for the 2D mapping of airflow distribution and pressure over the nasal and oral regions, providing rich spatiotemporal data for detailed respiratory pattern recognition and diagnosis. This level of detail is invaluable for diagnosing conditions like obstructive sleep apnea or tracking the progression of pulmonary diseases. Furthermore, the complexity in sensor adhesion to the skin's irregular surface was tackled by Drotlef et al., who proposed bioinspired composite microfibers to significantly improve skin adhesion and signal amplification for wearable sensors [7]. Their films consisted of elastomeric microfibers decorated with conformal, mushroom-shaped vinylsiloxane tips, mimicking the adhesive structures found in certain biological systems. Strong adhesion, up to 18 kPa, was achieved through the controlled crosslinking of the viscous tips directly onto the skin surface, allowing excellent shape adaptation to the skin's multiscale roughness. When integrated with a strain sensor, this microfibrillar adhesive system dramatically improved the signal-to-noise ratio to 59.7, demonstrating a considerable signal amplification effect that is critical for accurately monitoring subtle vital signs like heart rate and respiration under real-world conditions.

Moreover, the advanced control over fiber mechanics is not limited to passive sensing but extends to active components. For example, the work by Hou et al. on bioinspired liquid crystalline spinning to fabricate high-performing fibrous artificial muscles represents a foundational advance for future fiber-based diagnostic and therapeutic devices (Figure 9F) [357]. By drawing inspiration from the dragline silks of spiders, which utilize multiple drawdowns for alignment, they employed internal drawdown via a tapered-wall-induced-shearing mechanism and external mechanical stretching to shape liquid crystal elastomers (LCEs) into thin, aligned microfibers. This process enabled the continuous, high-speed production (up to 8400 m h^{-1}) of LCE microfibers with unprecedented actuation metrics, including a rapid deformation strain rate of 810% s^{-1} and powerful actuation stress of 5.3 MPa. Such high-performance active fibers could be integrated into smart micro-robotics or fiber-based soft actuators for *in vivo* manipulation or targeted drug delivery systems that are intrinsically linked to a fiber-optic diagnostic interface. This concept of intrinsic functionality was mirrored in the design of proprioceptive sensors by Lee et al., who developed an inherently integrated microfiber-based flexible proprioceptive sensor for feedback-controlled soft actuators (Figure 9G) [358]. In their system, two parallel conductive microfibers were embedded around an elastomeric chamber of a pneumatic soft actuator. These microfibers simultaneously served two purposes: they acted as the radial expansion limiting fibers, which are essential for the actuator's mechanical function, and also as a capacitive bending sensor to provide real-time proprioceptive feedback on the actuator's bending and expansion state. By leveraging the essential structural components for sensing, they eliminated the need for separate, bulky, or rigid sensing devices, significantly reducing structural complexity and manufacturing costs while enhancing interfacial stability, a strategy highly relevant to creating multi-functional, fiber-integrated diagnostic probes for endoscopy or surgical robotics.

In summary, microfibers offer a highly versatile platform for biosensing and diagnostics owing to their structural tunability, large surface area, and compatibility with functional nanomaterials and biomolecules. By enabling continuous monitoring of biochemical and physiological signals, microfiber-based sensors hold significant promise for wound monitoring, wearable health devices, implantable diagnostics, and theranostic systems. Future directions will focus on improving sensitivity and selectivity, integrating multiplexed detection, ensuring long-term stability in physiological environments, and coupling with wireless communication and AI-driven data analysis to create robust, real-world diagnostic tools.

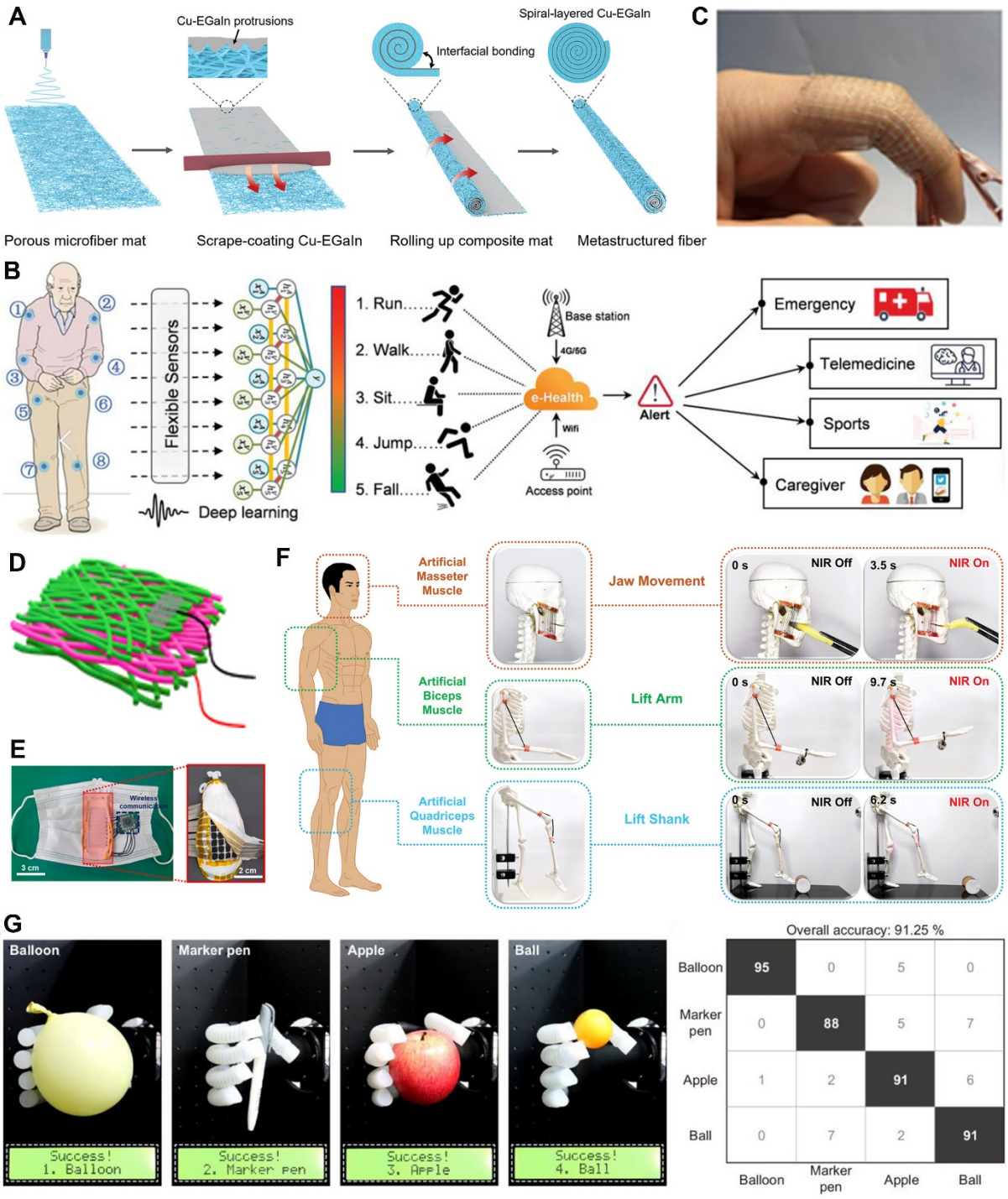

Figure 9. Applications in biosensing. (**A**) Schematic illustrating the preparation of the metastructured fibers for wearable electronics. Reproduced with permission [352]. Copyright 2025, Wiley-VCH. (**B**) Schematic showing the wireless wearable health monitoring and early warning system assisted by microfibers and artificial intelligence. Reproduced with permission [353]. Copyright 2021, Wiley-VCH. (**C**) Optical images of the mesh hydrogel during the finger bending. Reproduced with permission [207]. Copyright 2021, ACS Publications. (**D**) Schematic showing wearable microfiber piezoelectric sensor. Reproduced with permission [84]. Copyright 2025, Wiley-VCH. (**E**) Digital images of the microfiber-based array sensor equipped inside a commercial face mask. Reproduced with permission [356]. Copyright 2024, Elsevier. (**F**) Schematic illustrating the liquid crystal elastomer microfibers as masseter artificial muscle, biceps artificial muscle and quadriceps artificial muscle on a human skeleton. Reproduced with permission [357]. Copyright 2023, Wiley-VCH. (**G**) Photographs showing the object recognition and classification with the soft prosthetic hand, integrated with microfiber-based sensor. Reproduced with permission [358]. Copyright 2024, Springer Nature.

7.7. Cancer Treatment

The integration of polymer microfibers into advanced biomedical strategies has heralded a new epoch for cancer treatment, moving beyond conventional systemic limitations toward site-specific, stimuli-responsive, and highly localized therapies and diagnostic platforms [359,360]. The inherent structural versatility and biomimetic cues offered by fibrous scaffolds, particularly those fabricated via techniques like electrospinning, 3D printing and microfluidic spinning, provide an exceptional foundation for optimizing drug delivery, enhancing immunotherapy, and establishing high-fidelity *in vitro* tumor models [361]. A significant focus in recent years has been on applying these materials to address challenging clinical scenarios, such as preventing postoperative recurrence and developing personalized drug screening assays [362].

The postsurgical management of tumors remains a critical hurdle in oncological practice, as residual cancer cells often lead to recurrence. To combat this, Ye et al. explored the application of electrospun composite microfibers designed for dual-modal therapy, specifically for use in the postoperative niche (Figure 10A) [215]. Their work involved incorporating molybdenum disulfide (MoS_2) nanosheets, a photothermal agent, and the widely used anticancer drug doxorubicin (DOX) into a poly(lactic-co-glycolic acid) (PLGA) microfiber matrix. This durable photothermal agent exhibited excellent photothermal transformation and stability in both the near-infrared I (NIR I) and near-infrared II (NIR II) biowindows, which are crucial for deeper tissue penetration. Importantly, they demonstrated that the synergistic effect of photothermal therapy (PTT) and chemotherapy, delivered directly by the microfibers at the surgical site, was capable of completely prohibiting postoperative tumor reoccurrence *in vivo*. In addition to develop localized postsurgical care, Chen et al. further developed a strategy using microfluidic spinning to produce microfibers derived from natural origin materials for breast tumor postsurgical treatment (Figure 10B) [363]. The scaffold incorporated extracts from the traditional Chinese herb Premna microphylla alongside curcumin, a compound celebrated for its anti-inflammatory and anti-cancer properties. By utilizing the mild, biocompatible characteristics of natural polymers, this work provides a blueprint for effective, localized drug delivery platforms that seek to minimize systemic toxicity while maximizing therapeutic efficacy against residual tumor cells.

Beyond drug delivery systems, microfiber scaffolds are also being explored as platforms for cancer immunotherapy by acting as potent vaccination scaffolds. Huo et al. detailed the creation of Astragaloside IV (AS-IV) microfibers that spontaneously assemble into injectable 3D-scaffolds with intrinsic immunoactivity, serving as an injectable tumor vaccine platform [364]. This approach ingeniously minimizes the reliance on expensive synthetic adjuvants by utilizing a traditional Chinese herb component (AS-IV) as both a physical scaffold and a biological stimulant. The self-assembled microfiber network acts as a crucial reservoir for tumor antigens and simultaneously stimulates dendritic cells (DCs) within the tumor microenvironment (TME), leading to enhanced DC maturation and subsequent robust T-cell activation. This dual-role as an immunoadjuvant and physical cell-recruitment niche significantly boosts the overall efficacy of the tumor vaccine. Similarly, Sharma et al. developed an inorganic-organic hybrid nanocomposite using poly-$_L$-lactide (PLLA) microfibers decorated with radially grown zinc oxide (ZnO) nanowires (Figure 10C) [365]. This 3D complex was then loaded with a tumor antigen to function as a therapeutic cancer vaccine. This hybrid microfiber system efficiently delivered the tumor antigen into DCs, a critical step for initiating a robust anti-tumor immune response, showcasing a promising new avenue for cancer immunotherapy based on scaffold-mediated antigen presentation.

Besides therapeutic delivery and vaccination strategies, microfiber systems are also valuable for constructing biomimetic *in vitro* tumor models that can improve drug screening accuracy. Since tumor stiffness strongly influences cancer progression and treatment resistance, Song et al. engineered mechanically tunable hydrogel microfibers for a biomimetic drug testing platform focused on neuroblastoma (Figure 10D) [236]. The core innovation lay in fabricating alginate/poly(N-isopropyl acrylamide) (PNIPAM) shell microfibers that exhibit a rapid temperature response. This thermal sensitivity allowed for the precise and quick manipulation of the hydrogel's mechanical stiffness, thereby mimicking the changing stiffness of the ECM surrounding neuroblastoma cells. The resultant platforms successfully regulated the cellular pressure environment and rapidly formed highly active 3D tumor spheroids, which, crucially, displayed varying sensitivities to different chemotherapeutic agents, thus validating the model's predictive power for personalized treatment selection.

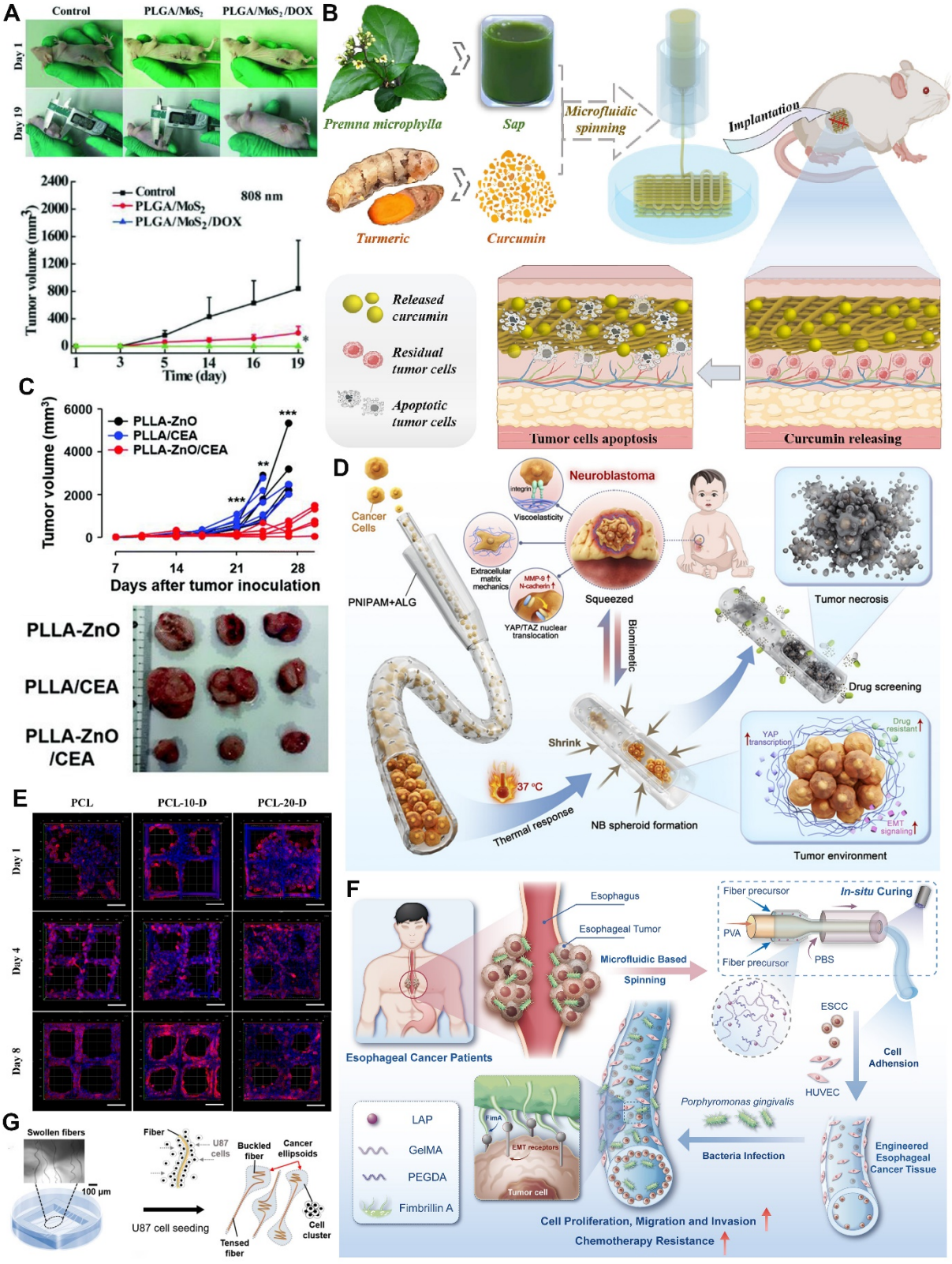

Figure 10. Applications in cancer research. (**A**) *In vivo* chemotherapy and photothermal therapy of HT 29 tumor bearing mice using PLGA/MoS_2/DOX composite microfibers. Reproduced with permission [215]. Copyright 2018, Wiley-VCH. (**B**) Schematic illustrating the application of microfluidic spun microfibers derived from herbal extracts for postsurgical treatment of breast tumor. Reproduced with permission [363]. Copyright 2023, Elsevier. (**C**) Cancer immunotherapy using PLLA-ZnO/CEA microfibers. (** $p < 0.01$; *** $p < 0.001$). Reproduced with permission [365]. Copyright 2019, RSC Publishing. (**D**) Schematic illustrating the use of microfluidic technology to fabricate core-shell microfibers encapsulating tumor cells, mimicking the mechanical environment of neuroblastoma *in vivo*, for antitumor drug evaluation. Reproduced with permission [236]. Copyright 2025, Wiley-

VCH. (**E**) CLSM images of A549 cells on different PCL microfibers based scaffolds after 1, 4, and 8 days of culture, Scale bar, 100 μm. Reproduced with permission [366]. Copyright 2021, ACS Publications. (**F**) Schematic illustrating a bionic esophageal cancer model featuring a hollow microfiber structure with esophageal squamous cell carcinoma (ESCC) cells lining the internal wall and HUVECs covering the surface, enabling the study of malignant progression following porphyromonas gingivalis infection. Reproduced with permission [241]. Copyright 2025, Cell Press. (**G**) Schematic depicting the cell seeding and cell aggregation on the gelatin microfibers. Reproduced with permission [367]. Copyright 2021, IOP Publishing.

Beyond mechanical regulation, the topographical characteristics of the tumor microenvironment also play a crucial role in tumor behavior. Jing et al. engineered scaffolds with precise nanotopography on microfibers of 3D-printed PCL scaffolds to modulate cellular responses and establish a superior *in vitro* tumor model (Figure 10E) [366]. They achieved tunable nanoscale features by simply leaching gliadin from PCL/gliadin composites using an ethanol solution. This approach provides a level of architectural control not possible with simpler 3D scaffolds, offering an optimized platform for drug screening. To further capture the complexity of tumor progression, Shi et al. engineered hydrogel-based hollow microfibers to functionally remodel esophageal carcinoma (esophageal squamous cell carcinoma or ESCC) (Figure 10F) [241]. This platform was specifically designed to study the malignant progression of ESCC under Porphyromonas gingivalis (Pg) infection, a known risk factor, providing a promising and high-fidelity ex vivo model for pathological research and the advancement of new tumor therapies. In addition to biochemical and structural cues, physical forces within the TME are also critical regulators of tumor growth and metastasis. To quantify these biomechanical interactions, Lee et al. detailed a method using suspended hydrogel microfibers for the guided assembly of a cancer ellipsoid (Figure 10G) [367]. This innovative platform allows for the estimation of multi-cellular traction force, a key biophysical parameter that regulates tumor growth, invasion, and metastasis, thus providing crucial quantitative data for understanding tumor-matrix interactions.

In summary, microfiber-based platforms hold significant promise for cancer treatment by enabling localized drug delivery, gene therapy, photothermal/photodynamic therapy, immunomodulation, and theranostic applications. Their structural versatility and ability to integrate multiple therapeutic functions make them superior to conventional delivery systems. With continued innovation in stimuli-responsive designs, multifunctional composites, and bioinspired architectures, microfiber technologies are poised to contribute to more effective, personalized, and minimally invasive cancer therapies in the near future.

8. Microfiber-Based Medical Products and Translational Challenges

Microfiber-based materials have transitioned from laboratory-scale research to a wide range of clinically approved biomedical products [368]. Over the past few decades, advances in fiber spinning technologies have enabled the large-scale manufacturing of fibrous medical devices with controlled fiber diameter, mechanical properties, and structural architecture. These technologies have facilitated the commercialization of various microfiber-based medical products, including surgical meshes, wound dressings, sutures, and vascular grafts, summarized in Table 3 [369].

Table 3. Clinically used microfiber products.

Materials	Brand Name (Company)	Fabrication Technique	Fiber Diameter (μm)	Final Structure	Application	Ref.
PP	Prolene® (Ethicon)	Melt extrusion	150	Knitted monofilament	Hernia mesh	[370,371]
Polyester	Acticoat® Flex7 (Smith & Nephew)	Melt extrusion	9–11	knitted mesh	Wound dressing	[372]
P4HB	GalaFLEX (Becton Dickinson)	Melt extrusion	154	Knitted monofilament	plastic and reconstructive surgery	[373,374]
P4HB	Phasix™ mesh (Becton Dickinson)	Melt extrusion	150–180	Wrap-knitted monofilament	Hernia repair	[375,376]
PVDF/ PP	DynaMesh® (FEG Textiltechnik mbH)	Melt extrusion	120–145	Interwoven knitted monofilament	abdominal wall repair	[377]
PGA	Neoveil® Sheet (Gunze)	Melt extrusion	15–17	Nonwoven felt/mesh	Reinforcement of soft tissue	[378]
Ca-Na alginate	Kaltostat® (Convatec)	-	14–19	Nonwoven mat	Wound dressing	[379]
Na-CMC	Durafiber® (Smith & Nephew)	-	9–13	Nonwoven sheet	Wound dressing	[380]
PVA	Exufiber® (Mölnlycke Health Care)	-	16–24	Nonwoven sheet	Wound dressing	[379]

Table 3. *Cont.*

Materials	Brand Name (Company)	Fabrication Technique	Fiber Diameter (μm)	Final Structure	Application	Ref.
Na-CMC	Aquacel® Extra (Convatec)	-	10–13	Nonwoven pad	Wound dressing	[379,381]
Calcium alginate	Suprasorb® A (Lohmann & Rauscher)	-	9–14	Nonwoven sheet	Wound dressing	[380]
Na-CMC	Kliniderm® Super Fiber (Klinion)	-	13–18	Nonwoven sheet	Wound dressing	[380]
PET	Mersilene® (Ethicon)	Melt extrusion	15	Woven/knitted mesh	Wound dressing	[382]
PET	Uni-Graft® K DV (B Braun)	Melt extrusion	15–20	Knitted graft	Vascular graft	[383,384]
Nylon	Supramid® Extra II (S JACKSON INC)	Melt extrusion	23	Multifilaments enclosed in outer sheath	Non-absorbable suture	[382]
PDO	PDS Plus® (Ethicon)	Melt extrusion	270	Monofilament	Absorbable suture	[385]
Polyglactin 910	Vicryl® (Ethicon)	Melt extrusion	10–15	Braided multifilament	Absorbable suture	[386]
PP	Surgipro® (Medtronic)	Melt extrusion	185	Monofilament	Non-absorbable suture	[387]
Poliglecaprone 25	Monocryl® (Ethicon)	Melt extrusion	295	Monofilament	Absorbable suture	[388,389]
PGA	Dexon® (Medtronic)	Melt extrusion	-	Braided multifilament	Absorbable suture	[390]
Natural collagen	Chromic Gut® (Medtronic)	-	196	Monofilament	Absorbable suture	[388]

A large proportion of commercial microfiber medical devices are fabricated using material extrusion process followed by textile processing techniques, such as knitting, weaving, or braiding, to produce mechanically robust fibrous constructs [5,370]. Synthetic polymers such as PP, PET, PVDF, poly-4-hydroxybutyrate (P4HB), and polydioxanone (PDO) are commonly used because of their excellent mechanical strength, stability, and biocompatibility [368]. For example, polypropylene meshes such as Prolene® are widely used for hernia repair, while P4HB-based scaffolds such as GalaFLEX® and Phasix™ meshes are biodegradable alternatives designed for soft-tissue reinforcement and reconstruction [373,382]. Similarly, PVDF-based meshes (e.g., DynaMesh®) are employed for abdominal wall repair due to their long-term mechanical stability and chemical resistance [377]. In addition to implantable surgical meshes, microfiber architectures are extensively utilized in wound care products. Hydrophilic fiber-based wound dressings produced through wet spinning techniques provide excellent fluid absorption, moisture retention, and conformability to irregular wound surfaces. Materials such as calcium alginate, sodium carboxymethyl cellulose (Na-CMC), and polyvinyl alcohol (PVA) are frequently used in commercial wound dressings including Kaltostat®, Durafiber®, Aquacel® Extra, and Exufiber® [379,380]. These fibrous dressings form highly absorbent nonwoven matrices that promote wound healing by maintaining a moist environment and facilitating exudate management. Microfiber are also widely employed in surgical sutures, where mechanical reliability and controlled degradation are essential. Both absorbable and non-absorbable sutures are produced using melt-extruded polymer filaments that are subsequently braided or formed into monofilaments [387]. Examples include polyglactin-based Vicryl® sutures, polydioxanone-based PDS Plus® sutures, and polypropylene-based Surgipro® sutures [377,386]. These materials are designed to provide temporary mechanical support during tissue healing while minimizing tissue reaction and maintaining high tensile strength. Furthermore, microfiber-based materials are used in vascular grafts and soft-tissue reinforcement devices, where fibrous structures provide both mechanical integrity and controlled porosity for tissue integration. The fibrous design of vascular grafts, such as Uni-Graft® K DV facilitates tissue ingrowth while maintaining sufficient mechanical stability to support physiological loads [383].

Thus, though there is the significant progress in microfiber based products, translation from laboratory-scale prototypes to clinically approved products remains challenging. The clinical success of microfiber-based systems depends not only on biological performance but also on regulatory classification, manufacturing reproducibility, biocompatibility, and degradation. From a regulatory perspective, microfiber-based products may follow different approval pathways depending on their intended use, composition, risk level, and mechanism of action. Relatively simple products such as sutures, hernia meshes, and some vascular grafts are generally regulated as medical devices. In the United States, many moderate-risk devices may require a 510 (k) submission to demonstrate substantial equivalence to a legally marketed predicate device [17,374]. High-risk implantable systems that support or sustain life, present significant risk, or lack sufficient safety history may require premarket approval, which involves more extensive evidence of safety and effectiveness. Regulatory translation also requires robust quality

control [391]. In the United States, manufacturers of finished medical devices must comply with the Quality Management System Regulation, which governs design, manufacturing, packaging, labeling, storage, installation, and servicing of finished devices intended for human use. The regulatory pathway becomes more demanding when microfiber scaffolds incorporate therapeutic agents, biologics, or living cells. Therefore, multifunctional microfiber systems must establish not only device safety but also drug release behavior, biological activity, dose control, pharmacokinetics, toxicity, and the interaction between components.

Manufacturing scalability is another major barrier [149]. Techniques such as melt extrusion, melt blowing, rotary jet spinning, and conventional electrospinning are more compatible with large-scale production because they can generate continuous fibers or large-area nonwoven mats. However, they often provide limited control over pore geometry, fiber placement, and 3D architecture. In contrast, melt electrowriting, microfluidic spinning, and direct-write 3D printing offer precise spatial control, defined pore size, and complex architectures, but they typically suffer from lower throughput, higher equipment cost, and more difficult process standardization. For clinical translation, key manufacturing requirements include batch-to-batch reproducibility, control of fiber diameter distribution, mechanical uniformity, residual solvent removal, sterilization compatibility, and quality management during scale-up.

Long-term biocompatibility and degradation behavior are especially important for implantable microfiber systems [255,327]. FDA guidance on ISO 10993-1 emphasizes a risk-based biological evaluation of medical devices based on the nature and duration of body contact, and the FDA notes that biocompatibility assessment should consider the device in its final finished form, including sterilization when applicable [392]. Nondegradable materials such as polypropylene, PET, and PTFE provide mechanical stability but may cause chronic foreign body responses, thrombosis, or long-term mechanical mismatch [17,203,365]. Biodegradable polymers such as PLA, PLGA, PCL, PDO, and PLCL can gradually transfer mechanical load to regenerating tissues, but their degradation rate, acidic byproducts, crystallinity changes, and loss of mechanical integrity must be carefully matched to the healing timeline [198,393].

Overall, successful clinical translation of microfiber-based biomedical systems requires an integrated design strategy that considers regulatory classification, scalable manufacturing, quality control, sterilization, degradation kinetics, and long-term biological response from the beginning of material development. Future progress will depend on establishing standardized testing protocols, improving scalable precision manufacturing, reducing variability, and generating long-term preclinical and clinical evidence. Addressing these translational barriers will be essential for moving advanced microfiber platforms from experimental studies toward clinically reliable regenerative, therapeutic, and diagnostic products.

9. Conclusions

The development of microfibers has opened new frontiers in biomedical engineering, offering platforms that combine biomimetic architecture, tunable material properties, and multifunctional performance. As this review highlights, advances in fabrication techniques, from electrospinning and melt electrowriting to microfluidic spinning, rotary jet spinning, and emerging methods like micro-adhesion guided spinning, have greatly expanded the design space for tailoring microfiber structure, composition, and functionality. By careful selection of materials and processing parameters, researchers can engineer fibers with diverse morphologies such as solid, hollow, porous, core–shell, and Janus structures, each serving distinct biomedical purposes.

Beyond structural engineering, microfiber functionalization strategies, including surface coating, plasma treatment, nanoparticle incorporation, and bioactive ligand conjugation, have transformed simple fibers into smart systems capable of dynamic interactions with their biological environment. Such modifications allow the integration of sensing, actuation, drug delivery, and regenerative functions within a single platform. This versatility has positioned microfibers as powerful tools across a broad spectrum of biomedical applications, ranging from wound healing and tissue regeneration to biosensing, diagnostics, and targeted cancer therapy. The unique combination of biocompatibility, high surface-to-volume ratio, and customizable properties enables microfibers not only to mimic natural ECM but also to surpass them by delivering controlled biochemical, mechanical, and electrical cues. Their adaptability further supports the convergence of regenerative medicine with precision diagnostics and theranostics, paving the way for next-generation personalized healthcare solutions.

Despite these advances, several challenges remain before microfiber technologies achieve widespread clinical translation. Key hurdles include scaling up fabrication processes while ensuring reproducibility, integrating multifunctionality without compromising mechanical integrity, achieving long-term biocompatibility and stability *in vivo*, and addressing sterilization and regulatory concerns. Furthermore, real-time monitoring and adaptive feedback within microfiber systems remain underexplored but are critical for safe and effective clinical use. Looking ahead,

the integration of microfiber fabrication with emerging technologies such as additive manufacturing, artificial intelligence-driven design optimization, and bioelectronic interfaces holds immense potential. Stimuli-responsive and multi-material microfiber systems capable of synergistically combining regenerative, diagnostic, and therapeutic functions are expected to play a transformative role in future biomedical devices.

In brief, microfibers represent a versatile and rapidly evolving class of biomaterials with profound implications for medicine. Continued interdisciplinary efforts bridging materials science, biology, engineering, and clinical research will be essential to unlock their full potential and translate laboratory innovations into clinically relevant therapies that improve patient outcomes.

Author Contributions: B.M.: conceptualization, writing—original draft preparation; S.M.S.S., S.M.A.: writing—reviewing and editing; J.X.: conceptualization, supervision, writing—reviewing and editing All authors have read and agreed to the published version of the manuscript.

Funding: This work was partially supported by startup funds from the University of Nebraska Medical Center (UNMC), National Institute of General Medical Sciences (NIGMS) and National Institute of Dental and Craniofacial Research (NIDCR) of the National Institutes of Health under Award Numbers R01GM138552 and R01DE031272, Nebraska Research Initiative grant, and NE LB606.

Conflicts of Interest: The authors declare no conflict of interest.

Use of AI and AI-Assisted Technologies: No AI tools were utilized for this paper.

References

1. Xue, J.; Niu, Y.; Gong, M.; Shi, R.; Chen, D.; Zhang, L.; Lvov, Y. Electrospun Microfiber Membranes Embedded with Drug-Loaded Clay Nanotubes for Sustained Antimicrobial Protection. *ACS Nano* **2015**, *9*, 1600–1612.
2. Haynl, C.; Hofmann, E.; Pawar, K.; Förster, S.; Scheibel, T. Microfluidics-Produced Collagen Fibers Show Extraordinary Mechanical Properties. *Nano Lett.* **2016**, *16*, 5917–5922.
3. Wei, D.; Charlton, L.; Glidle, A.; Qi, N.; Dobson, P.S.; Dalby, M.J.; Fan, H.; Yin, H. Dynamically Modulated Core-Shell Microfibers to Study the Effect of Depth Sensing of Matrix Stiffness on Stem Cell Fate. *ACS Appl. Mater. Interfaces* **2021**, *13*, 37997–38006.
4. Lanno, G.M.; Ramos, C.; Preem, L.; Putrins, M.; Laidmaë, I.; Tenson, T.; Kogermann, K. Antibacterial Porous Electrospun Fibers as Skin Scaffolds for Wound Healing Applications. *ACS Omega* **2020**, *5*, 30011–30022.
5. Kong, B.; Liu, R.; Guo, J.; Lu, L.; Zhou, Q.; Zhao, Y. Tailoring Micro/Nano-Fibers for Biomedical Applications. *Bioact. Mater.* **2023**, *19*, 328–347.
6. Daniele, M.A.; Boyd, D.A.; Adams, A.A.; Ligler, F.S. Microfluidic Strategies for Design and Assembly of Microfibers and Nanofibers with Tissue Engineering and Regenerative Medicine Applications. *Adv. Healthc. Mater.* **2015**, *4*, 11–28.
7. Drotlef, D.M.; Amjadi, M.; Yunusa, M.; Sitti, M. Bioinspired Composite Microfibers for Skin Adhesion and Signal Amplification of Wearable Sensors. *Adv. Mater.* **2017**, *29*, 1701353.
8. Lee, W.; Choi, J.H.; Lee, S.; Song, J.E.; Khang, G. Fabrication and Characterization of Silk Fibroin Microfiber-Incorporated Bone Marrow Stem Cell Spheroids to Promote Cell-Cell Interaction and Osteogenesis. *ACS Omega* **2020**, *5*, 18021–18027.
9. Guo, W.; Zhang, X.; Yu, X.; Wang, S.; Qiu, J.; Tang, W.; Li, L.; Liu, H.; Wang, Z.L. Self-Powered Electrical Stimulation for Enhancing Neural Differentiation of Mesenchymal Stem Cells on Graphene-Poly(3,4-Ethylenedioxythiophene) Hybrid Microfibers. *ACS Nano* **2016**, *10*, 5086–5095.
10. Fioretta, E.S.; Simonet, M.; Smits, A.I.P.M.; Baaijens, F.P.T.; Bouten, C.V.C. Differential Response of Endothelial and Endothelial Colony Forming Cells on Electrospun Scaffolds with Distinct Microfiber Diameters. *Biomacromolecules* **2014**, *15*, 821–829.
11. Salas-Ambrosio, P.; Morales-Patlan, E.; Cedillo-Servin, G.; Tronnet, A.; Villavicencio, K.P.; Gómez-Lizárraga, K.; Benítez-Martínez, J.A.; Sanchez-Arevalo, F.M.; Velasquillo, C.; Ceapă, C.D.; et al. Electrospinning Lysine-Polypeptide Copolymers: Creating Microfiber Meshes for Biomedical Applications. *ACS Appl. Polym. Mater.* **2024**, *6*, 8733–8744.
12. Zhu, J.; Zhu, Y.; Ye, Y.; Qiu, Z.; Zhang, Y.; Yu, Z.; Sun, X.; Bressler, D.C.; Jiang, F. Superelastic and Ultralight Aerogel Assembled from Hemp Microfibers. *Adv. Funct. Mater.* **2023**, *33*, 2300893.
13. Lim, J.; Choi, G.; Joo, K.Il; Cha, H.J.; Kim, J. Embolization of Vascular Malformations via *In Situ* Photocrosslinking of Mechanically Reinforced Alginate Microfibers Using an Optical-Fiber-Integrated Microfluidic Device. *Adv. Mater.* **2021**, *33*, 2006759.
14. Paxton, N.C.; Luposchainsky, S.; Reizabal, A.; Saiz, P.G.; Bade, S.; Woodruff, M.A.; Dalton, P.D. Manufacture of Biomimetic Auricular Surgical Implants Using 3D Printed High Density Polyethylene Microfibers. *Adv. Mater. Technol.* **2024**, *9*, 2301190.

15. Huynh, V.L.; Trung, T.Q.; Meeseepong, M.; Lee, H.B.; Nguyen, T.D.; Lee, N.E. Hollow Microfibers of Elastomeric Nanocomposites for Fully Stretchable and Highly Sensitive Microfluidic Immunobiosensor Patch. *Adv. Funct. Mater.* **2020**, *30*, 2004684.
16. Barroso-Solares, S.; Cuadra-Rodriguez, D.; Rodriguez-Mendez, M.L.; Rodriguez-Perez, M.A.; Pinto, J. A New Generation of Hollow Polymeric Microfibers Produced by Gas Dissolution Foaming. *J. Mater. Chem. B* **2020**, *8*, 8820–8829.
17. Varadharajan Idhaiam, K.S.; Oporto, G.; Barre, M.; Terada, M.; Boyd, J.; Goldsmith, W.; Nurkiewicz, T.; Gupta, R.K.; Sabolsky, E.M. Eco-Friendly Hierarchical Nanoporous Microfiber Respirator Filters Fabricated Using Rotary Jet Spinning Technology (RJS). *ACS Appl. Polym. Mater.* **2023**, *5*, 1657–1669.
18. Ma, W.; Liu, D.; Ling, S.; Zhang, J.; Chen, Z.; Lu, Y.; Xu, J. High-Throughput and Controllable Fabrication of Helical Microfibers by Hydrodynamically Focusing Flow. *ACS Appl. Mater. Interfaces* **2021**, *13*, 59392–59399.
19. Pham, Q.P.; Sharma, U.; Mikos, A.G. Electrospun Poly (ε-Caprolactone) Microfiber and Multilayer Nanofiber/Microfiber Scaffolds: Characterization of Scaffolds and Measurement of Cellular Infiltration. *Biomacromolecules* **2006**, *7*, 2796–2805.
20. Yu, Y.; Wei, W.; Wang, Y.; Xu, C.; Guo, Y.; Qin, J. Simple Spinning of Heterogeneous Hollow Microfibers on Chip. *Adv. Mater.* **2016**, *28*, 6649–6655.
21. Ding, C.; Breunig, M.; Timm, J.; Marschall, R.; Senker, J.; Agarwal, S. Flexible, Stable, Mechanically, Porous Self-Standing Microfiber Network Membranes of Covalent Organic Frameworks: Preparation Method and Characterization. *Adv. Funct. Mater.* **2021**, *31*, 2106507.
22. Shahriar, S.M.S.; Andrabi, S.M.; Al-Gahmi, A.M.; Yan, Z.; McCarthy, A.D.; Wang, C.; Yusuf, Z.A.; Sharma, N.S.; Busquets, M.E.; Nilles, M.I.; et al. Bicomponent Nano- and Microfiber Aerogels for Effective Management of Junctional Hemorrhage. *Nat. Commun.* **2025**, *16*, 2403.
23. Gong, J.; Schuurmans, C.C.L.; van Genderen, A.M.; Cao, X.; Li, W.; Cheng, F.; He, J.J.; López, A.; Huerta, V.; Manríquez, J.; et al. Complexation-Induced Resolution Enhancement of 3D-Printed Hydrogel Constructs. *Nat. Commun.* **2020**, *11*, 1267.
24. Roman, J.A.; Reucroft, I.; Martin, R.A.; Hurtado, A.; Mao, H.Q. Local Release of Paclitaxel from Aligned, Electrospun Microfibers Promotes Axonal Extension. *Adv. Healthc. Mater.* **2016**, *5*, 2628–2635.
25. Calejo, I.; Costa-Almeida, R.; Reis, R.L.; Gomes, M.E. A Textile Platform Using Continuous Aligned and Textured Composite Microfibers to Engineer Tendon-to-Bone Interface Gradient Scaffolds. *Adv. Healthc. Mater.* **2019**, *8*, 1900200.
26. Kim, B.J.; Choi, J.Y.; Choi, H.; Han, S.; Seo, J.; Kim, J.; Joo, S.; Kim, H.M.; Oh, C.; Hong, S.; et al. Astrocyte-Encapsulated Hydrogel Microfibers Enhance Neuronal Circuit Generation. *Adv. Healthc. Mater.* **2020**, *9*, 1901072.
27. Ning, H.; Wu, X.; Wu, Q.; Yu, W.; Wang, H.; Zheng, S.; Chen, Y.; Li, Y.; Su, J. Microfiber-Reinforced Composite Hydrogels Loaded with Rat Adipose-Derived Stem Cells and BMP-2 for the Treatment of Medication-Related Osteonecrosis of the Jaw in a Rat Model. *ACS Biomater. Sci. Eng.* **2019**, *5*, 2430–2443.
28. Daniele, M.A.; North, S.H.; Naciri, J.; Howell, P.B.; Foulger, S.H.; Ligler, F.S.; Adams, A.A. Rapid and Continuous Hydrodynamically Controlled Fabrication of Biohybrid Microfibers. *Adv. Funct. Mater.* **2013**, *23*, 698–704.
29. Patil, P.; Szymanski, J.M.; Feinberg, A.W. Defined Micropatterning of ECM Protein Adhesive Sites on Alginate Microfibers for Engineering Highly Anisotropic Muscle Cell Bundles. *Adv. Mater. Technol.* **2016**, *1*, 1600003.
30. Tian, L.; Shi, J.; Li, W.; Zhang, Y.; Gao, X. Hollow Microfiber Assembly-Based Endocrine Pancreas-on-a-Chip for Sugar Substitute Evaluation. *Adv. Healthc. Mater.* **2024**, *13*, 2302104.
31. Adamo, A.; Bartolacci, J.G.; Pedersen, D.D.; Traina, M.G.; Kim, S.; Pantano, A.; Ghersi, G.; Watkins, S.C.; Wagner, W.R.; Badylak, S.F.; et al. Continuous Microfiber Wire Mandrel-Less Biofabrication for Soft Tissue Engineering Applications. *Adv. Healthc. Mater.* **2022**, *11*, 2102613.
32. Chen, J.; Zhao, X.; Qiao, L.; Huang, Y.; Yang, Y.; Chu, D.; Guo, B. Multifunctional On-Demand Removability Hydrogel Dressing Based on in Situ Formed AgNPs, Silk Microfibers and Hydrazide Hyaluronic Acid for Burn Wound Healing. *Adv. Healthc. Mater.* **2024**, *13*, 2303157.
33. McNamara, M.C.; Aykar, S.S.; Alimoradi, N.; Niaraki Asli, A.E.; Pemathilaka, R.L.; Wrede, A.H.; Montazami, R.; Hashemi, N.N. Behavior of Neural Cells Post Manufacturing and After Prolonged Encapsulation within Conductive Graphene-Laden Alginate Microfibers. *Adv. Biol.* **2021**, *5*, 2101026.
34. Li, R.; McCarthy, A.; Zhang, Y.S.; Xie, J. Decorating 3D Printed Scaffolds with Electrospun Nanofiber Segments for Tissue Engineering. *Adv. Biosyst.* **2019**, *3*, 1900137.
35. Sharifi, S.; Sharifi, H. Electrospun-Reinforced Suturable Biodegradable Artificial Cornea. *ACS Appl. Bio Mater.* **2022**, *5*, 5716–5727.
36. Mondal, B.; Saini, D.; Mishra, H.K.; Mandal, D. Internet of Things and Machine Learning Enabled Smart E-Textile with Exceptional Breathability for Point-of-Care Diagnostics. *Adv. Mater. Technol.* **2024**, 2400206.
37. Acik, G.; Altinkok, C. Polypropylene Microfibers via Solution Electrospinning under Ambient Conditions. *J. Appl. Polym. Sci.* **2019**, *136*, 48199.

38. Kidoaki, S.; Kwon, I.K.; Matsuda, T. Mesoscopic Spatial Designs of Nano- and Microfiber Meshes for Tissue-Engineering Matrix and Scaffold Based on Newly Devised Multilayering and Mixing Electrospinning Techniques. *Biomaterials* **2005**, *26*, 37–46.
39. Devolder, R.J.; Bae, H.; Lee, J.; Kong, H. Directed Blood Vessel Growth Using an Angiogenic Microfiber/Microparticle Composite Patch. *Adv. Mater.* **2011**, *23*, 3139–3143.
40. Givens, S.R.; Gardner, K.H.; Rabolt, J.F.; Chase, D.B. High-Temperature Electrospinning of Polyethylene Microfibers from Solution. *Macromolecules* **2006**, *40*, 608–610.
41. Vaseashta, A. Controlled Formation of Multiple Taylor Cones in Electrospinning Process. *Appl. Phys. Lett.* **2007**, *90*, 093115.
42. Sun, D.; Chang, C.; Li, S.; Lin, L. Near-Field Electrospinning. *Nano Lett.* **2006**, *6*, 839–842.
43. Mondal, B.; Sarkar, R.; Saini, D.; Gupta, V.; Kundu, T.K.; Mandal, D. All-Electrospun, Water-Resistant, Breathable. Wearable, and Stable Metal Halide Perovskite Engineered Electroactive Polymer Textiles for Flexible Piezoelectric Nanogenerator. *Adv. Mater. Technol.* **2023**, *8*, 2300614.
44. Ura, D.P.; Rosell-Llompart, J.; Zaszczyńska, A.; Vasilyev, G.; Gradys, A.; Szewczyk, P.K.; Knapczyk-Korczak, J.; Avrahami, R.; Šišková, A.O.; Arinstein, A.; et al. The Role of Electrical Polarity in Electrospinning and on the Mechanical and Structural Properties of As-Spun Fibers. *Materials* **2020**, *13*, 4169.
45. Shao, H.; Fang, J.; Wang, H.; Lin, T. Effect of Electrospinning Parameters and Polymer Concentrations on Mechanical-to-Electrical Energy Conversion of Randomly-Oriented Electrospun Poly(Vinylidene Fluoride) Nanofiber Mats. *RSC Adv.* **2015**, *5*, 14345–14350.
46. Chi, H.; Jiang, A.; Wang, X.; Chen, G.; Song, C.; Prajapati, R.K.; Li, A.; Li, Z.; Li, J.; Zhang, Z.; et al. Dually Optimized Polycaprolactone/Collagen I Microfiber Scaffolds with Stem Cell Capture and Differentiation-Inducing Abilities Promote Bone Regeneration. *J. Mater. Chem. B* **2019**, *7*, 7052–7064.
47. Fang, J.; Niu, H.; Wang, H.; Wang, X.; Lin, T. Enhanced Mechanical Energy Harvesting Using Needleless Electrospun Poly(Vinylidene Fluoride) Nanofibre Webs. *Energy Environ. Sci.* **2013**, *6*, 2196–2202.
48. Wu, X.; Wang, Z.; Teng, J.; Yang, L.; Xu, S.; Luo, S.; Wu, Z.; Ye, C. Electrospun Microfiber Composite Scaffolds of Polyvinyl Alcohol, Polyhydroxybutyrate, and Multiwalled Carbon Nanotubes for Enhancing the Osteogenic Differentiation of Stem Cells to Promote Bone Regeneration. *Int. J. Biol. Macromol.* **2025**, *309*, 142988.
49. Adhikary, P.; Biswas, A.; Mandal, D. Improved Sensitivity of Wearable Nanogenerators Made of Electrospun Eu^{3+} Doped P(VDF-HFP)/Graphene Composite Nanofibers for Self-Powered Voice Recognition. *Nanotechnology* **2016**, *27*, 495501.
50. Schönlein, R.; Larrañaga, X.; Panfilo, A.; Li, Y.; Larrañaga, A.; Liu, G.; Müller, A.J.; Aguirresarobe, R.; Ugartemendia, J.M. Enhanced Piezoelectric Properties of Poly(L-Lactide) Nanocomposite Microfiber Scaffolds Due to Polydopamine-Coating of Barium Titanate Nanoparticles. *Adv. Mater. Interfaces* **2025**, *12*, 2400546.
51. Mares-Bou, S.; Serrano, M.A.; Gómez-Tejedor, J.A. Core–Shell Polyvinyl Alcohol (PVA) Base Electrospinning Microfibers for Drug Delivery. *Polymers* **2023**, *15*, 1554.
52. Li, Y.F.; Rubert, M.; Aslan, H.; Yu, Y.; Howard, K.A.; Dong, M.; Besenbacher, F.; Chen, M. Ultraporous Interweaving Electrospun Microfibers from PCL–PEO Binary Blends and Their Inflammatory Responses. *Nanoscale* **2014**, *6*, 3392–3402.
53. Steffi, C.; Wang, D.; Kong, C.H.; Wang, Z.; Lim, P.N.; Shi, Z.; San Thian, E.; Wang, W. Estradiol-Loaded Poly(ε-Caprolactone)/Silk Fibroin Electrospun Microfibers Decrease Osteoclast Activity and Retain Osteoblast Function. *ACS Appl. Mater. Interfaces* **2018**, *10*, 9988–9998.
54. Guo, Y.; Gilbert-Honick, J.; Somers, S.M.; Mao, H.Q.; Grayson, W.L. Modified Cell-Electrospinning for 3D Myogenesis of C2C12s in Aligned Fibrin Microfiber Bundles. *Biochem. Biophys. Res. Commun.* **2019**, *516*, 558–564.
55. Fattahi, P.; Dover, J.T.; Brown, J.L. 3D Near-Field Electrospinning of Biomaterial Microfibers with Potential for Blended Microfiber-Cell-Loaded Gel Composite Structures. *Adv. Healthc. Mater.* **2017**, *6*, 1700456.
56. Neuhäusler, A.; Rogg, K.; Schröder, S.; Spiehl, D.; Zora, H.; Arefaine, E.; Schettler, J.; Hartmann, H.; Blaeser, A. Electrospun Microfibers to Enhance Nutrient Supply in Bioinks and 3D-Bioprinted Tissue Precursors. *Biofabrication* **2024**, *17*, 015038.
57. Ko, J.; Kan, D.; Jun, M.B.G. Combining Melt Electrospinning and Particulate Leaching for Fabrication of Porous Microfibers. *Manuf. Lett.* **2015**, *3*, 5–8.
58. Hutmacher, D.W.; Dalton, P.D. Melt Electrospinning. *Chem.—Asian J.* **2011**, *6*, 44–56.
59. Afghah, F.; Dikyol, C.; Altunbek, M.; Koc, B. Biomimicry in Bio-Manufacturing: Developments in Melt Electrospinning Writing Technology Towards Hybrid Biomanufacturing. *Appl. Sci.* **2019**, *9*, 3540.
60. Yang, Z.; Peng, H.; Wang, W.; Liu, T. Crystallization Behavior of Poly(ε-Caprolactone)/Layered Double Hydroxide Nanocomposites. *J. Appl. Polym. Sci.* **2010**, *116*, 2658–2667.

61. Qin, C.C.; Duan, X.P.; Wang, L.; Zhang, L.H.; Yu, M.; Dong, R.H.; Yan, X.; He, H.W.; Long, Y.Z. Melt Electrospinning of Poly(Lactic Acid) and Polycaprolactone Microfibers by Using a Hand-Operated Wimshurst Generator. *Nanoscale* **2015**, *7*, 16611–16615.
62. Wang, C.; Xia, Q.; Yang, B.; Li, M.; Han, W.; Chen, H. Fabrication of Microfiber Bundles via Melt Electrospinning Technique. *Fibers Polym.* **2025**, *26*, 3843–3853.
63. Wang, Y.; Tan, J.; Xu, J.; Li, H.; Yang, W. The Preparation of Polypropylene Microfiber Yarns via Vortex Airflow-Assisted Melt Differential Electrospinning. *J. Appl. Polym. Sci.* **2024**, *141*, 55382.
64. Ko, J.; Ahsani, V.; Yao, S.X.; Mohtaram, N.K.; Lee, P.C.; Jun, M.B.G. Fabricating and Controlling PCL Electrospun Microfibers Using Filament Feeding Melt Electrospinning Technique. *J. Micromech. Microeng.* **2016**, *27*, 025007.
65. Lee, J.K.; Ko, J.; Jun, M.B.G.; Lee, P.C. Manufacturing and Characterization of Encapsulated Microfibers with Different Molecular Weight Poly(ε-Caprolactone) (PCL) Resins Using a Melt Electrospinning Technique. *Mater. Res. Express* **2016**, *3*, 025301.
66. Nayak, R.; Padhye, R.; Kyratzis, I.L.; Truong, Y.B.; Arnold, L. Effect of Viscosity and Electrical Conductivity on the Morphology and Fiber Diameter in Melt Electrospinning of Polypropylene. *Text. Res. J.* **2013**, *83*, 606–617.
67. Li, Y.-M.; Wang, X.-X.; Yu, S.-X.; Zhao, Y.-T.; Yan, X.; Zheng, J.; Yu, M.; Yan, S.-Y.; Long, Y.-Z. Bubble Melt Electrospinning for Production of Polymer Microfibers. *Polymers* **2018**, *10*, 1246.
68. O'Neill, K.L.; Dalton, P.D. A Decade of Melt Electrowriting. *Small Methods* **2023**, *7*, 2201589.
69. Nayak, R.; Padhye, R.; Arnold, L. *Melt-Electrospinning of Nanofibers*; Elsevier Ltd.: Amsterdam, The Netherlands, 2017.
70. Koenig, K.; Beukenberg, K.; Langensiepen, F.; Seide, G. A New Prototype Melt-Electrospinning Device for the Production of Biobased Thermoplastic Sub-Microfibers and Nanofibers. *Biomater. Res.* **2019**, *23*.
71. Castilho, M.; Feyen, D.; Flandes-Iparraguirre, M.; Hochleitner, G.; Groll, J.; Doevendans, P.A.F.; Vermonden, T.; Ito, K.; Sluijter, J.P.G.; Malda, J. Melt Electrospinning Writing of Poly-Hydroxymethylglycolide-Co-ε-Caprolactone-Based Scaffolds for Cardiac Tissue Engineering. *Adv. Healthc. Mater.* **2017**, *6*, 1700311.
72. Talebpour, P.; Mighri, F.; Ajji, A.; Heuzey, M.-C.; Virgilio, N. Tailoring the Morphology and Orientation in Immiscible Binary Polymer Blends during Melt-Electrospinning. *ACS Appl. Polym. Mater.* **2025**, *7*, 9555–9567.
73. Koenig, K.; Hermanns, S.; Ellerkmann, J.; Saralidze, K.; Langensiepen, F.; Seide, G. The Effect of Additives and Process Parameters on the Pilot-Scale Manufacturing of Polylactic Acid Sub-Microfibers by Melt Electrospinning. *Text. Res. J.* **2020**, *90*, 1948–1961.
74. Robinson, T.M.; Hutmacher, D.W.; Dalton, P.D.; Robinson, T.M.; Dalton, P.D.; Hutmacher, D.W. The Next Frontier in Melt Electrospinning: Taming the Jet. *Adv. Funct. Mater.* **2019**, *29*, 1904664.
75. Bachs-Herrera, A.; Yousefzade, O.; Del Valle, L.J.; Puiggali, J. Melt Electrospinning of Polymers: Blends, Nanocomposites, Additives and Applications. *Appl. Sci.* **2021**, *11*, 1808.
76. Zhang, L.H.; Duan, X.P.; Yan, X.; Yu, M.; Ning, X.; Zhao, Y.; Long, Y.Z. Recent Advances in Melt Electrospinning. *RSC Adv.* **2016**, *6*, 53400–53414.
77. Yang, H.; Wang, Y.; Jang, Y.; Shani, K.; Jiao, Q.; Peters, M.; Parker, K.K.; Vlassak, J.J. Biomimetic Hierarchical Fibrous Hydrogels with High Alignment and Flaw Insensitivity. *Matter* **2025**, *8*, 102054.
78. Golecki, H.M.I.; Yuan, H.; Glavin, C.; Potter, B.; Badrossamay, M.R.; Goss, J.A.; Phillips, M.D.; Parker, K.K. Effect of Solvent Evaporation on Fiber Morphology in Rotary Jet Spinning. *Langmuir* **2014**, *30*, 13369–13374.
79. Badrossamay, M.R.; McIlwee, H.A.; Goss, J.A.; Parker, K.K. Nanofiber Assembly by Rotary Jet-Spinning. *Nano Lett.* **2010**, *10*, 2257–2261.
80. Zander, N.E. Formation of Melt and Solution Spun Polycaprolactone Fibers by Centrifugal Spinning. *J. Appl. Polym. Sci.* **2015**, 132 2.
81. Rosa, J.C.; Bonvent, J.J.; Santos, A.R. Poly (ε-Caprolactone)/Poly (Lactic Acid) Fibers Produced by Rotary Jet Spinning for Skin Dressing with Antimicrobial Activity. *J. Biomater. Appl.* **2022**, *36*, 1641–1651.
82. Dantas, F.L.; Rodriguez Llanos, J.H.; Pereira Rodrigues, I.C.; Pereira, K.D.; Luchessi, A.D.; Sawazaki, R.; Najar Lopes, É.S.; Gabriel, L.P. PLLA Scaffolds Functionalized with Ketoprofen via Rotary Jet Spinning for Biomedical Applications. *J. Mater. Res. Technol.* **2024**, *30*, 9020–9027.
83. Atıcı, B.; Ünlü, C.H.; Yanilmaz, M. A Review on Centrifugally Spun Fibers and Their Applications. *Polym. Rev.* **2022**, *62*, 1–64.
84. Mondal, B.; Arora, M.; Panwar, V.; Ghosh, D.; Mandal, D. Piezoelectret Textile Dressing for Biosignal Monitored Wound Healing. *Small* **2025**, *21*, 2503130.
85. Zamproni, L.N.; Grinet, M.A.V.M.; Mundim, M.T.V.V.; Reis, M.B.C.; Galindo, L.T.; Marciano, F.R.; Lobo, A.O.; Porcionatto, M. Rotary Jet-Spun Porous Microfibers as Scaffolds for Stem Cells Delivery to Central Nervous System Injury. *Nanomed. Nanotechnol. Biol. Med.* **2019**, *15*, 98–107.

86. Kwak, B.E.; Yoo, H.J.; Lee, E.; Kim, D.H. Large-Scale Centrifugal Multispinning Production of Polymer Micro- and Nanofibers for Mask Filter Application with a Potential of Cospinning Mixed Multicomponent Fibers. *ACS Macro Lett.* **2021**, *10*, 382–388.
87. Machado-Paula, M.M.; Corat, M.A.F.; De Vasconcellos, L.M.R.; Araújo, J.C.R.; Mi, G.; Ghannadian, P.; Toniato, T.V.; Marciano, F.R.; Webster, T.J.; Lobo, A.O. Rotary Jet-Spun Polycaprolactone/Hydroxyapatite and Carbon Nanotube Scaffolds Seeded with Bone Marrow Mesenchymal Stem Cells Increase Bone Neoformation. *ACS Appl. Bio Mater.* **2022**, *5*, 1013–1024.
88. Motta, S.E.; Peters, M.M.; Chantre, C.O.; Chang, H.; Cera, L.; Liu, Q.; Cordoves, E.M.; Fioretta, E.S.; Zaytseva, P.; Cesarovic, N.; et al. On-Demand Heart Valve Manufacturing Using Focused Rotary Jet Spinning. *Matter* **2023**, *6*, 1860–1879.
89. MacQueen, L.A.; Alver, C.G.; Chantre, C.O.; Ahn, S.; Cera, L.; Gonzalez, G.M.; O'Connor, B.B.; Drennan, D.J.; Peters, M.M.; Motta, S.E.; et al. Muscle Tissue Engineering in Fibrous Gelatin: Implications for Meat Analogs. *NPJ Sci. Food* **2019**, *3*, 20.
90. Ahn, S.; Chantre, C.O.; Ardoña, H.A.M.; Gonzalez, G.M.; Campbell, P.H.; Parker, K.K. Biomimetic and Estrogenic Fibers Promote Tissue Repair in Mice and Human Skin via Estrogen Receptor β. *Biomaterials* **2020**, *255*, 120149.
91. Fu, F.; Zuo, X.; Wang, Y.; Zhao, F.; Li, C.; Zeng, Y.; Wang, L.; Wang, F. Centrifugal Spinning-Derived Biomimetic Aerogel for Rapid Hemostasis with Minimal Blood Loss. *Nano Lett.* **2025**, *25*, 6040–6050.
92. Pereira Rodrigues, I.C.; Tamborlin, L.; Rodrigues, A.A.; Jardini, A.L.; Ducati Luchessi, A.; Maciel Filho, R.; Najar Lopes, É.S.; Pellizzer Gabriel, L. Polyurethane Fibrous Membranes Tailored by Rotary Jet Spinning for Tissue Engineering Applications. *J. Appl. Polym. Sci.* **2020**, *137*, 48455.
93. Guner, M.B.; Dalgic, A.D.; Tezcaner, A.; Yilanci, S.; Keskin, D. A Dual-Phase Scaffold Produced by Rotary Jet Spinning and Electrospinning for Tendon Tissue Engineering. *Biomed. Mater.* **2020**, *15*, 065014.
94. Chang, H.; Liu, Q.; Zimmerman, J.F.; Lee, K.Y.; Jin, Q.; Peters, M.M.; Rosnach, M.; Choi, S.; Kim, S.L.; Ardoña, H.A.M.; et al. Recreating the Heart's Helical Structure-Function Relationship with Focused Rotary Jet Spinning. *Science* **2022**, *377*, 180–185.
95. Bitay, E.; Gergely, A.L.; Kántor, J.; Szabó, Z.I. Evaluation of Lapatinib-Loaded Microfibers Prepared by Centrifugal Spinning. *Polymers* **2022**, *14*, 5557.
96. Robert, M.; Shambaugh, L. A Macroscopic View of the Melt-Blowing Process for Producing Microfibers. *Ind. Eng. Chem. Res.* **2002**, *27*, 2363–2372.
97. Drabek, J.; Zatloukal, M. Meltblown Technology for Production of Polymeric Microfibers/Nanofibers: A Review. *Phys. Fluids* **2019**, *31*, 091301.
98. Hoda, N.; Mert, F.; Kara, F.; Atasagun, H.G.; Bhat, G.S. Effect of Process Parameters on Fiber Diameter and Fiber Distribution of Melt-Blown Polypropylene Microfibers Produced by Biax Line. *Fibers Polym.* **2021**, *22*, 285–293.
99. Liu, G.; Guan, J.; Wang, X.; Yu, J.; Ding, B. Polylactic Acid (PLA) Melt-Blown Nonwovens with Superior Mechanical Properties. *ACS Sustain. Chem. Eng.* **2023**, *11*, 4279–4288.
100. Jin, K.; Kim, S.S.; Xu, J.; Bates, F.S.; Ellison, C.J. Melt-Blown Cross-Linked Fibers from Thermally Reversible Diels–Alder Polymer Networks. *ACS Macro Lett.* **2018**, *7*, 1339–1345.
101. Sun, G.; Han, W.; Wang, Y.; Xin, S.; Yang, J.; Zou, F.; Wang, X.; Xiao, C. Overview of the Fiber Dynamics during Melt Blowing. *Ind. Eng. Chem. Res.* **2022**, *61*, 1004–1021.
102. Dzierzkowska, E.; Scisłowska-Czarnecka, A.; Kudzin, M.; Boguń, M.; Szatkowski, P.; Gajek, M.; Kornaus, K.; Chadzinska, M.; Stodolak-Zych, E. Effects of Process Parameters on Structure and Properties of Melt-Blown Poly(Lactic Acid) Nonwovens for Skin Regeneration. *J. Funct. Biomater.* **2021**, *12*, 16.
103. Wang, R.; Zhang, H.; Cao, Y.; Zhai, Q.; Hu, J.; Zhen, Q.; Qian, X. Preparation of PLA/PEG@SDS Microfibers-Based Nonwovens via Melt-Blown Process Parameters: Wound Dressings with Enhanced Water Wetting Performance. *J. Appl. Polym. Sci.* **2023**, *140*, 54234.
104. Brochocka, A.; Nowak, A.; Majchrzycka, K.; Puchalski, M.; Sztajnowski, S. Multifunctional Polymer Composites Produced by Melt-Blown Technique to Use in Filtering Respiratory Protective Devices. *Materials* **2020**, *13*, 712.
105. González-Sánchez, A.; Rosas-Macías, R.; Hernández-Bautista, J.E.; Valdez-Garza, J.A.; Rodríguez-Fuentes, N.; Soriano-Corral, F.; Ledezma-Pérez, A.S.; Ávila-Orta, C.A.; Cruz-Delgado, V.J. Antimicrobial Properties of Polyester/Copper Nanocomposites by Melt-Spinning and Melt-Blowing Techniques. *Textiles* **2024**, *4*, 1–16.
106. Kang, Y.O.; Im, J.N.; Park, W.H. Morphological and Permeable Properties of Antibacterial Double-Layered Composite Nonwovens Consisting of Microfibers and Nanofibers. *Compos. Part B: Eng.* **2015**, *75*, 256–263.
107. Volpi, M.; Paradiso, A.; Walejewska, E.; Gargioli, C.; Costantini, M.; Swieszkowski, W. Automated Microfluidics-Assisted Hydrogel-Based Wet-Spinning for the Biofabrication of Biomimetic Engineered Myotendinous Junction. *Adv. Healthc. Mater.* **2024**, *13*, 2402075.

108. Lavin, D.M.; Stefani, R.M.; Zhang, L.; Furtado, S.; Hopkins, R.A.; Mathiowitz, E. Multifunctional Polymeric Microfibers with Prolonged Drug Delivery and Structural Support Capabilities. *Acta Biomater.* **2012**, *8*, 1891–1900.
109. Wang, C.; Li, Y.; Yu, H.Y.; Abdalkarim, S.Y.H.; Zhou, J.; Yao, J.; Zhang, L. Continuous Meter-Scale Wet-Spinning of Cornlike Composite Fibers for Eco-Friendly Multifunctional Electronics. *ACS Appl. Mater. Interfaces* **2021**, *13*, 40953–40963.
110. Paradiso, A.; Volpi, M.; Martinez, D.C.; Jaroszewicz, J.; Costantini, M.; Swieszkowski, W. Engineering Biomimetic Microvascular Capillary Networks in Hydrogel Fibrous Scaffolds via Microfluidics-Assisted Co-Axial Wet-Spinning. *ACS Appl. Mater. Interfaces* **2024**, *16*, 65927–65941.
111. Lüken, A.; Geiger, M.; Steinbeck, L.; Joel, A.-C.; Lampert, A.; Linkhorst, J.; Wessling, M.; Lüken, A.; Geiger, M.; Steinbeck, L.; et al. Biocompatible Micron-Scale Silk Fibers Fabricated by Microfluidic Wet Spinning. *Adv. Healthc. Mater.* **2021**, *10*, 2100898.
112. Lee, B.R.; Lee, K.H.; Kang, E.; Kim, D.S.; Lee, S.H. Microfluidic Wet Spinning of Chitosan-Alginate Microfibers and Encapsulation of HepG2 Cells in Fibers. *Biomicrofluidics* **2011**, *5*, 022208.
113. Xu, B.; Du, L.; Zhang, J.; Zhu, M.; Ji, S.; Zhang, Y.; Kong, D.; Ma, X.; Yang, Q.; Wang, L. Circumferentially Oriented Microfiber Scaffold Prepared by Wet-Spinning for Tissue Engineering of Annulus Fibrosus. *RSC Adv.* **2015**, *5*, 42705–42713.
114. Li, Y.; Hu, H.; Salim, T.; Cheng, G.; Lam, Y.M.; Ding, J. Flexible Wet-Spun PEDOT:PSS Microfibers Integrating Thermal-Sensing and Joule Heating Functions for Smart Textiles. *Polymers* **2023**, *15*, 3432.
115. Zeng, H.; Gao, C.; Yu, Y.; Jiang, M.; Deng, T.; Zhu, J. Wet Spinning Enabled Advanced PEDOT:PSS Composite Fibers for Smart Devices. *Accounts Mater. Res.* **2025**, *6*, 952–963.
116. Lavin, D.M.; Zhang, L.; Furtado, S.; Hopkins, R.A.; Mathiowitz, E. Effects of Protein Molecular Weight on the Intrinsic Material Properties and Release Kinetics of Wet Spun Polymeric Microfiber Delivery Systems. *Acta Biomater.* **2013**, *9*, 4569–4578.
117. Han, L.H.; Yu, S.; Wang, T.; Behn, A.W.; Yang, F. Microribbon-Like Elastomers for Fabricating Macroporous and Highly Flexible Scaffolds That Support Cell Proliferation in 3D. *Adv. Funct. Mater.* **2013**, *23*, 346–358.
118. Wang, L.; Zhang, J.; Wang, L.; Zhu, M.; Xiao, N.; Kong, D. Wet-Spun Poly(ε-Caprolactone) Microfiber Scaffolds for Oriented Growth and Infiltration of Smooth Muscle Cells. *Mater. Lett.* **2014**, *132*, 59–62.
119. Zheng, T.; Pour Shahid Saeed Abadi, P.; Seo, J.; Cha, B.H.; Miccoli, B.; Li, Y.C.; Park, K.; Park, S.; Choi, S.J.; Bayaniahangar, R.; et al. Biocompatible Carbon Nanotube-Based Hybrid Microfiber for Implantable Electrochemical Actuator and Flexible Electronic Applications. *ACS Appl. Mater. Interfaces* **2019**, *11*, 20615–20627.
120. Puppi, D.; Braccini, S.; Battisti, A.; Manariti, A.; Pecorini, G.; Samal, S.K. Additive Manufacturing of Wet-Spun Polysulfone Medical Implants. *ACS Biomater. Sci. Eng.* **2023**, *9*, 5418–5429.
121. Yang, Y.; Sun, J.; Liu, X.; Guo, Z.; He, Y.; Wei, D.; Zhong, M.; Guo, L.; Fan, H.; Zhang, X. Wet-Spinning Fabrication of Shear-Patterned Alginate Hydrogel Microfibers and the Guidance of Cell Alignment. *Regen. Biomater.* **2017**, *4*, 299–307.
122. Gong, R.; Dong, Y.; Ge, D.; Miao, Z.; Yu, H.Y. Wet Spinning Fabrication of Robust and Uniform Intrinsically Conductive Cellulose Nanofibril/Silk Conductive Fibers as Bifunctional Strain/Humidity Sensor in Potential Smart Dressing. *Adv. Fiber Mater.* **2024**, *6*, 993–1007.
123. Su, R.; Ai, Y.; Wang, J.; Wu, L.; Sun, H.; Ding, M.; Xie, R.; Liang, Q. Engineered Microfibers for Tissue Engineering. *ACS Appl. Bio Mater.* **2024**.
124. Ren, N.; Qiao, A.; Cui, M.; Huang, R.; Qi, W.; Su, R. Design and Fabrication of Nanocellulose-Based Microfibers by Wet Spinning. *Chem. Eng. Sci.* **2023**, *282*, 119320.
125. Pullagura, B.K.; Gundabala, V. Microfluidics-Based On-Demand Generation of Nonwoven and Single Polymer Microfibers. *Langmuir* **2020**, *36*, 1227–1234.
126. Abrishamkar, A.; Nilghaz, A.; Saadatmand, M.; Naeimirad, M.; Demello, A.J. Microfluidic-Assisted Fiber Production: Potentials, Limitations, and Prospects. *Biomicrofluidics* **2022**, *16*, 61504.
127. Hwang, C.M.; Khademhosseini, A.; Park, Y.; Sun, K.; Lee, S.H. Microfluidic Chip-Based Fabrication of PLGA Microfiber Scaffolds for Tissue Engineering. *Langmuir* **2008**, *24*, 6845–6851.
128. Guo, J.; Yu, Y.; Wang, H.; Zhang, H.; Zhang, X.; Zhao, Y. Conductive Polymer Hydrogel Microfibers from Multiflow Microfluidics. *Small* **2019**, *15*, 1805162.
129. Zhao, M.; Liu, H.; Zhang, X.; Wang, H.; Tao, T.; Qin, J. A Flexible Microfluidic Strategy to Generate Grooved Microfibers for Guiding Cell Alignment. *Biomater. Sci.* **2021**, *9*, 4880–4890.
130. Lee, D.; Yang, K.; Xie, J. Innovative Microfluidic Technologies in Precision Research and Therapy Development in Diabetic Neuropathy: A Narrative Review. *Adv. Technol. Neurosci.* **2024**, *1*, 123–137.
131. Liu, W.; Xu, Z.; Sun, L.; Guo, P.; Zeng, C.; Wang, C.; Zhang, L. Polymerization-Induced Phase Separation Fabrication: A Versatile Microfluidic Technique to Prepare Microfibers with Various Cross Sectional Shapes and Structures. *Chem. Eng. J.* **2017**, *315*, 25–34.

132. Lu, L.; Fan, S.; Niu, Q.; Peng, Q.; Geng, L.; Yang, G.; Shao, H.; Hsiao, B.S.; Zhang, Y. Strong Silk Fibers Containing Cellulose Nanofibers Generated by a Bioinspired Microfluidic Chip. *ACS Sustain. Chem. Eng.* **2019**, *7*, 14765–14774.
133. Zhao, Z.; Wang, J.; Yuan, H.; Xu, J.; Gao, H.; Nie, Y. Preparation of Antibacterial Biobased Fibers by Triaxial Microfluidic Spinning Technology Using Ionic Liquids as the Solvents. *ACS Appl. Mater. Interfaces* **2024**, *16*, 18063–18074.
134. Chen, N.; Wei, W.; Ning, N.; Wu, H.; Tian, M. All-Polymeric Stretchable Conductive Fiber with Versatile Intelligent Wearable Applications via Microfluidic Spinning Technology. *Chem. Eng. J.* **2024**, *487*, 150741.
135. Geiger, M.; Frank, J.; Schmitz, F.; Paul, R.; Rauer, S.B.; Koulchitsky, S.; Lampert, A.; Linkhorst, J.; Wessling, M. Microfluidic Spinning of PEDOT:PSS Microfibers for Nerve Guidance Conduits. *Adv. Mater. Technol.* **2025**, 2401996.
136. Shang, L.; Fu, F.; Cheng, Y.; Yu, Y.; Wang, J.; Gu, Z.; Zhao, Y. Bioinspired Multifunctional Spindle-Knotted Microfibers from Microfluidics. *Small* **2017**, *13*, 1600286.
137. Peng, Y.; Shang, Y.; Che, J.; Yu, Y.; Zhao, Y.; Gu, X. Multifunctional Analgesic Sutures from Microfluidic Spinning Technology. *Adv. Healthc. Mater.* **2025**, *14*, 2402420.
138. Masuda, A.; Kurashina, Y.; Tani, H.; Soma, Y.; Muramatsu, J.; Itai, S.; Tohyama, S.; Onoe, H. Maturation of Human IPSC-Derived Cardiac Microfiber with Electrical Stimulation Device. *Adv. Healthc. Mater.* **2024**, *13*, 2303477.
139. Liu, J.D.; Du, X.Y.; Chen, S. A Phase Inversion-Based Microfluidic Fabrication of Helical Microfibers towards Versatile Artificial Abdominal Skin. *Angew. Chem. Int. Ed.* **2021**, *60*, 25089–25096.
140. Magnani, J.S.; Montazami, R.; Hashemi, N.N. Recent Advances in Microfluidically Spun Microfibers for Tissue Engineering and Drug Delivery Applications. *Annu. Rev. Anal. Chem.* **2021**, *14*, 185–205.
141. Jun, Y.; Kang, E.; Chae, S.; Lee, S.H. Microfluidic Spinning of Micro- and Nano-Scale Fibers for Tissue Engineering. *Lab. Chip* **2014**, *14*, 2145–2160.
142. Cheng, Y.; Yu, Y.; Fu, F.; Wang, J.; Shang, L.; Gu, Z.; Zhao, Y. Controlled Fabrication of Bioactive Microfibers for Creating Tissue Constructs Using Microfluidic Techniques. *ACS Appl. Mater. Interfaces* **2016**, *8*, 1080–1086.
143. Huang, Q.; He, F.; Yu, J.; Zhang, J.; Du, X.; Li, Q.; Wang, G.; Yu, Z.; Chen, S. Microfluidic Spinning-Induced Heterotypic Bead-on-String Fibers for Dual-Cargo Release and Wound Healing. *J. Mater. Chem. B* **2021**, *9*, 2727–2735.
144. Lin, H.H.; Chao, P.H.G.; Tai, W.C.; Chang, P.C. 3d-Printed Collagen-Based Waveform Microfibrous Scaffold for Periodontal Ligament Reconstruction. *Int. J. Mol. Sci.* **2021**, *22*, 7725.
145. Bojedla, S.S.R.; Kattimani, V.; Alwala, A.M.; Nikzad, M.; Masood, S.H.; Riza, S.; Pati, F. Augmented Repair and Regeneration of Critical Size Rabbit Calvaria Defects with 3D Printed Silk Fibroin Microfibers Reinforced PCL Composite Scaffolds. *Biomed. Mater. Devices* **2023**, *1*, 942–955.
146. Luo, Z.; Lian, L.; Stocco, T.; Guo, J.; Mei, X.; Cai, L.; Andrabi, S.M.; Su, Y.; Tang, G.; Ravanbakhsh, H.; et al. 3D Assembly of Cryo(Bio)Printed Modular Units for Shelf-Ready Scalable Tissue Fabrication. *Adv. Funct. Mater.* **2024**, *34*, 2309173.
147. Jiang, X.; Kong, Y.; Kuss, M.; Weisenburger, J.; Haider, H.; Harms, R.; Shi, W.; Liu, B.; Xue, W.; Dong, J.; et al. 3D Bioprinting of Multilayered Scaffolds with Spatially Differentiated ADMSCs for Rotator Cuff Tendon-to-Bone Interface Regeneration. *Appl. Mater. Today* **2022**, *27*, 101510.
148. Heinrich, M.A.; Liu, W.; Jimenez, A.; Yang, J.; Akpek, A.; Liu, X.; Pi, Q.; Mu, X.; Hu, N.; Schiffelers, R.M.; et al. 3D Bioprinting: From Benches to Translational Applications. *Small* **2019**, *15*, 1805510.
149. Lee, D.; Tran, H.Q.; Sharma, N.S.; Andrabi, S.M.; Yan, Z.; Killeen, A.C.; Reinhardt, R.A.; Zhu, W.; Xie, J. 3D-Printed Microfluidic Platform for Creating Porous Nanofibrous Microspheres to Regulate Cell Response and Enhance Tissue Regeneration. *Small* **2025**, 2502033.
150. Prendergast, M.E.; Burdick, J.A. Recent Advances in Enabling Technologies in 3D Printing for Precision Medicine. *Adv. Mater.* **2020**, *32*, 1902516.
151. Jiang, Z.; Diggle, B.; Tan, M.L.; Viktorova, J.; Bennett, C.W.; Connal, L.A. Extrusion 3D Printing of Polymeric Materials with Advanced Properties. *Adv. Sci.* **2020**, *7*, 2001379.
152. Zhou, L.Y.; Fu, J.; He, Y. A Review of 3D Printing Technologies for Soft Polymer Materials. *Adv. Funct. Mater.* **2020**, *30*, 2000187.
153. Zhou, X.; Yu, X.; You, T.; Zhao, B.; Dong, L.; Huang, C.; Zhou, X.; Xing, M.; Qian, W.; Luo, G.; et al. 3D Printing-Based Hydrogel Dressings for Wound Healing. *Adv. Sci.* **2024**, *11*, 2404580.
154. Yu, C.; Zhu, W.; Sun, B.; Mei, D.; Gou, M.; Chen, S. Modulating Physical, Chemical, and Biological Properties in 3D Printing for Tissue Engineering Applications. *Appl. Phys. Rev.* **2018**, *5*, 41107.
155. Diloksumpan, P.; De Ruijter, M.; Castilho, M.; Gbureck, U.; Vermonden, T.; Van Weeren, P.R.; Malda, J.; Levato, R. Combining Multi-Scale 3D Printing Technologies to Engineer Reinforced Hydrogel-Ceramic Interfaces. *Biofabrication* **2020**, *12*, 025014.
156. Cedillo-Servin, G.; Dahri, O.; Meneses, J.; van Duijn, J.; Moon, H.; Sage, F.; Silva, J.; Pereira, A.; Magalhães, F.D.; Malda, J.; et al. 3D Printed Magneto-Active Microfiber Scaffolds for Remote Stimulation and Guided Organization of 3D In Vitro Skeletal Muscle Models. *Small* **2024**, *20*, 2307178.

157. Ainsworth, M.J.; Lotz, O.; Gilmour, A.; Zhang, A.; Chen, M.J.; McKenzie, D.R.; Bilek, M.M.M.; Malda, J.; Akhavan, B.; Castilho, M. Covalent Protein Immobilization on 3D-Printed Microfiber Meshes for Guided Cartilage Regeneration. *Adv. Funct. Mater.* **2023**, *33*, 2206583.
158. Shen, Y.; Pan, Y.; Liang, F.; Song, J.; Yu, X.; Cui, J.; Cai, G.; El-Newehy, M.; Abdulhameed, M.M.; Gu, H.; et al. Development of 3D Printed Electrospun Vascular Graft Loaded with Tetramethylpyrazine for Reducing Thrombosis and Restraining Aneurysmal Dilatation. *Burn. Trauma.* **2024**, *12*, 8.
159. Iturriaga, L.; Van Gordon, K.D.; Larrañaga-Jaurrieta, G.; Camarero-Espinosa, S. Strategies to Introduce Topographical and Structural Cues in 3D-Printed Scaffolds and Implications in Tissue Regeneration. *Adv. NanoBiomed Res.* **2021**, *1*, 2100068.
160. Deng, X.; Qi, C.; Meng, S.; Dong, H.; Wang, T.; Liu, Z.; Kong, T. All-Aqueous Embedded 3D Printing for Freeform Fabrication of Biomimetic 3D Constructs. *Adv. Mater.* **2024**, *36*, 2406825.
161. Wang, C.; Shahriar, S.M.S.; Su, Y.; Hayati, F.; Andrabi, S.M.; Xiao, Y.; Busquets, M.E.; Sharma, N.S.; Xie, J. Three-Dimensional Bioprinting of Biphasic Nanobioink for Enhanced Diabetic Wound Healing. *ACS Nano* **2025**, *19*, 21411–21425.
162. von Witzleben, M.; Stoppe, T.; Ahlfeld, T.; Bernhardt, A.; Polk, M.L.; Bornitz, M.; Neudert, M.; Gelinsky, M. Biomimetic Tympanic Membrane Replacement Made by Melt Electrowriting. *Adv. Healthc. Mater.* **2021**, *10*, 2002089.
163. Hrynevich, A.; Elçi, B.; Haigh, J.N.; McMaster, R.; Youssef, A.; Blum, C.; Blunk, T.; Hochleitner, G.; Groll, J.; Dalton, P.D. Dimension-Based Design of Melt Electrowritten Scaffolds. *Small* **2018**, *14*, 1800232.
164. Mueller, K.M.A.; Hangleiter, A.; Burkhardt, S.; Rojas-González, D.M.; Kwade, C.; Pammer, S.T.; Leonhardt, S.; Mela, P. Filament-Based Melt Electrowriting Enables Dual-Mode Additive Manufacturing for Multiscale Constructs. *Small Sci.* **2023**, *3*, 2300021.
165. Mondadori, C.; Chandrakar, A.; Lopa, S.; Wieringa, P.; Talò, G.; Perego, S.; Lombardi, G.; Colombini, A.; Moretti, M.; Moroni, L. Assessing the Response of Human Primary Macrophages to Defined Fibrous Architectures Fabricated by Melt Electrowriting. *Bioact. Mater.* **2023**, *21*, 209–222.
166. Florczak, S.; Lorson, T.; Zheng, T.; Mrlik, M.; Hutmacher, D.W.; Higgins, M.J.; Luxenhofer, R.; Dalton, P.D. Melt Electrowriting of Electroactive Poly(Vinylidene Difluoride) Fibers. *Polym. Int.* **2019**, *68*, 735–745.
167. Mueller, K.M.A.; Unterrainer, A.; Rojas-González, D.M.; De-Juan-Pardo, E.; Willner, M.S.; Herzen, J.; Mela, P. Introducing Controlled Microporosity in Melt Electrowriting. *Adv. Mater. Technol.* **2023**, *8*, 2201158.
168. Sarfraz, M.H.; Chen, Y.; Xie, M.; He, Y. 3D Printing of High-Resolution Multi-Layer Scaffolds With Melt Electrowriting. *Adv. Mater. Technol.* **2025**, 2402029.
169. Pang, L.; Paxton, N.C.; Ren, J.; Liu, F.; Zhan, H.; Woodruff, M.A.; Bo, A.; Gu, Y. Development of Mechanically Enhanced Polycaprolactone Composites by a Functionalized Titanate Nanofiller for Melt Electrowriting in 3D Printing. *ACS Appl. Mater. Interfaces* **2020**, *12*, 47993–48006.
170. Saidy, N.T.; Wolf, F.; Bas, O.; Keijdener, H.; Hutmacher, D.W.; Mela, P.; De-Juan-Pardo, E.M. Biologically Inspired Scaffolds for Heart Valve Tissue Engineering via Melt Electrowriting. *Small* **2019**, *15*, 1900873.
171. Saiz, P.G.; Reizabal, A.; Vilas-Vilela, J.L.; Dalton, P.D.; Lanceros-Mendez, S. Materials and Strategies to Enhance Melt Electrowriting Potential. *Adv. Mater.* **2024**, *36*, 2312084.
172. Snow, F.; Doyle, S.E.; Liu, E.; Rauch, D.De; Millett, D.; Wilding-Mcbride, J.; Kita, M.; Pirogova, E.; Kapsa, R.M.I.; Quigley, A. A Detailed Guide to Melt Electro-Writing for Tissue Engineering Applications. *Biofabrication* **2025**, *17*, 042004.
173. Castilho, M.; van Mil, A.; Maher, M.; Metz, C.H.G.; Hochleitner, G.; Groll, J.; Doevendans, P.A.; Ito, K.; Sluijter, J.P.G.; Malda, J. Melt Electrowriting Allows Tailored Microstructural and Mechanical Design of Scaffolds to Advance Functional Human Myocardial Tissue Formation. *Adv. Funct. Mater.* **2018**, *28*, 1803151.
174. Kim, J.; Bakirci, E.; O'Neill, K.L.; Hrynevich, A.; Dalton, P.D. Fiber Bridging during Melt Electrowriting of Poly(ε-Caprolactone) and the Influence of Fiber Diameter and Wall Height. *Macromol. Mater. Eng.* **2021**, *306*, 2000685.
175. Kong, X.; Zhu, D.; Hu, Y.; Liu, C.; Zhang, Y.; Wu, Y.; Tan, J.; Luo, Y.; Chen, J.; Xu, T.; et al. Melt Electrowriting (MEW)-PCL Composite Three-Dimensional Exosome Hydrogel Scaffold for Wound Healing. *Mater. Des.* **2024**, *238*, 112717.
176. Luxenhofer, R.; Keßler, L.; Mirzaei, Z.; Kade, J.C. Highly Porous and Drug-Loaded Amorphous Solid Dispersion Microfiber Scaffolds of Indomethacin Prepared by Melt Electrowriting. *ACS Appl. Polym. Mater.* **2023**, *5*, 913–922.
177. Kilian, D.; Witzleben, M.von; Lanaro, M.; Wong, C.S.; Vater, C.; Lode, A.; Allenby, M.C.; Woodruff, M.A.; Gelinsky, M. 3D Plotting of Calcium Phosphate Cement and Melt Electrowriting of Polycaprolactone Microfibers in One Scaffold: A Hybrid Additive Manufacturing Process. *J. Funct. Biomater.* **2022**, *13*, 75.
178. Loewner, S.; Heene, S.; Baroth, T.; Heymann, H.; Cholewa, F.; Blume, H.; Blume, C. Recent Advances in Melt Electro Writing for Tissue Engineering for 3D Printing of Microporous Scaffolds for Tissue Engineering. *Front. Bioeng. Biotechnol.* **2022**, *10*, 896719.
179. Mueller, K.M.A.; Ahrens, C.; Grefen, L.; Mansi, S.; Arcuti, D.; De-Juan-Pardo, E.; Kur, F.; Hagl, C.; Mela, P. Programmable Compliance in Small-Diameter Vascular Grafts by Design of Melt-Electrowritten Scaffold Architectures for *In Situ* Tissue Engineering. *Adv. Healthc. Mater.* **2025**, 02038.

180. Lai, X.; Huang, J.; Huang, S.; Wang, J.; Zheng, Y.; Luo, Y.; Tang, L.; Gao, B.; Tang, Y. Antibacterial and Osteogenic Dual-Functional Micronano Composite Scaffold Fabricated via Melt Electrowriting and Solution Electrospinning for Bone Tissue Engineering. *ACS Appl. Mater. Interfaces* **2024**, *16*, 37707–37721.
181. Janssen, R.; Schulze, H.S.; Nelissen, C.M.L.; Valverde, M.G.; Hrynevich, A.; Jong, G.A.H.; Genderen, A.M.; Malda, J.; Bastiaan-Net, S.; Willemsen, L.E.M.; et al. Half-Pipe Melt Electrowritten Scaffolds Support Engineering of an Immunocompetent Hydrogel-Embedded Intestine-on-a-Chip. *Adv. Sci.* **2025**, 07132.
182. Shahverdi, M.; Seifi, S.; Akbari, A.; Mohammadi, K.; Shamloo, A.; Movahhedy, M.R. Melt Electrowriting of PLA, PCL, and Composite PLA/PCL Scaffolds for Tissue Engineering Application. *Sci. Rep.* **2022**, *12*, 19935.
183. Ranat, K.; Phan, H.; Ellythy, S.; Kenter, M.; Akkouch, A. Advancements in Musculoskeletal Tissue Engineering: The Role of Melt Electrowriting in 3D-Printed Scaffold Fabrication. *J. Funct. Biomater.* **2025**, *16*, 163.
184. Ross, M.T.; Kilian, D.; Lode, A.; Ren, J.; Allenby, M.C.; Gelinsky, M.; Woodruff, M.A. Using Melt-Electrowritten Microfibres for Tailoring Scaffold Mechanics of 3D Bioprinted Chondrocyte-Laden Constructs. *Bioprinting* **2021**, *23*, 00158.
185. Sun, T.; Lu, H.; Luposchainsky, S.; Yang, L.; Zhang, X.; Hirano, A.; Nakano, Y.; Shinichi, Y.; Xu, H. Challenges of High-Temperature Melt Electrowriting: A Study of EVOH Printing. *Polymer* **2025**, *331*, 128518.
186. Chandrakar, A.; van der Spoel, M.; Beeren, I.; Giacomini, F.; Mondadori, C.; Eischen-Loges, M.J.; Truckenmüller, R.; Moroni, L.; Wieringa, P. Melt Electrowriting of Hydrophilic/Hydrophobic Multiblock Copolymers for Bone Tissue Regeneration. *Biomater. Adv.* **2025**, *169*, 214167.
187. Ni, Z.; Zhu, Z.; Ji, Y.; He, X.; Fu, X.; Yang, W.; Wang, Y. Biomimetic Microadhesion Guided Instant Spinning. *Nano Lett.* **2022**, *22*, 9396–9404.
188. Liu, Y.; Wang, C.; Liu, Z.; Qu, X.; Gai, Y.; Xue, J.; Chao, S.; Huang, J.; Wu, Y.; Li, Y.; et al. Self-Encapsulated Ionic Fibers Based on Stress-Induced Adaptive Phase Transition for Non-Contact Depth-of-Field Camouflage Sensing. *Nat. Commun.* **2024**, *15*, 663.
189. Zhao, Y.; Gumyusenge, A.; He, J.; Qu, G.; McNutt, W.W.; Long, Y.; Zhang, H.; Huang, L.; Diao, Y.; Mei, J.; et al. Continuous Melt-Drawing of Highly Aligned Flexible and Stretchable Semiconducting Microfibers for Organic Electronics. *Adv. Funct. Mater.* **2018**, *28*, 1705584.
190. Zhang, T.; Yin, L.; Hui, Z.; Zhang, R.; Fu, J.; Xu, H.; Zhou, J.; Hou, W.; Yao, Y.; An, J.; et al. Biomimetic Spinning of Glassy Ionogel Fibers with Tailorable Mechanical Properties for Versatile Applications. *Chem. Eng. J.* **2025**, *524*, 169443.
191. Xue, J.; Wu, T.; Dai, Y.; Xia, Y. Electrospinning and Electrospun Nanofibers: Methods, Materials, and Applications. *Chem. Rev.* **2019**, *119*, 5298–5415.
192. Yu, Y.; Fu, F.; Shang, L.; Cheng, Y.; Gu, Z.; Zhao, Y. Bioinspired Helical Microfibers from Microfluidics. *Adv. Mater.* **2017**, *29*, 1605765.
193. Lan, D.; Shang, Y.; Su, H.; Liang, M.; Liu, Y.; Li, H.; Feng, Q.; Cao, X.; Dong, H. Facile Fabrication of Hollow Hydrogel Microfiber via 3D Printing-Assisted Microfluidics and Its Application as a Biomimetic Blood Capillary. *ACS Biomater. Sci. Eng.* **2021**, *7*, 4971–4981.
194. Chen, Y.; Deng, Z.; Ouyang, R.; Zheng, R.; Jiang, Z.; Bai, H.; Xue, H. 3D Printed Stretchable Smart Fibers and Textiles for Self-Powered e-Skin. *Nano Energy* **2021**, *84*, 105866.
195. Tibbitt, M.W.; Rodell, C.B.; Burdick, J.A.; Anseth, K.S. Progress in Material Design for Biomedical Applications. *Proc. Natl. Acad. Sci.* **2015**, *112*, 14444–14451.
196. Guo, B.; Glavas, L.; Albertsson, A.C. Biodegradable and Electrically Conducting Polymers for Biomedical Applications. *Prog. Polym. Sci.* **2013**, *38*, 1263–1286.
197. Du, X.Y.; Li, Q.; Wu, G.; Chen, S. Multifunctional Micro/Nanoscale Fibers Based on Microfluidic Spinning Technology. *Adv. Mater.* **2019**, *31*, 1903733.
198. Song, R.; Murphy, M.; Li, C.; Ting, K.; Soo, C.; Zheng, Z. Current Development of Biodegradable Polymeric Materials for Biomedical Applications. *Drug Des. Devel. Ther.* **2018**, *12*, 3117–3145.
199. Shahriar, S.M.S.; McCarthy, A.D.; Andrabi, S.M.; Su, Y.; Polavoram, N.S.; John, J.V.; Matis, M.P.; Zhu, W.; Xie, J. Mechanically Resilient Hybrid Aerogels Containing Fibers of Dual-Scale Sizes and Knotty Networks for Tissue Regeneration. *Nat. Commun.* **2024**, *15*, 1080.
200. Yu, Y.; Jin, B.; Chen, J.; Lou, C.; Guo, J.; Yang, C.; Zhao, Y. Nerve-on-a-Chip Derived Biomimicking Microfibers for Peripheral Nerve Regeneration. *Adv. Sci.* **2023**, *10*, 2207536.
201. Mondal, B.; Mandal, D. Geometry-Modulated All Organic 3D Printed Smart PLA Fibers for Flextension Amplified Giant Mechanical Energy Harvesting and Machine Learning Assisted Pressure Mapping. *Chem. Eng. J.* **2024**, *496*, 154281.
202. Shao, L.; Gao, Q.; Xie, C.; Fu, J.; Xiang, M.; He, Y. Bioprinting of Cell-Laden Microfiber: Can It Become a Standard Product? *Adv. Healthc. Mater.* **2019**, *8*, 1900014.
203. Dias, Y.J.; Robles, J.R.; Sinha-Ray, S.; Abiade, J.; Pourdeyhimi, B.; Niemczyk-Soczynska, B.; Kolbuk, D.; Sajkiewicz, P.; Yarin, A.L. Solution-Blown Poly(Hydroxybutyrate) and ε-Poly-l-Lysine Submicro- and Microfiber-Based Sustainable Nonwovens with Antimicrobial Activity for Single-Use Applications. *ACS Biomater. Sci. Eng.* **2021**, *7*, 3980–3992.

204. Yuan, S.; Li, Z.; Song, L.; Shi, H.; Luan, S.; Yin, J. Liquid-Infused Poly(Styrene-*b*-Isobutylene-*b*-Styrene) Microfiber Coating Prevents Bacterial Attachment and Thrombosis. *ACS Appl. Mater. Interfaces* **2016**, *8*, 21214–21220.
205. Miele, D.; Nomicisio, C.; Musitelli, G.; Boselli, C.; Icaro Cornaglia, A.; Sànchez-Espejo, R.; Vigani, B.; Viseras, C.; Rossi, S.; Sandri, G. Design and Development of Polydioxanone Scaffolds for Skin Tissue Engineering Manufactured via Green Process. *Int. J. Pharm.* **2023**, *634*, 122669.
206. Jia, Z.; Gong, J.; Zeng, Y.; Ran, J.; Liu, J.; Wang, K.; Xie, C.; Lu, X.; Wang, J. Bioinspired Conductive Silk Microfiber Integrated Bioelectronic for Diagnosis and Wound Healing in Diabetes. *Adv. Funct. Mater.* **2021**, *31*, 2010461.
207. Guo, J.; Yu, Y.; Zhang, H.; Sun, L.; Zhao, Y. Elastic MXene Hydrogel Microfiber-Derived Electronic Skin for Joint Monitoring. *ACS Appl. Mater. Interfaces* **2021**, *13*, 47800–47806.
208. Yang, X.; Cai, H.; Li, R.; He, Z.; Liu, Y.; Wu, J.; Xu, Z.; Yang, L.; Zhu, Z.; Wang, J.; et al. Macro- or Microfiber Scaffolds with Different Fiber Arrangements: Determining the Best Design for Osteogenesis. *Ind. Eng. Chem. Res.* **2024**, *63*, 7540–7555.
209. Tian, Y.; Wang, J.; Wang, L. Microfluidic Fabrication of Bioinspired Cavity-Microfibers for 3D Scaffolds. *ACS Appl. Mater. Interfaces* **2018**, *10*, 29219–29226.
210. Han, W.; Wang, L.; Li, Q.; Ma, B.; He, C.; Guo, X.; Nie, J.; Ma, G. A Review: Current Status and Emerging Developments on Natural Polymer-Based Electrospun Fibers. *Macromol. Rapid Commun.* **2022**, *43*, 2200456.
211. Satchanska, G.; Davidova, S.; Petrov, P.D. Natural and Synthetic Polymers for Biomedical and Environmental Applications. *Polymers* **2024**, *16*, 1159.
212. Wei, S.; Hu, Q.; Dong, J.; Sun, Y.; Bai, J.; Shan, H.; Gao, X.; Sheng, L.; Dai, J.; Jiang, F.; et al. Mechanically Enhanced Biodegradable Scaffold Based on SF Microfibers for Repairing Bone Defects in the Distal Femur of Rats. *Int. J. Biol. Macromol.* **2024**, *282*, 137372.
213. Moghimi, N.; Kamaraj, M.; Zehtabi, F.; Amin Yavari, S.; Kohandel, M.; Khademhosseini, A.; John, J.V. Development of Bioactive Short Fiber-Reinforced Printable Hydrogels with Tunable Mechanical and Osteogenic Properties for Bone Repair. *J. Mater. Chem. B* **2024**, *12*, 2818–2830.
214. Tian, H.; Tang, Z.; Zhuang, X.; Chen, X.; Jing, X. Biodegradable Synthetic Polymers: Preparation, Functionalization and Biomedical Application. *Prog. Polym. Sci.* **2012**, *37*, 237–280.
215. Ye, C.; Zhao, J.; Zheng, Y.; Wu, C.; Chen, Y.; Wu, H.; An, X.; Huang, M.; Wang, S. Preparation of Poly(Lactic-Co-Glycolic Acid)-Based Composite Microfibers for Postoperative Treatment of Tumor in NIR I and NIR II Biowindows. *Macromol. Biosci.* **2018**, *18*, 1800206.
216. Jung, J.H.; Choi, C.H.; Chung, S.; Chung, Y.M.; Lee, C.S. Microfluidic Synthesis of a Cell Adhesive Janus Polyurethane Microfiber. *Lab. Chip* **2009**, *9*, 2596–2602.
217. Ranjan, V.D.; Zeng, P.; Li, B.; Zhang, Y. *In Vitro* Cell Culture in Hollow Microfibers with Porous Structures. *Biomater. Sci.* **2020**, *8*, 2175–2188.
218. Dores, R.; Oliveira, M.S.N.; Bimbo, L.M. Microfluidic Manufacture of Composite Fibers for Biomedical Applications. *Adv. Mater. Technol.* **2025**, *10*, 2400976.
219. Ramakrishna, S.; Mayer, J.; Wintermantel, E.; Leong, K.W. Biomedical Applications of Polymer-Composite Materials: A Review. *Compos. Sci. Technol.* **2001**, *61*, 1189–1224.
220. De las Heras Alarcón, C.; Pennadam, S.; Alexander, C. Stimuli Responsive Polymers for Biomedical Applications. *Chem. Soc. Rev.* **2005**, *34*, 276–285.
221. Delaey, J.; Dubruel, P.; Van Vlierberghe, S. Shape-Memory Polymers for Biomedical Applications. *Adv. Funct. Mater.* **2020**, *30*, 1909047.
222. Buratti, E.; Sanzari, I.; Dinelli, F.; Prodromakis, T.; Bertoldo, M. Formation and Stability of Smooth Thin Films with Soft Microgels Made of Poly(N-Isopropylacrylamide) and Poly(Acrylic Acid). *Polymers* **2020**, *12*, 2638.
223. Wu, R.; Kim, T. Review of Microfluidic Approaches for Fabricating Intelligent Fiber Devices: Importance of Shape Characteristics. *Lab. Chip* **2021**, *21*, 1217–1240.
224. Chen, C.; Chen, X.; Zhang, H.; Zhang, Q.; Wang, L.; Li, C.; Dai, B.; Yang, J.; Liu, J.; Sun, D. Electrically-Responsive Core-Shell Hybrid Microfibers for Controlled Drug Release and Cell Culture. *Acta Biomater.* **2017**, *55*, 434–442.
225. Zou, W.; Yan, Y.; Fang, J.; Yang, Y.; Liang, J.; Deng, K.; Yao, J.; Wei, Z. Biomimetic Superhelical Conducting Microfibers with Homochirality for Enantioselective Sensing. *J. Am. Chem. Soc.* **2014**, *136*, 578–581.
226. Xie, R.; Xu, P.; Liu, Y.; Li, L.; Luo, G.; Ding, M.; Liang, Q.; Xie, R.; Xu, P.; Liu, Y.; et al. Necklace-Like Microfibers with Variable Knots and Perfusable Channels Fabricated by an Oil-Free Microfluidic Spinning Process. *Adv. Mater.* **2018**, *30*, 1705082.
227. Liu, Y.; Yang, L.; Chen, G.; Liu, Z.; Lu, T.; Yang, Y.; Yu, J.; Kang, D.; Yan, W.; He, M.; et al. PBAT Hollow Porous Microfibers Prepared via Electrospinning and Their Functionalization for Potential Peptide Release. *Mater. Des.* **2021**, *207*, 109880.

228. Cao, X.; Chen, W.; Zhao, P.; Yang, Y.; Yu, D.G. Electrospun Porous Nanofibers: Pore−Forming Mechanisms and Applications for Photocatalytic Degradation of Organic Pollutants in Wastewater. *Polymers* **2022**, *14*, 3990.
229. Xing, J.; Zhang, W.; Sun, S.; Liu, Z. Preparation of Porous Polylactic Acid Nanofibers and Application in Non-Electret High-Efficiency Filtration Composites. *RSC Adv.* **2024**, *14*, 14857–14867.
230. Wagner, A.; Poursorkhabi, V.; Mohanty, A.K.; Misra, M. Analysis of Porous Electrospun Fibers from Poly(l-Lactic Acid)/Poly(3-Hydroxybutyrate-Co-3-Hydroxyvalerate) Blends. *ACS Sustain. Chem. Eng.* **2014**, *2*, 1976–1982.
231. Katsogiannis, K.A.G.; Vladisavljević, G.T.; Georgiadou, S. Porous Electrospun Polycaprolactone Fibers: Effect of Process Parameters. *J. Polym. Sci. Part. B Polym. Phys.* **2016**, *54*, 1878–1888.
232. Huang, C.; Thomas, N.L. Fabricating Porous Poly(Lactic Acid) Fibres via Electrospinning. *Eur. Polym. J.* **2018**, *99*, 464–476.
233. Katsogiannis, K.A.G.; Vladisavljević, G.T.; Georgiadou, S. Porous Electrospun Polycaprolactone (PCL) Fibres by Phase Separation. *Eur. Polym. J.* **2015**, *69*, 284–295.
234. McNamara, M.C.; Niaraki-Asli, A.E.; Guo, J.; Okuzono, J.; Montazami, R.; Hashemi, N.N. Enhancing the Conductivity of Cell-Laden Alginate Microfibers with Aqueous Graphene for Neural Applications. *Front. Mater.* **2020**, *7*, 500340.
235. Wang, Y.; Guo, J.; Luo, Z.; Shen, Y.; Wang, J.; Yu, Y.; Zhao, Y. Biopolymer-Assembled Porous Hydrogel Microfibers from Microfluidic Spinning for Wound Healing. *Adv. Healthc. Mater.* **2024**, *13*, 2302170.
236. Song, T.; Shen, Q.; Cheng, Y.; Zhi, Y.; Liu, G.; Ren, H.; Wang, J. Mechanically Tunable Hydrogel Microfibers for Biomimetic Tumor Drug Testing. *Adv. Funct. Mater.* **2025**, 2502840.
237. Yu, Y.; Wen, H.; Ma, J.; Lykkemark, S.; Xu, H.; Qin, J. Flexible Fabrication of Biomimetic Bamboo-like Hybrid Microfibers. *Adv. Mater.* **2014**, *26*, 2494–2499.
238. Cheung, T.W.; Li, L. A Review of Hollow Fibers in Application-Based Learning: From Textiles to Medical. *Text. Res. J.* **2019**, *89*, 237–253.
239. Tian, Y.; Wang, Z.; Wang, L. Hollow Fibers: From Fabrication to Applications. *Chem. Commun.* **2021**, *57*, 9166–9177.
240. Liu, H.; Wang, Y.; Chen, W.; Yu, Y.; Jiang, L.; Qin, J. A Microfluidic Strategy to Fabricate Ultra-Thin Polyelectrolyte Hollow Microfibers as 3D Cellular Carriers. *Mater. Sci. Eng. C* **2019**, *104*, 109705.
241. Shi, L.; Hao, S.; Li, J.; Fan, L.; Li, W.; Chen, T.; Shi, J.; Yang, P.; Yu, Y.; Gao, S. Hydrogel-Based Hollow Microfibers for Functional Esophageal Carcinoma Remodeling. *Cell Rep. Phys. Sci.* **2025**, *6*, 102358.
242. Liu, H.; Wang, Y.; Yu, Y.; Chen, W.; Jiang, L.; Qin, J. Simple Fabrication of Inner Chitosan-Coated Alginate Hollow Microfiber with Higher Stability. *J. Biomed. Mater. Res. Part. B Appl. Biomater.* **2019**, *107*, 2527–2536.
243. Jiang, M.Y.; Ju, X.J.; Deng, K.; Fan, X.X.; He, X.H.; Wu, F.; He, F.; Liu, Z.; Wang, W.; Xie, R.; et al. The Microfluidic Synthesis of Composite Hollow Microfibers for K+-Responsive Controlled Release Based on a Host–Guest System. *J. Mater. Chem. B* **2016**, *4*, 3925–3935.
244. Wang, M.; Ge, R.; Zhao, P.; Williams, G.R.; Yu, D.G.; Bligh, S.W.A. Exploring Wettability Difference-Driven Wetting by Utilizing Electrospun Chimeric Janus Microfiber Comprising Cellulose Acetate and Polyvinylpyrrolidone. *Mater. Des.* **2023**, *226*, 111652.
245. Lee, K.J.; Park, T.H.; Hwang, S.; Yoon, J.; Lahann, J. Janus-Core and Shell Microfibers. *Langmuir* **2013**, *29*, 6181–6186.
246. Tian, J.; Ma, Q.; Yu, W.; Li, D.; Dong, X.; Liu, G.; Wang, J. Preparation of Janus Microfibers with Magnetic and Fluorescence Functionality via Conjugate Electro-Spinning. *Mater. Des.* **2019**, *170*, 107701.
247. Jia, L.; Han, F.; Yang, H.; Turnbull, G.; Wang, J.; Clarke, J.; Shu, W.; Guo, M.; Li, B. Microfluidic Fabrication of Biomimetic Helical Hydrogel Microfibers for Blood-Vessel-on-a-Chip Applications. *Adv. Healthc. Mater.* **2019**, *8*, 1900435.
248. Teh, T.K.H.; Toh, S.L.; Goh, J.C.H. Aligned Fibrous Scaffolds for Enhanced Mechanoresponse and Tenogenesis of Mesenchymal Stem Cells. *Tissue Eng.-Part A* **2013**, *19*, 1360–1372.
249. Tan, Y.; Yi, J.; Shi, P.; Wei, Q.; Cui, Y.; Guan, Y.; Cheng, H.; Su, T.; Yao, Q.; Liu, H.; et al. Extracellular Matrix-Modified Helix-Flexible Nerve Conduit with Optimal Mechanics and Nerve Regenerating Properties. *Mater. Today Bio* **2025**, *35*, 102501.
250. Zhu, C.; Pongkitwitoon, S.; Qiu, J.; Thomopoulos, S.; Xia, Y. Design and Fabrication of a Hierarchically Structured Scaffold for Tendon-to-Bone Repair. *Adv. Mater.* **2018**, *30*, 1707306.
251. Huang, D.; Li, Z.; Li, G.; Zhou, F.; Wang, G.; Ren, X.; Su, J. Biomimetic Structural Design in 3D-Printed Scaffolds for Bone Tissue Engineering. *Mater. Today Bio* **2025**, *32*, 101664.
252. Liu, Y.; Wan, Y.; Li, C.; Guan, G.; Wang, F.; Gao, J.; Wang, L. Gradient Scaffolds in Bone-Soft Tissue Interface Engineering: Structural Characteristics, Fabrication Techniques, and Emerging Trends. *J. Orthop. Transl.* **2025**, *50*, 333–353.
253. Cao, X.; Chen, R.; Wang, Z.; Zhang, H.; Ma, X.; Bao, F. Microfluidic Spun Self-Healable Janus-Core Composite Microfibers as Smart Fiber Actuators. *ACS Appl. Mater. Interfaces* **2025**, *17*, 20225–20235.
254. Jeon, H.J.; Lee, H.; Kim, G.H. Nano-Sized Surface Patterns on Electrospun Microfibers Fabricated Using a Modified Plasma Process for Enhancing Initial Cellular Activities. *Plasma Process. Polym.* **2014**, *11*, 142–148.

255. Meng, J.; Boschetto, F.; Yagi, S.; Marin, E.; Adachi, T.; Chen, X.; Pezzotti, G.; Sakurai, S.; Sasaki, S.; Aoki, T.; et al. Enhancing the Bioactivity of Melt Electrowritten PLLA Scaffold by Convenient, Green, and Effective Hydrophilic Surface Modification. *Biomater. Adv.* **2022**, *135*, 112686.
256. Liu, S.M.; Chen, W.C.; Huang, S.M.; Chen, J.C.; Lin, C.L. Characterization of Electrospun Fibers and Electrospray Vancomycin-Containing Beads through the Interstitial or Lamellar Separation of Bead Composite Fiber Membranes to Evaluate Their Biomedical Application *in Vitro*. *J. Ind. Text.* **2022**, *52*. https://doi.org/10.1177/15280837221139326
257. Jensen, B.N.; Wang, Y.; Le Friec, A.; Nabavi, S.; Dong, M.; Seliktar, D.; Chen, M. Wireless Electromagnetic Neural Stimulation Patch with Anisotropic Guidance. *NPJ Flex. Electron.* **2023**, *7*, 34.
258. Truong, Y.B.; Glattauer, V.; Briggs, K.L.; Zappe, S.; Ramshaw, J.A.M. Collagen-Based Layer-by-Layer Coating on Electrospun Polymer Scaffolds. *Biomaterials* **2012**, *33*, 9198–9204.
259. Can-Herrera, L.A.; Ávila-Ortega, A.; de la Rosa-García, S.; Oliva, A.I.; Cauich-Rodríguez, J.V.; Cervantes-Uc, J.M. Surface Modification of Electrospun Polycaprolactone Microfibers by Air Plasma Treatment: Effect of Plasma Power and Treatment Time. *Eur. Polym. J.* **2016**, *84*, 502–513.
260. Correia, D.M.; Ribeiro, C.; Botelho, G.; Borges, J.; Lopes, C.; Vaz, F.; Carabineiro, S.A.C.; MacHado, A.V.; Lanceros-Méndez, S. Superhydrophilic Poly(l-Lactic Acid) Electrospun Membranes for Biomedical Applications Obtained by Argon and Oxygen Plasma Treatment. *Appl. Surf. Sci.* **2016**, *371*, 74–82.
261. Sankar, D.; Shalumon, K.T.; Chennazhi, K.P.; Menon, D.; Jayakumar, R. Surface Plasma Treatment of Poly(Caprolactone) Micro, Nano, and Multiscale Fibrous Scaffolds for Enhanced Osteoconductivity. *Tissue Eng. Part A* **2014**, *20*, 1689–1702.
262. Esmail, A.; Pereira, J.R.; Zoio, P.; Silvestre, S.; Menda, U.D.; Sevrin, C.; Grandfils, C.; Fortunato, E.; Reis, M.A.M.; Henriques, C.; et al. Oxygen Plasma Treated-Electrospun Polyhydroxyalkanoate Scaffolds for Hydrophilicity Improvement and Cell Adhesion. *Polymers* **2021**, *13*, 1056.
263. Transito-Medina, J.; Vázquez-Vélez, E.; Castillo, M.C.; Martínez, H.; Campillo, B. Gentamicin Release Study in Uniaxial and Coaxial Polyhydroxybutyrate–Polyethylene Glycol–Gentamicin Microfibers Treated with Atmospheric Plasma. *Polymers* **2023**, *15*, 3889.
264. El Khatib, M.; Mauro, A.; Wyrwa, R.; Di Mattia, M.; Turriani, M.; Di Giacinto, O.; Kretzschmar, B.; Seemann, T.; Valbonetti, L.; Berardinelli, P.; et al. Fabrication and Plasma Surface Activation of Aligned Electrospun Plga Fiber Fleeces with Improved Adhesion and Infiltration of Amniotic Epithelial Stem Cells Maintaining Their Teno-Inductive Potential. *Molecules* **2020**, *25*, 3176.
265. Kim, S.; Sitti, M. Biologically Inspired Polymer Microfibers with Spatulate Tips as Repeatable Fibrillar Adhesives. *Appl. Phys. Lett.* **2006**, *89*, 261911.
266. Gharib, G.; Bütün, İ.; Muganlı, Z.; Kozalak, G.; Namlı, İ.; Sarraf, S.S.; Ahmadi, V.E.; Toyran, E.; Wijnen, A.J.; Koşar, A. Biomedical Applications of Microfluidic Devices: A Review. *Biosensors* **2022**, *12*, 1023.
267. Boda, S.K.; Chen, S.; Chu, K.; Kim, H.J.; Xie, J. Electrospraying Electrospun Nanofiber Segments into Injectable Microspheres for Potential Cell Delivery. *ACS Appl. Mater. Interfaces* **2018**, *10*, 25069–25079.
268. Xie, J.; Wang, C.H. Electrospray in the Dripping Mode for Cell Microencapsulation. *J. Colloid Interface Sci.* **2007**, *312*, 247–255.
269. Stankevich, K.S.; Kudryavtseva, V.L.; Bolbasov, E.N.; Shesterikov, E.V.; Larionova, I.V.; Shapovalova, Y.G.; Domracheva, L.V.; Volokhova, A.A.; Kurzina, I.A.; Zhukov, Y.M.; et al. Modification of PCL Scaffolds by Reactive Magnetron Sputtering: A Possibility for Modulating Macrophage Responses. *ACS Biomater. Sci. Eng.* **2020**, *6*, 3967–3974.
270. Fiaschini, N.; Giuliani, C.; Vitali, R.; Tammaro, L.; Valerini, D.; Rinaldi, A. Design and Manufacturing of Antibacterial Electrospun Polysulfone Membranes Functionalized by Ag Nanocoating via Magnetron Sputtering. *Nanomaterials* **2022**, *12*, 3962.
271. Kalakonda, P.; Thudumu, S.; Mynepally, S.L.; Mandal, P.; Banne, S.; Kalakonda, P.B.; Podili, B.B. Engineering Micro/Nano-Fibrous Scaffolds with Silver Coating for Tailored Wound Repair Applications. *J. Nanopart. Res.* **2023**, *25*, 254.
272. Zhang, H.; Cao, Y.; Zhen, Q.; Hu, J.J.; Cui, J.Q.; Qian, X.M. Facile Preparation of PET/PA6 Bicomponent Microfilament Fabrics with Tunable Porosity for Comfortable Medical Protective Clothing. *ACS Appl. Bio Mater.* **2022**, *5*, 3509–3518.
273. Joseph, E.; Patil, A.; Hirlekar, S.; Shete, A.; Parekh, N.; Prabhune, A.; Nisal, A. Glycomonoterpene-Functionalized Crack-Resistant Biocompatible Silk Fibroin Coatings for Biomedical Implants. *ACS Appl. Bio Mater.* **2019**, *2*, 675–684.
274. Innocent, M.; Zhai, G.; Innocent, M.T.; Zhou, J.; Dai, X.; Jiang, T.; Wang, J.; Xiang, H.; Zhu, M. Bifunctional Catechol-Based Coating Strategy to Construct Highly Effective Antimicrobial Polyethylene Microfibers for Personal Protective Equipment. *Prog. Org. Coat.* **2025**, *198*, 108916.
275. McCarthy, A.; Avegnon, K.L.M.; Holubeck, P.A.; Brown, D.; Karan, A.; Sharma, N.S.; John, J.V.; Weihs, S.; Ley, J.; Xie, J. Electrostatic Flocking of Salt-Treated Microfibers and Nanofiber Yarns for Regenerative Engineering. *Mater. Today Bio* **2021**, *12*, 100166.

276. Hosseini, V.; Evrova, O.; Hoerstrup, S.P.; Vogel, V.; Hosseini, V.; Evrova, O.; Vogel, V.; Hoerstrup, S.P. A Simple Modification Method to Obtain Anisotropic and Porous 3D Microfibrillar Scaffolds for Surgical and Biomedical Applications. *Small* **2018**, *14*, 1702650.
277. Schneider, R.; Facure, M.H.M.; Chagas, P.A.M.; Andre, R.S.; dos Santos, D.M.; Correa, D.S. Tailoring the Surface Properties of Micro/Nanofibers Using 0D, 1D, 2D, and 3D Nanostructures: A Review on Post-Modification Methods. *Adv. Mater. Interfaces* **2021**, *8*, 2100430.
278. Xiao, F.X.; Pagliaro, M.; Xu, Y.J.; Liu, B. Layer-by-Layer Assembly of Versatile Nanoarchitectures with Diverse Dimensionality: A New Perspective for Rational Construction of Multilayer Assemblies. *Chem. Soc. Rev.* **2016**, *45*, 3088–3121.
279. Ravikrishnan, A.; Zhang, H.; Fox, J.M.; Jia, X. Core–Shell Microfibers via Bioorthogonal Layer-by-Layer Assembly. *ACS Macro Lett.* **2020**, *9*, 1369–1375.
280. Ariga, K.; Lvov, Y.; Decher, G. There Is Still Plenty of Room for Layer-by-Layer Assembly for Constructing Nanoarchitectonics-Based Materials and Devices. *Phys. Chem. Chem. Phys.* **2022**, *24*, 4097–4115.
281. Wang, J.; Wang, H.; Mo, X.; Wang, H. Reduced Graphene Oxide-Encapsulated Microfiber Patterns Enable Controllable Formation of Neuronal-Like Networks. *Adv. Mater.* **2020**, *32*, 2004555.
282. Gilbert-Honick, J.; Iyer, S.R.; Somers, S.M.; Takasuka, H.; Lovering, R.M.; Wagner, K.R.; Mao, H.Q.; Grayson, W.L. Engineering 3D Skeletal Muscle Primed for Neuromuscular Regeneration Following Volumetric Muscle Loss. *Biomaterials* **2020**, *255*, 120154.
283. Obata, A.; Hotta, T.; Wakita, T.; Ota, Y.; Kasuga, T. Electrospun Microfiber Meshes of Silicon-Doped Vaterite/Poly(Lactic Acid) Hybrid for Guided Bone Regeneration. *Acta Biomater.* **2010**, *6*, 1248–1257.
284. Shahriar, S.M.S.; Tran, H.Q.; Hayati, F.; Andrabi, S.M.; Yan, Z.; Rather, I.I.G.; Sharma, N.S.; Xie, J. Swallowable Expandable Fibrous Capsules for Nonendoscopic Sampling of Esophageal Cells. *Sci. Adv.* **2025**, *11*, eaeb3892.
285. Xu, Y.; Cui, W.; Zhang, Y.; Zhou, P.; Gu, Y.; Shen, X.; Li, B.; Chen, L. Hierarchical Micro/Nanofibrous Bioscaffolds for Structural Tissue Regeneration. *Adv. Healthc. Mater.* **2017**, *6*, 1601457.
286. Lund, A.; Rundqvist, K.; Nilsson, E.; Yu, L.; Hagström, B.; Müller, C. Energy Harvesting Textiles for a Rainy Day: Woven Piezoelectrics Based on Melt-Spun PVDF Microfibres with a Conducting Core. *NPJ Flex. Electron.* **2018**, *2*, 9.
287. Zhou, Y.; He, J.; Wang, H.; Qi, K.; Nan, N.; You, X.; Shao, W.; Wang, L.; Ding, B.; Cui, S. Highly Sensitive. Self-Powered and Wearable Electronic Skin Based on Pressure-Sensitive Nanofiber Woven Fabric Sensor. *Sci. Rep.* **2017**, *7*, 12949.
288. Fan, W.; He, Q.; Meng, K.; Tan, X.; Zhou, Z.; Zhang, G.; Yang, J.; Wang, Z.L. Machine-Knitted Washable Sensor Array Textile for Precise Epidermal Physiological Signal Monitoring. *Sci. Adv.* **2020**, *6*, 2840.
289. Mokhtari, F.; Foroughi, J.; Zheng, T.; Cheng, Z.; Spinks, G.M. Triaxial Braided Piezo Fiber Energy Harvesters for Self-Powered Wearable Technologies. *J. Mater. Chem. A* **2019**, *7*, 8245–8257.
290. Girard, F.; Lajoye, C.; Camman, M.; Tissot, N.; Berthelot Pedurand, F.; Tandon, B.; Moedder, D.; Liashenko, I.; Salameh, S.; Dalton, P.D.; et al. First Advanced Bilayer Scaffolds for Tailored Skin Tissue Engineering Produced via Electrospinning and Melt Electrowriting. *Adv. Funct. Mater.* **2024**, *34*, 2314757.
291. Lu, Z.; Zhang, H.; Hu, X.; Lu, J.; Wang, D. Probiotic-Free Microfiber Membrane for Promoting Infected Wound Healing by Regulating Wound Flora Balance. *ACS Mater. Lett.* **2022**, *4*, 2547–2554.
292. Wang, C.; Su, Y.; Xie, J. Advances in Electrospun Nanofibers: Versatile Materials and Diverse Biomedical Applications. *Accounts Mater. Res.* **2024**, *5*, 987–999.
293. Chen, S.; Liu, B.; Carlson, M.A.; Gombart, A.F.; Reilly, D.A.; Xie, J. Recent Advances in Electrospun Nanofibers for Wound Healing. *Nanomedicine* **2017**, *12*, 1335–1352.
294. Huang, Q.; Wu, T.; Wang, L.; Zhu, J.; Guo, Y.; Yu, X.; Fan, L.; Xin, J.H.; Yu, H. A Multifunctional 3D Dressing Unit Based on the Core-Shell Hydrogel Microfiber for Diabetic Foot Wound Healing. *Biomater. Sci.* **2022**, *10*, 2568–2576.
295. Wang, X.; Sun, K.; Wang, C.; Yang, M.; Qian, K.; Ye, B.; Guo, X.; Shao, Y.; Chu, C.; Xue, F.; et al. Ultrasound-Responsive Microfibers Promoted Infected Wound Healing with Neuro-Vascularization by Segmented Sonodynamic Therapy and Electrical Stimulation. *Biomaterials* **2025**, *313*, 122803.
296. Hema Naveena, A.; Kumar, A.; Agrawal, A.; Mavely, L.; Bhatia, D. Characterization of a Bioactive Chitosan Dressing: A Comprehensive Solution for Different Wound Healing Phases. *ACS Appl. Bio Mater.* **2025**, *8*, 1921–1933.
297. Nakayama, K.H.; Shayan, M.; Huang, N.F. Engineering Biomimetic Materials for Skeletal Muscle Repair and Regeneration. *Adv. Healthc. Mater.* **2019**, *8*, 1801168.
298. Li, J.; Wang, Y.; Wang, X.; Shang, L.; Zhao, Y.; Zhang, H. Photo-Responsive Antibacterial Patches Composed of Liquid Metal-Encapsulated Core-Shell Microfibers for Wound Healing. *Chem. Eng. J.* **2025**, *516*, 164218.
299. Yang, X.; Li, W.; Liu, Y.; Cao, N.; He, Y.; Sun, Q.; Zhou, S. Charged Fibrous Dressing to Promote Diabetic Chronic Wound Healing. *Adv. Healthc. Mater.* **2024**, *13*, 2302183.
300. Xue, J.; Wu, T.; Xia, Y. Perspective: Aligned Arrays of Electrospun Nanofibers for Directing Cell Migration. *APL Mater.* **2018**, *6*, 120902.

301. Zhang, X.; Hao, R.; Tong, J.; Hu, H.; Du, J.; Gong, B.; Tian, F.; Lu, Y.; Xue, J. A Radially Aligned Nanofiber Scaffold with Engineered Guidance Gradients for Directed Cell Migration and Accelerated Wound Healing. *Biomaterials* **2026**, *327*, 123797.
302. Homaeigohar, S.; Li, M.; Boccaccini, A.R. Bioactive Glass-Based Fibrous Wound Dressings. *Burn. Trauma* **2022**, *1*, tkac038.
303. Meng, Q.; Li, C.; Jiang, J.; Guo, F.; Fu, Y.; Gu, S.; Jiang, T.; Pan, J.; Zeng, Y.; Sun, L.; et al. A Fibrous Dressing Integrating Advanced Nanomicro Hybrid Structure with Effective Drug Delivery for Accelerated Wound Healing. *ACS Appl. Bio Mater.* **2025**, *9*, 315–332.
304. Kou, J.; Li, Y.; Zhou, C.; Wang, X.; Ni, J.; Lin, Y.; Ge, H.; Zheng, D.; Chen, G.; Sun, X.; et al. Electrospinning in Promoting Chronic Wound Healing: Materials, Process, and Applications. *Front. Bioeng. Biotechnol.* **2025**, *6*, 1550553.
305. Shen, Y.; Liu, Y.; Nunes, J.K.; Wang, C.; Xu, M.; To, M.K.T.; Stone, H.A.; Shum, H.C. Fibro-Gel: An All-Aqueous Hydrogel Consisting of Microfibers with Tunable Release Profile and Its Application in Wound Healing. *Adv. Mater.* **2023**, *35*, 2211637.
306. Yu, Y.; Chen, G.; Guo, J.; Liu, Y.; Ren, J.; Kong, T.; Zhao, Y. Vitamin Metal-Organic Framework-Laden Microfibers from Microfluidics for Wound Healing. *Mater. Horizons* **2018**, *5*, 1137–1142.
307. Ha, J.H.; Kim, J.Y.; Kim, D.; Ahn, J.; Jeong, Y.; Ko, J.; Hwang, S.; Jeon, S.; Jung, Y.; Gu, J.; et al. Multifunctional Micro/Nanofiber Based-Dressing Patch with Healing, Protection, and Monitoring Capabilities for Advanced Wound Care. *Adv. Mater. Technol.* **2023**, *8*, 2201765.
308. Tan, L.; Fu, J.; Feng, F.; Liu, X.; Cui, Z.; Li, B.; Han, Y.; Zheng, Y.; Yeung, K.W.K.; Li, Z.; et al. Engineered Probiotics Biofilm Enhances Osseointegration via Immunoregulation and Anti-Infection. *Sci. Adv.* **2020**, *6*, 5723–5736.
309. Xu, Z.; Shi, L.; Yang, M.; Zhang, H.; Zhu, L. Fabrication of a Novel Blended Membrane with Chitosan and Silk Microfibers for Wound Healing: Characterization, in Vitro and in Vivo Studies. *J. Mater. Chem. B* **2015**, *3*, 3634–3642.
310. Sharma, N.S.; Hayati, F.; Andrabi, S.M.; Su, Y.; Mondal, B.; Xie, J. Functional Nanofiber Scaffolds Enabling Local Immunomodulation and Inhibition of Ectopic Bone Formation. *ACS Appl. Mater. Interfaces* **2026**, *18*, 9559–9572.
311. Shi, L.; Wang, F.; Zhu, W.; Xu, Z.; Fuchs, S.; Hilborn, J.; Zhu, L.; Ma, Q.; Wang, Y.; Weng, X.; et al. Self-Healing Silk Fibroin-Based Hydrogel for Bone Regeneration: Dynamic Metal-Ligand Self-Assembly Approach. *Adv. Funct. Mater.* **2017**, *27*, 1700591.
312. Wang, J.; Yang, Q.; Saiding, Q.; Chen, L.; Liu, M.; Wang, Z.; Xiang, L.; Deng, L.; Chen, Y.; Cui, W.; et al. Geometric Angles and Gene Expression in Cells for Structural Bone Regeneration. *Adv. Sci.* **2023**, *10*, 2304111.
313. Zhou, Y.H.; Zou, Z.H.; Teng, J.X.; Wu, Z.Y.; Luo, S.W.; Ning, X.; Ye, C.; Yang, L.; Toh, W.S. Injectable Alginate/β-TCP Composite Hydrogel Incorporating P34HB/MgO+PEG Coaxial Electrospun Microfibers for Minimally Invasive Treatment of Osteonecrosis. *Adv. Healthc. Mater.* **2025**, *14*, 2500617.
314. Xu, Z.; Shi, L.; Hu, D.; Hu, B.; Yang, M.; Zhu, L. Formation of Hierarchical Bone-like Apatites on Silk Microfiber Templates via Biomineralization. *RSC Adv.* **2016**, *6*, 76426–76433.
315. Yan, Z.; Tran, H.; Ma, D.; Xie, J. Emerging Piezoelectric Metamaterials for Biomedical Applications. *Mater. Interfaces* **2024**, *1*, 13–34.
316. Zhou, Y.; Jiao, Z.; Zhang, H.; Zhao, G.; Zhao, Z.; Li, C.; Zhang, P.; Zhao, L.; Zhao, Y.; Wu, G. Collagen-Enhanced Piezoelectric PLLA/ZnO Microfiber Barrier Membranes for Superior Bone Regeneration. *Int. J. Biol. Macromol.* **2025**, *319*, 145443.
317. Somers, S.M.; Zhang, N.Y.; Morrissette-McAlmon, J.B.F.; Tran, K.; Mao, H.Q.; Grayson, W.L. Myoblast Maturity on Aligned Microfiber Bundles at the Onset of Strain Application Impacts Myogenic Outcomes. *Acta Biomater.* **2019**, *94*, 232–242.
318. Kamaraj, M.; Rezayof, O.; Barer, A.; Kim, H.; Moghimi, N.; Joshi, A.; Dokmeci, M.R.; Khademhosseini, A.; Alambeigi, F.; John, J.V. Development of Silk Microfiber-Reinforced Bioink for Muscle Tissue Engineering and in Situ Printing by a Handheld 3D Printer. *Biomater. Adv.* **2025**, *166*, 214057.
319. Gilbert-Honick, J.; Ginn, B.; Zhang, Y.; Salehi, S.; Wagner, K.R.; Mao, H.Q.; Grayson, W.L. Adipose-Derived Stem/Stromal Cells on Electrospun Fibrin Microfiber Bundles Enable Moderate Muscle Reconstruction in a Volumetric Muscle Loss Model. *Cell Transplant.* **2018**, *27*, 1644–1656.
320. Chen, X.; Du, W.; Cai, Z.; Ji, S.; Dwivedi, M.; Chen, J.; Zhao, G.; Chu, J. Uniaxial Stretching of Cell-Laden Microfibers for Promoting C2C12 Myoblasts Alignment and Myofibers Formation. *ACS Appl. Mater. Interfaces* **2020**, *12*, 2162–2170.
321. Campiglio, C.E.; Carcano, A.; Draghi, L. RGD-Pectin Microfiber Patches for Guiding Muscle Tissue Regeneration. *J. Biomed. Mater. Res. Part A* **2022**, *110*, 515–524.
322. Li, M.; Deng, W.; Zhang, J.; Zheng, W.; Yu, T.; Zhou, Q. Aligned Electrospun PLLA/Graphene Microfibers with Nanotopographical Surface Modulate the Mitochondrial Responses of Vascular Smooth Muscle Cells. *Adv. Mater. Interfaces* **2021**, *8*, 2100229.

323. Uribe-Gomez, J.; Posada-Murcia, A.; Shukla, A.; Ergin, M.; Constante, G.; Apsite, I.; Martin, D.; Schwarzer, M.; Caspari, A.; Synytska, A.; et al. Shape-Morphing Fibrous Hydrogel/Elastomer Bilayers Fabricated by a Combination of 3D Printing and Melt Electrowriting for Muscle Tissue Regeneration. *ACS Appl. Bio Mater.* **2021**, *4*, 1720–1730.
324. Nam, S.; Seo, B.R.; Najibi, A.J.; McNamara, S.L.; Mooney, D.J. Active Tissue Adhesive Activates Mechanosensors and Prevents Muscle Atrophy. *Nat. Mater.* **2022**, *22*, 249–259.
325. Christensen, K.W.; Turner, J.; Coughenour, K.; Maghdouri-White, Y.; Bulysheva, A.A.; Sergeant, O.; Rariden, M.; Randazzo, A.; Sheean, A.J.; Christ, G.J.; et al. Fiber Bioprinted Implants with Musculoskeletal Tissue Properties Promote Functional Recovery in Volumetric Muscle Loss. *Adv. Healthc. Mater.* **2022**, *11*, 2101357.
326. Kim, W.J.; Kim, M.; Kim, G.H. 3D-Printed Biomimetic Scaffold Simulating Microfibril Muscle Structure. *Adv. Funct. Mater.* **2018**, *28*, 1800405.
327. Chen, Y.; Guo, C.; Manousiouthakis, E.; Wang, X.; Cairns, D.M.; Roh, T.T.; Du, C.; Kaplan, D.L. Bi-Layered Tubular Microfiber Scaffolds as Functional Templates for Engineering Human Intestinal Smooth Muscle Tissue. *Adv. Funct. Mater.* **2020**, *30*, 2000543.
328. Chen, X.; Sun, T.; Shimoda, S.; Wang, H.; Huang, Q.; Fukuda, T.; Shi, Q.; Chen, X.; Sun, T.; Wang, H.; et al. A Micromanipulation-Actuated Large-Scale Screening to Identify Optimized Microphysiological Model Parameters in Skeletal Muscle Regeneration. *Adv. Sci.* **2024**, *11*, 2403622.
329. Xie, J.; MacEwan, M.R.; Li, X.; Sakiyama-Elbert, S.E.; Xia, Y. Neurite Outgrowth on Nanofiber Scaffolds with Different Orders, Structures, and Surface Properties. *ACS Nano* **2009**, *3*, 1151–1159.
330. Zhang, C.; Gong, J.; Zhang, J.; Zhu, Z.; Qian, Y.; Lu, K.; Zhou, S.; Gu, T.; Wang, H.; He, Y.; et al. Three Potential Elements of Developing Nerve Guidance Conduit for Peripheral Nerve Regeneration. *Adv. Funct. Mater.* **2023**, *33*, 2302251.
331. Puhl, D.L.; Funnell, J.L.; Nelson, D.W.; Gottipati, M.K.; Gilbert, R.J. Electrospun Fiber Scaffolds for Engineering Glial Cell Behavior to Promote Neural Regeneration. *Bioengineering* **2021**, *8*, 4.
332. Fang, Y.; Wang, C.; Liu, Z.; Ko, J.; Chen, L.; Zhang, T.; Xiong, Z.; Zhang, L.; Sun, W. 3D Printed Conductive Multiscale Nerve Guidance Conduit with Hierarchical Fibers for Peripheral Nerve Regeneration. *Adv. Sci.* **2023**, *10*, 2205744.
333. Dong, X.; Liu, S.; Yang, Y.; Gao, S.; Li, W.; Cao, J.; Wan, Y.; Huang, Z.; Fan, G.; Chen, Q.; et al. Aligned Microfiber-Induced Macrophage Polarization to Guide Schwann-Cell-Enabled Peripheral Nerve Regeneration. *Biomaterials* **2021**, *272*, 120767.
334. Kim, T.; Jeon, J.; Lee, M.S.; Park, J.H.; Chung, Y.; Yang, H.S. Development of Electrospun Nerve Guidance Conduits by a Milk-Derived Protein with Biodegradable Polymers for Peripheral Nerve Regeneration. *ACS Appl. Bio Mater.* **2025**, *8*, 3498–3512.
335. Yao, S.; He, F.; Cao, Z.; Sun, Z.; Chen, Y.; Zhao, H.; Yu, X.; Wang, X.; Yang, Y.; Rosei, F.; et al. Mesenchymal Stem Cell-Laden Hydrogel Microfibers for Promoting Nerve Fiber Regeneration in Long-Distance Spinal Cord Transection Injury. *ACS Biomater. Sci. Eng.* **2020**, *6*, 1165–1175.
336. Nakielski, P.; Pierini, F. Blood Interactions with Nano- and Microfibers: Recent Advances, Challenges and Applications in Nano- and Microfibrous Hemostatic Agents. *Acta Biomater.* **2019**, *84*, 63–76.
337. Zhang, F.; King, M.W. Immunomodulation Strategies for the Successful Regeneration of a Tissue-Engineered Vascular Graft. *Adv. Healthc. Mater.* **2022**, *11*, 2200045.
338. Ravi, S.; Chaikof, E.L. Biomaterials for Vascular Tissue Engineering. *Regen. Med.* **2010**, *5*, 107–120.
339. Liu, S.; Yao, L.; Wang, Y.; Li, Y.; Jia, Y.; Yang, Y.; Li, N.; Hu, Y.; Kong, D.; Dong, X.; et al. Immunomodulatory Hybrid Micro-Nanofiber Scaffolds Enhance Vascular Regeneration. *Bioact. Mater.* **2023**, *21*, 464–482.
340. Fahad, M.A.Al; Lee, H.Y.; Park, S.; Choi, M.; Shanto, P.C.; Park, M.; Bae, S.H.; Lee, B.T. Small-Diameter Vascular Graft Composing of Core-Shell Structured Micro-Nanofibers Loaded with Heparin and VEGF for Endothelialization and Prevention of Neointimal Hyperplasia. *Biomaterials* **2024**, *306*, 122507.
341. Wang, H.; Cui, L.; Luo, Y.; Chen, H.; Liu, X.; Shi, Q. Inflammation-Responsive PCL/Gelatin Microfiber Scaffold with Sustained Nitric Oxide Generation and Heparin Release for Blood-Contacting Implants. *Int. J. Biol. Macromol.* **2024**, *281*, 136544.
342. Li, P.; Shahriar, S.M.S.; Tang, L.; Prachyl, H.; Chaliki, H.; Scott, L.; Xie, J.; Zhu, W. Minimally Invasive Delivery of Engineered Heart Tissues Restores Cardiac Function in Rats with Chronic Myocardial Infarction. *Acta Biomater.* **2026**, *211*, 74–91.
343. Federici, A.S.; Garcia, O.; Kelly, D.J.; Hoey, D.A. Muticomponent Melt-Electrowritten Vascular Graft to Mimic and Guide Regeneration of Small Diameter Blood Vessels. *Adv. Funct. Mater.* **2024**, *34*, 2409883.
344. Wang, Q.; Zhang, Y.; Shao, F.; Yang, X.; Wang, S.; Shen, Y.; Wang, H. Bio-Inspired Design of 4D-Printed Scaffolds Capable of Programmable Multi-Step Transformations Toward Vascular Reconstruction. *Adv. Funct. Mater.* **2024**, *34*, 2407592.

345. Wang, H.; Xing, M.; Deng, W.; Qian, M.; Wang, F.; Wang, K.; Midgley, A.C.; Zhao, Q. Anti-Sca-1 Antibody-Functionalized Vascular Grafts Improve Vascular Regeneration via Selective Capture of Endogenous Vascular Stem/Progenitor Cells. *Bioact. Mater.* **2022**, *16*, 433–450.
346. Wu, Z.; Cai, H.; Ao, Z.; Xu, J.; Heaps, S.; Guo, F. Microfluidic Printing of Tunable Hollow Microfibers for Vascular Tissue Engineering. *Adv. Mater. Technol.* **2021**, *6*, 2000683.
347. Sun, T.; Shi, Q.; Huang, Q.; Wang, H.; Xiong, X.; Hu, C.; Fukuda, T. Magnetic Alginate Microfibers as Scaffolding Elements for the Fabrication of Microvascular-like Structures. *Acta Biomater.* **2018**, *66*, 272–281.
348. Yu, L.; Feng, Y.; Yao, L.; Soon, R.H.; Yeo, J.C.; Lim, C.T. Dual-Core Capacitive Microfiber Sensor for Smart Textile Applications. *ACS Appl. Mater. Interfaces* **2019**, *11*, 33347–33355.
349. Zhao, Y.; Zhai, Q.; Dong, D.; An, T.; Gong, S.; Shi, Q.; Cheng, W. Highly Stretchable and Strain-Insensitive Fiber-Based Wearable Electrochemical Biosensor to Monitor Glucose in the Sweat. *Anal. Chem.* **2019**, *91*, 6569–6576.
350. Chinnamani, M.V.; Hanif, A.; Kannan, P.K.; Kaushal, S.; Sultan, M.J.; Lee, N.E. Soft Microfiber-Based Hollow Microneedle Array for Stretchable Microfluidic Biosensing Patch with Negative Pressure-Driven Sampling. *Biosens. Bioelectron.* **2023**, *237*, 115468.
351. Jiang, C.; Dai, P.; Li, X.; Cong, Z.; Dong, T.; Sun, Y.; Liu, X.; Sui, Y.; Chen, P.; Yu, X.; et al. Flexible Wearable Microfiber Respiratory Sensor Based on Microspheres Coupling. *IEEE Sens. J.* **2023**, *23*, 27324–27330.
352. Yu, R.; Wu, L.; Yang, Z.; Wu, J.; Chen, H.; Pan, S.; Zhu, M. Dynamic Liquid Metal–Microfiber Interlocking Enables Highly Conductive and Strain-Insensitive Metastructured Fibers for Wearable Electronics. *Adv. Mater.* **2025**, *37*, 2415268.
353. Gao, J.; Fan, Y.; Zhang, Q.; Luo, L.; Hu, X.; Li, Y.; Song, J.; Jiang, H.; Gao, X.; Zheng, L.; et al. Ultra-Robust and Extensible Fibrous Mechanical Sensors for Wearable Smart Healthcare. *Adv. Mater.* **2022**, *34*, 2107511.
354. Hanif, A.; Park, J.; Kim, D.; Youn, J.; Jeong, U.; Kim, D.S. A Stretchable and Strain-Limiting, Bio-Inspired Nanofiber-Reinforced Microfiber for Wearable Electronics. *Adv. Mater. Technol.* **2024**, *9*, 2301643.
355. Jiang, Q.; Ma, X.; Chai, Y.; Ma, H.; Tang, F.; Hua, K.; Chen, R.; Jin, Z.; Wang, X.; Ji, J.; et al. Reduced Graphene Oxide-Polypyrrole Aerogel-Based Coaxial Heterogeneous Microfiber Enables Ultrasensitive Pressure Monitoring of Living Organisms. *ACS Appl. Mater. Interfaces* **2021**, *13*, 5425–5434.
356. Kim, J.; Roh, H.; Moon, S.; Jeon, C.; Baek, S.; Cho, W.; Sim, J.Y.; Jeong, U. Wireless Breathable Face Mask Sensor for Spatiotemporal 2D Respiration Profiling and Respiratory Diagnosis. *Biomaterials* **2024**, *309*, 122579.
357. Hou, W.; Wang, J.; Lv, J.an. Bioinspired Liquid Crystalline Spinning Enables Scalable Fabrication of High-Performing Fibrous Artificial Muscles. *Adv. Mater.* **2023**, *35*, 2211800.
358. Kim, H.; Na, H.; Noh, S.; Chang, S.; Kim, J.; Kong, T.; Shin, G.; Lee, C.; Lee, S.; Park, Y.L.; et al. Inherently Integrated Microfiber-Based Flexible Proprioceptive Sensor for Feedback-Controlled Soft Actuators. *NPJ Flex. Electron.* **2024**, *8*, 15.
359. Chen, S.; Boda, S.K.; Batra, S.K.; Li, X.; Xie, J. Emerging Roles of Electrospun Nanofibers in Cancer Research. *Adv. Healthc. Mater.* **2018**, *7*, 1701024.
360. Tian, L.; Ma, J.; Li, W.; Zhang, X.; Gao, X. Microfiber Fabricated via Microfluidic Spinning toward Tissue Engineering Applications. *Macromol. Biosci.* **2023**, *23*, 2200429.
361. Neufeld, L.; Yeini, E.; Pozzi, S.; Satchi-Fainaro, R. 3D Bioprinted Cancer Models: From Basic Biology to Drug Development. *Nat. Rev. Cancer* **2022**, *22*, 679–692.
362. Zhao, J.; Cui, W. Functional Electrospun Fibers for Local Therapy of Cancer. *Adv. Fiber Mater.* **2020**, *2*, 229–245.
363. Chen, Y.; Guo, J.; Wu, X.; Xu, Y.; Wang, J.; Ren, H.; Zhao, Y. Microfluidic Spinning of Natural Origin Microfibers for Breast Tumor Postsurgical Treatment. *Chem. Eng. J.* **2023**, *472*, 144901.
364. Huo, J.; Zou, J.; Ma, H.; Meng, G.; Huang, Y.; Yan, X.; Yang, Y.; Zhang, M. Astragaloside IV Microfibers Assembling into Injectable 3D-Scaffolds with Intrinsic Immunoactivity for Enhanced Tumor Vaccine Efficacy. *Chem. Eng. J.* **2024**, *498*, 155511.
365. Sharma, P.; Shin, J.B.; Park, B.C.; Lee, J.W.; Byun, S.W.; Jang, N.Y.; Kim, Y.J.; Kim, Y.; Kim, Y.K.; Cho, N.H. Application of Radially Grown ZnO Nanowires on Poly-L-Lactide Microfibers Complexed with a Tumor Antigen for Cancer Immunotherapy. *Nanoscale* **2019**, *11*, 4591–4600.
366. Jing, L.; Wang, X.; Leng, B.; Zhan, N.; Liu, H.; Wang, S.; Lu, Y.; Sun, J.; Huang, D. Engineered Nanotopography on the Microfibers of 3D-Printed PCL Scaffolds to Modulate Cellular Responses and Establish an in Vitro Tumor Model. *ACS Appl. Bio Mater.* **2021**, *4*, 1381–1394.
367. Lee, C.T.; Gill, E.L.; Wang, W.; Gerigk, M.; Terentjev, E.M.; Shery Huang, Y.Y. Guided Assembly of Cancer Ellipsoid on Suspended Hydrogel Microfibers Estimates Multi-Cellular Traction Force. *Phys. Biol.* **2021**, *18*, 036001.
368. Shiroud Heidari, B.; Dodda, J.M.; El-Khordagui, L.K.; Focarete, M.L.; Maroti, P.; Toth, L.; Pacilio, S.; El-Habashy, S.E.; Boateng, J.; Catanzano, O.; et al. Emerging Materials and Technologies for Advancing Bioresorbable Surgical Meshes. *Acta Biomater.* **2024**, *184*, 1–21.
369. Pluchino, M.; Vivarelli, L.; Giavaresi, G.; Dallari, D.; Govoni, M. Commercial Biomaterial-Based Products for Tendon Surgical Augmentation: A Scoping Review on Currently Available Medical Devices. *J. Funct. Biomater.* **2025**, *16*, 130.

370. Baylón, K.; Rodríguez-Camarillo, P.; Elías-Zúñiga, A.; Díaz-Elizondo, J.A.; Gilkerson, R.; Lozano, K.Past. Present and Future of Surgical Meshes: A Review. *Membranes* **2017**, *22*, 47.
371. Plencner, M.; East, B.; Tonar, Z.; Otáhal, M.; Prosecká, E.; Rampichová, M.; Krejčí, T.; Litvinec, A.; Buzgo, M.; Míčková, A.; et al. Abdominal Closure Reinforcement by Using Polypropylene Mesh Functionalized with Poly-Ɛ-Caprolactone Nanofibers and Growth Factors for Prevention of Incisional Hernia Formation. *Int. J. Nanomed.* **2014**, *9*, 3263–3277.
372. Cazzagon, V.; Giubilato, E.; Bonetto, A.; Blosi, M.; Zanoni, I.; Costa, A.L.; Vineis, C.; Varesano, A.; Marcomini, A.; Hristozov, D.; et al. Identification of the Safe(r) by Design Alternatives for Nanosilver-Enabled Wound Dressings. *Front. Bioeng. Biotechnol.* **2022**, *10*, 987650.
373. Williams, S.F.; Martin, D.P.; Moses, A.C. The History of GalaFLEX P4HB Scaffold. *Aesthetic Surg. J.* **2016**, *36*, 33–42.
374. Williams, S.F.; Rizk, S.; Martin, D.P. Poly-4-Hydroxybutyrate (P4HB): A New Generation of Resorbable Medical Devices for Tissue Repair and Regeneration. *Biomed. Eng.* **2013**, *58*, 439–452.
375. Martin, D.P.; Badhwar, A.; Shah, D.V.; Rizk, S.; Eldridge, S.N.; Gagne, D.H.; Ganatra, A.; Darois, R.E.; Williams, S.F.; Tai, H.C.; et al. Characterization of Poly-4-Hydroxybutyrate Mesh for Hernia Repair Applications. *J. Surg. Res.* **2013**, *184*, 766–773.
376. Deeken, C.R.; Gagne, D.H.; Badhwar, A. Mechanical and Histological Characteristics of PhasixTM ST Mesh in a Porcine Model of Hernia Repair. *J. Investig. Surg.* **2022**, *35*, 415–423.
377. Gómez-Gil, V.; Rodríguez, M.; García-Moreno Nisa, F.; Pérez-Köhler, B.; Pascual, G. Evaluation of Synthetic Reticular Hybrid Meshes Designed for Intraperitoneal Abdominal Wall Repair Preclinical and *In Vitro* Behavior. *PLoS One 2019 14*, 0213005.
378. Horii, T.; Tsujimoto, H.; Hagiwara, A.; Isogai, N.; Sueyoshi, Y.; Oe, Y.; Kageyama, S.; Yoshida, T.; Kobayashi, K.; Minato, H.; et al. Effects of Fiber Diameter and Spacing Size of an Artificial Scaffold on the In Vivo Cellular Response and Tissue Remodeling. *ACS Appl. Bio Mater.* **2021**, *4*, 6924–6936.
379. Minsart, M.; Vlierberghe, S.; Dubruel, P.; Mignon, A. Commercial Wound Dressings for the Treatment of Exuding Wounds: An in-Depth Physico-Chemical Comparative Study. *Burn. Trauma* **2022**, *10*, tkac024.
380. Sopata, M.; Piasecki, A.; Sopata, M. Scanning Electron Microscopic Examination of Absorption Potency of Various Fibrous Dressings. *J. Wound Care* **2019**, *28*, 82–88.
381. Hurlow, J. AQUACEL® Ag Dressing with Hydrofiber® Technology. *Adv. Wound Care* **2012**, *1*, 104–107.
382. Kwon, K.A.; Shipley, R.J.; Edirisinghe, M.; Ezra, D.G.; Rose, G.E.; Rayment, A.W.; Best, S.M.; Cameron, R.E. Microstructure and Mechanical Properties of Synthetic Brow-Suspension Materials. *Mater. Sci. Eng. C* **2014**, *35*, 220–230.
383. Sun, H.; Cheng, Z.; Guo, X.; Gu, H.; Tang, D.; Wang, L. Comparison of Biomechanical and Microstructural Properties of Aortic Graft Materials in Aortic Repair Surgeries. *J. Funct. Biomater.* **2024**, *15*, 248.
384. Herten, M.; Bisdas, T.; Knaack, D.; Becker, K.; Osada, N.; Torsello, G.B.; Idelevich, E.A. Rapid *In Vitro* Quantification of S. Aureus Biofilms on Vascular Graft Surfaces. *Front. Microbiol.* **2017**, *8*, 2333.
385. Abhari, R.E.; Snelling, S.J.B.; Augustynak, E.; Davis, S.; Fischer, R.; Carr, A.J.; Mouthuy, P.A. A Hybrid Electrospun-Extruded Polydioxanone Suture for Tendon Tissue Regeneration. *Tissue Eng. Part A* **2024**, *30*, 214–224.
386. Shiga, T.; Okada, H.; Isobe, M.; Furui, T. Tissue Damage between Barbed Suture and Conventional Sutures in Animal Laboratory Model Using Scanning Electron Microscopy. *J. Obs. Gynaecol.* **2024**, *44*, 2370973.
387. Dragovic, M.; Pejovic, M.; Stepic, J.; Colic, S.; Dozic, B.; Dragovic, S.; Lazarevic, M.; Nikolic, N.; Milasin, J.; Milicic, B. Comparison of Four Different Suture Materials in Respect to Oral Wound Healing, Microbial Colonization, Tissue Reaction and Clinical Features—Randomized Clinical Study. *Clin. Oral. Investig.* **2019**, *24*, 1527–1541.
388. Andrade, M.G.S.; Weissman, R.; Reis, S.R.A. Tissue Reaction and Surface Morphology of Absorbable Sutures after in Vivo Exposure. *J. Mater. Sci. Mater. Med.* **2006**, *17*, 949–961.
389. Tomihata, K.; Suzuki, M.; Ikada, Y. The PH Dependence of Monofilament Sutures on Hydrolytic Degradation. *J. Biomed. Mater. Res.* **2001**, *58*, 511–518.
390. Lee, K.H.; Chu, C.C. The Role of Superoxide Ions in the Degradation of Synthetic Absorbable Sutures. *J. Biomed. Mater. Res.* **2000**, *49*, 25–35.
391. Jadhav, S.A.; Raval, A.J.; Patravale, V.B. Drug Delivery, Development, and Technological Aspects for Peripheral Drug Eluting Stents. *Adv. Drug Deliv. Rev.* **2025**, *226*, 115678.
392. Pires, L.S.; Melo, D.S.; Borges, J.P.; Henriques, C.R. PEDOT-Coated PLA Fibers Electrospun from Solutions Incorporating Fe(III)Tosylate in Different Solvents by Vapor-Phase Polymerization for Neural Regeneration. *Polymers* **2023**, *15*, 4004.
393. Shahriar, S.M.S.; Sharma, N.; Andrabi Syed, M.; Mondal, B.; Yan, Z.; Rainu, S.; Hellman, A.; Buesquets, M.; Rensch, J.; Perez, R.; et al. Nanofiber, Microfiber, or Hybrid: Which Architecture Excels in Soft Tissue Reinforcement and Constructive Regeneration? *ACS Appl. Mater. Interfaces* **2026**. https://doi.org/10.1021/acsami.6c04938.